2008-10-15

Modulation of Voltage-Gated N-Type Calcium Channels by G Protein-Coupled Receptors Involves Lipids and Proteins: A Dissertation

Tora Mitra Ganguli
University of Massachusetts Medical School

MODULATION OF VOLTAGE-GATED N-TYPE CALCIUM CHANNELS BY G PROTEIN-COUPLED RECEPTORS INVOLVES LIPIDS AND PROTEINS

A Dissertation Presented

By

TORA MITRA GANGULI

Submitted to the Faculty of the

University of Massachusetts Graduate School of Biomedical Sciences, Worcester

in partial fulfillment of the requirements for the degree of

DOCTOR OF PHILOSOPHY

(OCTOBER 15, 2008)

NEUROSCIENCE

MODULATION OF VOLTAGE-GATED N-TYPE CALCIUM CHANNELS BY G PROTEIN-COUPLED RECEPTORS INVOLVES LIPIDS AND PROTEINS

A Dissertation Presented
By
TORA MITRA GANGULI

The signatures of the Dissertation Defense Committee signifies
completion and approval as to style and content of the Dissertation

Ann R. Rittenhouse, Ph.D., Thesis Advisor

Julie Jonassen, Ph.D., Member of Committee

Stephen R. Ikeda, Ph.D., Member of Committee

José R. Lemos, Ph.D., Member of Committee

Hong-Sheng Li, Ph.D., Member of Committee

The signature of the Chair of the Committee signifies that the written dissertation meets
the requirements of the Dissertation Committee

William R. Kobertz, Ph.D., Chair of Committee

The signature of the Dean of the Graduate School of Biomedical Sciences signifies
that the student has met all graduation requirements of the school.

Anthony Carruthers, Ph.D.,
Dean of the Graduate School of Biomedical Sciences
Neuroscience
September 30, 2008

ACKNOWLEDGEMENTS

My sincere thanks to my advisor Dr. Ann Rittenhouse for providing such an excellent mentorship that helped me develop as a scientist and enjoy research as much as I do now. I have learned a lot from her and the numerous conversations that we had, helped me a lot in developing ideas and concepts. I am especially indebted to Ann for her enthusiasm and unwavering support throughout these years.

I am also thankful to the past members of the Rittenhouse laboratory- Dr. Liwang Liu, Dr. Rubing Zhao, Dr. John Heneghan, Dr. Mandy Roberts-Crowley and Lee Stanish for helping me transition into the lab, teaching me techniques and engaging in scientific discussions that have supported my growth tremendously.

I would like to thank all my committee members for their patient guidance during the entire process and for guiding me with techniques and suggestions whenever the need arose. Many thanks to Drs. Robert Carraway, Daniel Kilpatrick, James Dobson, Mitsuo Ikebe, Gregory Pazour and members of their laboratories for helpful discussions and for letting me use reagents and instruments. I would also like to thank Ms Cheryl Barry and Ms Patricia Keith of the Physiology department for their administrative support.

I would like to thank my parents for their unconditional love and support. I also acknowledge the contribution of Dr. Tushar Kanti Ghosh (University of Calcutta), for imbibing in me the interest in Neuroscience twelve years ago that ultimately led me to pursue research in this field. I am also thankful to my husband, Abhijit, for believing in me and supporting me immensely every step of the way. Finally, I bow before my motherland for providing me with the will and the strength to succeed in difficult times.

ABSTRACT

Pain signaling involves transmission of nociceptive stimuli in the spinal cord where a critical balance between excitatory and inhibitory inputs determines the response to noxious stimuli. The neuropeptide, substance P (SP), mediates transmission of pain in part by binding to the tachykinin receptor (NK-1R) in the dorsal horn (DH) of the spinal cord. One of SP's downstream effects is to modulate N-type Ca^{2+} (N-) channels. While phospholipid breakdown is a part of the inflammatory process that accompanies tissue damage, the role of this metabolic pathway has not been completely described with respect to N-channel modulation during pain signaling. Despite the incomplete understanding of this modulation, pharmacological antagonists of both NK-1R and N-channels have been used to treat pain.

In Chapter II, using whole-cell patch clamp recording techniques, the SP signaling cascade that mediates inhibition of recombinant N-channel activity was characterized. By adopting a pharmacological approach, I show that this pathway resembles the slow pathway that was earlier described for modulation of N-current by the M_1 muscarinic receptor (M_1R). M_1R couples to G_q to stimulate phospholipid breakdown. Together with previous observations, the data presented in this chapter provide evidence for involvement of the extracellular receptor kinase (ERK1/2), phospholipase A_2 and release of phospholipid metabolites in the modulation of N-current by SP. Overall, this chapter shows that phospholipid metabolism involved in modulation of N-currents is not specific to M_1Rs but that other G_q-coupled receptors may also modulate N-currents via the same signal transduction pathway.

In Chapter III, enhancement of N-current by SP was studied as part of a collaborative project to understand current enhancement that occurs when a palmitoylated accessory $Ca_V\beta2a$ subunit is co-expressed with the pore-forming subunit $Ca_V2.2$ and the accessory subunit $\alpha_2\delta$-1. When $Ca_V\beta3$ is present, SP inhibits N-current as described in Chapter II. However, when palmitoylated $Ca_V\beta2a$ is co-expressed with $Ca_V2.2$ (and $\alpha_2\delta$-1), current enhancement is observed at negative test potentials, demonstrating that both M_1Rs and NK-1Rs exhibit the same profile of N-current modulation. This change in modulation by muscarinic agonists is not observed in the presence of a depalmitoylated $Ca_V\beta2a$. However a chimeric $Ca_V\beta2a\beta1b$ subunit that contains the palmitoylated N-terminus from $Ca_V\beta2a$ confers enhancement. Normally expression of the β1b subunit resulted in current inhibition. These findings indicated that the palmitoylated $Ca_V\beta2a$ participates in enhancement of current. Our data support a model where inhibition dominates over enhancement; when inhibition is blocked, enhancement may be observed. Lastly, we show that N-current inhibition by SP is minimized when exogenous palmitic acid is applied to cells co-expressing $Ca_V\beta3$ subunits with N-channels. These results indicate that the presence of palmitic acid can prevent N-current inhibition when SP is applied most likely by interacting with $Ca_V2.2$. We propose a model where palmitic acid occupies the inhibitory site and serves to antagonize inhibition by a lipid metabolite, which is most likely arachidonic acid. The $Ca_V\beta2a$ protein seems to have a role in positioning the palmitoyl groups near $Ca_V2.2$. This chapter provides a new role for protein palmitoylation where the palmitoyl groups of $Ca_V\beta2a$ are both necessary and sufficient to block inhibition of another protein: $Ca_V2.2$.

In Chapter IV, I probe the role of the relative orientation of $Ca_V\beta2a$ and the pore-forming subunit of the N-channel in N-current modulation. Evidence is presented that shows that not just the presence of a palmitoylated $Ca_V\beta2a$ is necessary, but the relative orientation of $Ca_V\beta2a$ to $Ca_V2.2$ is critical for blocking inhibition. Using N-channel mutants that cause a change in the orientation of $Ca_V\beta2a$ relative to $Ca_V2.2$, I show that the block of inhibition is disrupted; inhibition by the slow pathway is rescued. These findings further support my model that the palmitoyl groups of $Ca_V\beta2a$ normally reside in a specific location that overlaps with the slow pathway inhibitory site on $Ca_V2.2$. Lastly I present data showing that the enhancement of N-current, observed when palmitoylated $Ca_V\beta2a$ is present, occurs via the slow pathway.

In Chapter V the effect of $Ca_V\beta$'s orientation on N-channel modulation by the dopamine D2 receptor is tested. In this form of modulation, inhibition is rapid and voltage-dependent. The signaling pathway is membrane-delimited since $G\beta\gamma$, released after receptor stimulation, directly interacts with the N-channel at a site that overlaps with a high affinity binding site for $Ca_V\beta$s. While N-currents are modulated by this pathway, the deletion mutants show aberrant membrane-delimited modulation. The findings in this chapter further underscore the importance of proper positioning of $Ca_V\beta$ to $Ca_V2.2$ for eliciting proper N-current modulation after GPCR stimulation.

Overall, the data presented in this dissertation provides a mechanistic approach into examining modulation of N-current by different GPCRs via two different signaling pathways as well as the role $Ca_V\beta$ subunits serve in each modulatory pathway.

TABLE OF CONTENTS

LIST OF FIGURES

LIST OF FIGURES (continued)

LIST OF FIGURES (continued)

ACKNOWLEDGEMENT OF CONTRIBUTION OF CO-AUTHORS

Chapter III: The data collected using substance P are my contributions to this chapter. The experiments using Oxo-M were performed jointly by Lee Stanish and Dr. John Heneghan. The data using SCG neurons were collected by Dr. Liwang Liu.

Chapter IV: The BIFC images were obtained by Dr. Iuliia Vitko and Dr. Edward Perez-Reyes at University of Virginia.

Chapter V: Data in Figures 5.3 and 5.5 were collected by Dr. Iuliia Vitko and Dr. Edward Perez-Reyes at University of Virginia.

CHAPTER I:

BACKGROUND

A. Introduction

One in five people worldwide suffer from pain at any given time (Lewis, 2005). The American Pain Foundation estimates that 1 in 4 patients with pain are undertreated. In spite of intense research directed towards understanding the mechanisms underlying pain and analgesia, much remains unclear. My research aims at understanding the basic mechanism by which an ion channel is modulated by a neuropeptide with possible implications in pain perception. The N-type calcium channel (N-channel), which when pharmacologically blocked, relieves pain and its modulation by the neuropeptide substance P (SP) which mediates transmission of pain, are the key players of my thesis. During the course of my research, I have found that modulation of N-channel activity not only involves physical interactions between the channel and its accessory subunit, but the relative orientation between the two interacting subunits is also important for channel modulation.

B. Brief overview of pain perception

Pain is caused by intense stimuli (thermal, mechanical or chemical) from the environment, which generates signals at the site of insult in the periphery and visceral

organs that travel to the brain. These noxious signals are transmitted by small diameter, Aδ and C nerve fibres: the Aδ fibres are myelinated whereas the C fibres are unmyelinated (Kandel et al., 2000). These primary afferent nociceptive neurons have their cell bodies in the dorsal root ganglion (DRG), contain the neuropeptide SP (Lawson, 2002), and terminate predominantly in laminae I and II of the dorsal horn of the spinal cord (Todd, 2002) (Fig 1.1). Thus, the synapse between the DRG and the dorsal horn of the spinal cord forms the first synapse in the pain pathway.

Pain may be described as chronic, "neuropathic" pain or nociceptive, "inflammatory" pain. Chronic pain following traumatic nerve injury or associated with diabetes or with neuropathies is characterized by hyperalgesia (increase in the pain elicited by a noxious stimulus) (Abdulla et al., 2003). Nociceptive pain is an acute response generated by the activation of nociceptors by painful stimuli (Millan, 1999). Both types of pain are characterized by hypersensitivity at the site of damage and in adjacent normal tissue. Hypersensitivity due to inflammatory pain usually diminishes once the disease process is controlled. In contrast, neuropathic pain persists long after the initiating event has healed; it is considered a pathological state of the nervous system. Stimulation of G-protein coupled receptors (GPCRs) and tyrosine-kinase receptors cause parallel activation of numerous intracellular kinases such as protein kinase A, protein kinase C and mitogen activated protein kinase (MAPK). These kinases in turn cause altered modulation of ion channels ultimately leading to facilitation in excitatory synaptic output of dorsal horn neurons (Woolf and Salter, 2000; Abdulla et al., 2003).

C. Substance P mediates pain signaling

SP was the first peptide identified in the mammalian tachykinin family. Originally identified in 1931 by Von Euler and Gaddum and later purified (Chang and Leeman, 1970; Chang et al., 1971), its peptide structure was identified as H-Arg-Pro-Lys-Pro-Gln-Gln-Phe-Phe-Gly-Leu-Met-NH_2 (Carraway and Leeman, 1979). Neurokinin A (NKA) and Neurokinin B (NKB) are two additional tachykinin family members that were identified more recently (Kangawa et al., 1983; Kimura et al., 1984; Nawa et al., 1984). SP and NKA are encoded by the preprotachykinin-A (PPT-A) gene (Almeida et al., 2004). NKB is the only known sequence encoded by PPT-B. The three tachykinin receptors, NK-1R, NK-2R and NK-3R, recognize all three tachykinins, although SP, NKA and NKB exhibit preferential binding to NK-1R, NK-2R and NK-3R respectively (Mussap et al., 1993). SP serves as the principal neurotransmitter that mediates pain signaling. In response to nociceptive stimulation, SP is released from nociceptive DRG neurons onto dorsal horn neurons (Fig 1.2) which express NK-1R (Cheunsuang et al., 2002) as well as N-channels (Yaksh, 2006) .

NK-1R has seven transmembrane domains and is G_q-coupled (Macdonald et al., 1996). It was considered a putative drug target for pain, emesis and wound healing because its activation by SP is involved in diverse functions such as transmission of painful stimuli, neurogenic inflammation, smooth muscle contraction, secretion and activation of the immune system (Ulfers et al., 2002). Activation of NK-1R is associated with depression and anxiety; blocking NK-1R, either pharmacologically or by generating

knock-out mice, causes behavioral and physiological effects associated with anti-depressant and anxiolytic behavior (Santarelli et al., 2002).

D. Voltage-gated calcium channels

Voltage-gated Ca^{2+} channels are the fastest Ca^{2+} signaling proteins (Clapham, 2007) regulating numerous cellular processes in every organism (Hille, 2001). Ca^{2+} currents were first identified by Paul Fatt and Bernard Katz in crustacean muscle where they observed generation of action potentials in Na^{+}-free medium (Fatt and Katz, 1953). The first evidence that cells express more than one type of Ca^{2+} channel came from electrophysiological studies on starfish eggs (Hagiwara et al., 1975). Subsequently, currents in mammalian sensory neurons were divided into two categories. Carbone and Lux first used the term low- and high-voltage activated (LVA and HVA) channels to describe these two components (Carbone and Lux, 1984, 1987). The HVA are further classified into L-type for "Long lasting", N-type for "Non-L and non-T" (Nowycky et al., 1985), P-type for "Purkinje cell" (Llinas et al., 1989)/Q-type for "cerebellar granule cells" and R-type for channels giving rise to a "Residual" current (Randall and Tsien, 1995). The T-type calcium channels for "Transient" and "Tiny" were identified as LVA since they activated at negative voltages (Nowycky et al., 1985). We now know that at least 10 different genes encode Ca^{2+} channels (Catterall et al., 2005), which are classified into three subfamilies, Ca_V1, Ca_V2 and Ca_V3, based on their amino acid sequence homologies (Fig 1.3).

E. Structure of the α1 subunit

Initial purification studies and later biochemical analyses identified α1, β, γ and $\alpha_2\delta$ subunits as part of the Ca^{2+} channel complex (Fig 1.4) (Yang et al., 1993; Catterall et al., 2005). The α1 subunit forms the pore of the channel and is found in association with auxillary subunits- intracellular β, a disulfide-linked α2δ and a transmembrane γ subunit (Catterall, 2000; Arikkath and Campbell, 2003). The α1 subunit $Ca_V1.1$ was first cloned from rabbit skeletal muscle (Tanabe et al., 1987). Analysis of hydrophobic and hydrophilic amino acids suggest that similar to the Na^+ channel, the α1 subunit of the Ca^{2+} channel is organized in four internal repeat domains (I-IV) (Noda et al., 1984) that are connected by intracellular loops (Fig 1.4). The domains are equivalent to one subunit of K^+ channels. The intracellular loops or linker regions are targets for phosphorylation as well as binding sites for regulatory proteins discussed later.

Each domain or subunit consists of six hydrophobic transmembrane segments (S1 - S6). The bacterial K^+ channel K_{csa} has been crystallized providing insight into the organization of how the four subunit regions form the selectivity pore (Doyle et al., 1998). The membrane-associated loop between segments S5 and S6 consist of four highly conserved glutamate residues that form the selectivity filter of the channel. The pore region determines ion conductance and selectivity. S6 segments span the membrane at an angle in such a way that they are separated from one another at the outer pore region, but cross one another as they emerge from the inner membrane leaflet forming the helix cross bundle (Doyle et al., 1998).

Extensive mutagenesis studies (MacKinnon, 1991) as well as crystal structures of a chimeric voltage-gated K^+ channel (Long et al., 2005) have provided a general picture of how voltage-gated ion channels are topologically organized and suggest what regions of the channel give rise to the "gates" for opening and inactivation. The S4 segment consists of positively charged residues that appear to serve as the voltage sensor. S4 appears to move during depolarization allowing the channel to transition from the closed to the open state (Liman et al., 1991; Jiang et al., 2003). The movements of S4 appear coupled to flexing of S6. Slow forms of inactivation also involve S6 though are not well understood. While few of these details have been confirmed in Ca_V channels, their sequence homology indicates that their biophysical properties arise due to a similar structural organization.

F. Structure of the β subunit

The $Ca_V\beta$ subunit is a 55 kDa cytosolic accessory subunit of the Ca^{2+} channel (Fig 1.4). There are four different $Ca_V\beta$ subunit genes: β1- β4 and alternative splicing gives rise to additional variants (Pragnell et al., 1991; Perez-Reyes et al., 1992; Castellano et al., 1993a, 1993b; Birnbaumer et al., 1998). All $Ca_V\beta$ subunits are found in the brain (Birnbaumer et al., 1998). Among the different β subunits, β2a is uniquely palmitoylated on its N-terminus at residues Cys3 and Cys4 (Chien et al., 1996). Palmitoylation occurs post-translationally and is achieved by reversible esterification of cysteine-thiol groups with a 16-carbon palmitate (Mumby, 1997; Chien et al., 1998). Addition of palmitate groups to protein substrates is catalyzed by palmitoyl acyl transferases (Resh, 2006). Although palmitoylation of proteins usually serves to influence membrane targeting or

subcellular localization of the modified proteins (Resh, 2006), both palmitoylated as well as non-palmitoylated $Ca_V\beta$s show plasma membrane association (Chien et al., 1998). Whether palmitoylation serves additional roles involving either the $Ca_V\beta$2a or the α1 subunit will be discussed later.

The amino acid structure of $Ca_V\beta$ subunits contains five domains (D1-D5). The N-terminal D1, middle D3 and C-terminal D5 regions are highly variable while D2 and D4 are highly conserved (Birnbaumer et al., 1998). The D2 and D4 regions are homologous to *src* homology 3 (SH3) and guanylate kinase (GK)-like motifs respectively. These two domains establish a resemblance between $Ca_V\beta$s and the membrane-associated guanylate kinase (MAGUK) family of proteins raising the possibility that these domains could interact with other proteins, including calcium channel α1 subunits. Unlike canonical SH3 domains, $Ca_V\beta$'s SH3 domain contains a long and flexible HOOK region which is also known to mediate protein-protein interactions with similar sites on the PSD95 family of proteins. Except for the 13- amino terminal residues, this HOOK region is variable in both length and amino acid sequence between different $Ca_V\beta$ family members (Chien et al., 1998; Hanlon et al., 1999; Chen et al., 2004; Opatowsky et al., 2004; Van Petegem et al., 2004).

$Ca_V\beta$s bind the α1 subunit between domains I and II (I-II linker) at a sequence of residues called the α-interacting domain (AID) (Pragnell et al., 1994) thereby masking an endoplasmic retention site. This interaction enhances membrane expression of Ca^{2+} channels (Bichet et al., 2000) and was earlier proposed to occur via the amino terminus of $Ca_V\beta$'s D4 domain, referred to as β-interaction domain (BID) (De Waard et al., 1994).

However, crystallography studies later showed that the BID is crucial for the association of the SH3 with the GK domains, but the AID binds to the $Ca_V\beta$ at a hydrophobic pocket in the GK domain near to but distinct from the BID (Chen et al., 2004; Opatowsky et al., 2004; Van Petegem et al., 2004). A key point here is that the crystallography studies were performed using a $Ca_V\beta$ core protein that did not include the N-terminal amino acid residues, hence information regarding positioning of the palmitoyl groups is lacking. Depending on the $Ca_V\beta$ subunit co-expressed with the channel protein, $Ca_V\beta$ also affects the cellular distribution of channels (Brice and Dolphin, 1999) as well as their sensitivity to pharmacological antagonists (Hering, 2002). To understand the clinical importance of $Ca_V\beta$ subunits in affecting the binding of drugs to channels, it is important to know how $Ca_V\beta$ affects the channel's activity. $Ca_V\beta$ subunits modify the channel's biophysical properties such as channel opening, inactivation and inhibition by $G_{\beta\gamma}$ proteins (Birnbaumer et al., 1998). Besides these known functions, the role of $Ca_V\beta$ in modulation of $Ca_V2.2$ currents via two different pathways will be discussed in Chapters III, IV, and V of my thesis.

G. Structure of the $\alpha_2\delta$ subunit

Four known genes that undergo splicing encode $\alpha_2\delta$ subunits. α_2 and δ proteins arise from the same gene where the gene product undergoes post-translational proteolytic cleavage that separates α_2 from the δ subunit. Molecular weight of $\alpha_2\delta$ subunits varies between 160 to 200 kDa. While both α_2 and δ are highly glycosylated, α_2 is located extracellularly and linked by disulfide bonds to the δ subunit located in the plasma membrane (Fig 1.4). $\alpha_2\delta$-1 subunit is ubiquitously expressed; $\alpha_2\delta$-2 and $\alpha_2\delta$-3 are found

in neurons in the brain and $\alpha_2\delta$-4 is found in non-neuronal cells (Klugbauer et al., 2003; Davies et al., 2007). All calcium channels have an $\alpha_2\delta$ co-expressed with them. The $\alpha_2\delta$ subunit increases current amplitude by an undefined mechanism and is a target for binding by analgesic drugs such as gabapentin (Davies et al., 2007).

H. Structure of the γ subunit

The γ subunit is a 33 kDa transmembrane subunit. Unlike the other subunits, it does not affect membrane expression of channels nor does it affect the structural or functional integrity of the channels. This subunit has also been found associated with AMPA receptors (Sharp et al., 2001). The status of this protein serving as a calcium channel subunit rather than some other, more general function remains unresolved. Hence, this subunit was not included in our expression system and will not be further discussed.

I. N-type ($Ca_V2.2$) calcium channel

N-type calcium channels or N-channels belong to the high voltage-activated class of calcium channels. N-currents were first identified in chick dorsal root ganglion using whole-cell and single-channel recording techniques (Nowycky et al., 1985). N-channels are blocked by a toxin, ω-conotoxin GVIA, isolated from the cone shell mollusc *Conus geographus* (McCleskey et al., 1987; Plummer et al., 1989). This pharmacological tool aided in cloning N-channels from rat brain tissue and cell lines (Dubel et al., 1992). $Ca_V2.2$ undergoes alternative splicing in the I-II linker, II-III linker, S3-S4 extracellular linker and carboxy terminus giving rise to multiple tissue- and developmentally specific

variants. These variants differ in their activation and inactivation kinetics (Lin et al., 1996; Ghasemzadeh et al., 1999; Lin et al., 1999; Lu and Dunlap, 1999; Pan and Lipscombe, 2000; Bell et al., 2004; Lin et al., 2004; Gray et al., 2007). One splice variant is associated with pain transmission since it is specifically expressed in nociceptive DRG neurons that respond to capsaicin (Bell et al., 2004). Hence N-channel antagonists such as ω-conotoxin GV1A and ω-conotoxin-MVIIA have been used therapeutically for pain relief (Snutch, 2005).

Calcium influx through N-channels regulates closely associated ion channels, such as calcium-activated K^+ channels (Wisgirda and Dryer, 1994), activates specific enzymes (Rittenhouse and Zigmond, 1999), initiates neurotransmitter release from nerve endings (Hirning et al., 1988) and triggers gene transcription (Brosenitsch and Katz, 2001; Zhao et al., 2007). In turn, a number of GPCRs modulate N-channels via different pathways. Multiple GPCRs couple neurotransmitter release to membrane excitability by regulating the opening and closing of N-channels. Different modulatory pathways activate different classes of G-proteins. While all G proteins involve α, β and γ subunits, they are distinguished on the basis of their sensitivity to pertussis toxin (PTX) or cholera toxin (Hille, 1994; Zhu and Ikeda, 1994). While cholera toxin prevents the G_α-bound GTP from converting into GDP so that the G protein remains in the active state, PTX prevents release of GDP from the G_α so that the G protein remains in the inactive state. Following receptor coupling to specific G proteins, signaling can then diverge; some pathways are well characterized while some remain incompletely understood and will be discussed in this thesis.

J. Modulation of N-channels by GPCRs via the membrane-delimited pathway

Inhibition of voltage-gated Ca^{2+} currents by GPCRs in neurons (Reuter, 1974) was first described by Dunlap and Fischbach where application of norepinephrine on chick DRG neurons reduced the contribution of Ca^{2+} currents to the action potentials (Dunlap and Fischbach, 1978, 1981). Numerous other studies showed similar inhibition of native Ca^{2+} currents by other GPCRs (Tedford and Zamponi, 2006). Transmitter-mediated inhibition of Ca^{2+} was blocked by pre-treatment of DRG cultures with PTX or dialyzing cells with GDP-β-S. GDP-β-S competes with GTP for binding to the guanine-nucleotide site on G-proteins thus antagonizing their activation following transmitter binding to receptor. These initial experiments implicated PTX-sensitive $G_{i/o}$-proteins in this form of Ca^{2+} current inhibition (Holz et al., 1986).

Subsequently, this form of inhibition was defined as membrane-delimited. This nomenclature was adopted because current inhibition did not occur when the Ca^{2+} channels were isolated in a cell-attached patch and the agonist applied to the bath. This observation indicated that inhibition must occur due to tight receptor-channel coupling rather than by indirect diffusible mediators (Forscher et al., 1986; Hille, 1994). Activation of GPCRs causes dissociation of the heterotrimeric complexes of Gαβγ subunits into Gα-GTP and Gβγ both of which serve as rapid signaling components. Isoprenylation of Gγ's C-terminus facilitates membrane association of Gβγ (Resh, 2006; Tedford and Zamponi, 2006).

During membrane-delimited inhibition of Ca^{2+} currents, application of neuro-transmitters shifts the channels' voltage-sensitivity whereby the channels require a more

positive membrane voltage before opening (Dunlap and Fischbach, 1978; Bean, 1989). There is no obvious change in the number of functional channels. Bean (1989) presented a model of membrane-delimited inhibition where N-channels exist in “willing” or “reluctant” modes in the absence or presence respectively of a neurotransmitter. The “willing” mode describes channels that are willing to open in response to moderate depolarizations. The “reluctant” mode describes channels that are reluctant to open; larger depolarizations are required for the channels to open. In the presence of neurotransmitters, activation of GPCRs shifts most N-channels to the “reluctant” mode while a large depolarization is required for channel opening. The voltage-dependence of this modulation, elicited by membrane-delimited inhibition by neurotransmitters or internal dialysis with GTP-γS, was elegantly revealed by Elmslie et al. (1990) using a novel voltage protocol (Fig 1.5A). A large depolarizing “prepulse”, also referred to as the “facilitating prepulse” relieved reluctant gating in a subsequent test pulse that followed within ms of the prepulse (Elmslie et al., 1990). Membrane-delimited inhibition was later reconstituted in a recombinant system and a series of depolarizations mimicking an action potential could relieve the inhibition (Brody et al., 1997) reinforcing the physiological relevance of this inhibition during trains of action potentials.

Re-inhibition rapidly occurs after prepulse facilitation. Its dependence on the concentration of activated G-proteins suggested that G-proteins might directly bind to channels (Lopez and Brown, 1991). However, which subunit of the G protein and where on the channel it might bind remained unresolved for a number of years. Definitive evidence that Gβγ-mediated inhibition was provided by two back-to-back publications in

Nature. These papers showed that intracellular dialysis or over-expression of Gβγ subunits mimicked voltage-dependent, membrane-delimited inhibition, whereas over-expression of Gα had no effect (Herlitze et al., 1996; Ikeda, 1996). Three sites of interaction of Gβγ with the channel have so far been described: the AID region on the I-II linker (Pragnell et al., 1994; De Waard et al., 1997; Zamponi et al., 1997), the carboxy cytoplasmic tail (Qin et al., 1997) and the N-terminus (Zhang et al., 1996; Page et al., 1998; Canti et al., 1999), which physically interacts with the I-II linker to promote Gβγ mediated inhibition (Agler et al., 2005).

Phosphorylation by protein kinase C blocks membrane-delimited inhibition (Swartz, 1993; Swartz et al., 1993) apparently by preventing G protein subunits from binding to the channel (Fig 1.5C). PKC phosphorylation sites exist on the I-II linker of N-channels in close proximity to where Gβγ bind (Hamid et al., 1999). However in mutational studies, additional phosphorylation sites were identified on the II-III linker (Kamatchi et al., 2004). These studies underscore the difficulties in attempting to deconstruct membrane-delimited modulation.

The “willing” (Gβγ-free) and “reluctant” (Gβγ-bound) states of calcium channels can also be observed at the single channel level where with a moderate depolarization, an increased first latency to open gives rise to slowed activation kinetics of whole-cell currents (Tedford and Zamponi, 2006). Transition between the reluctant and willing states was also proposed to occur via binding of phosphatidylinositol-4,5-bisphosphate (PIP_2), to a particular low-affinity “R” (reluctant and regulatory) site (Wu et al., 2002;

Michailidis et al., 2007). How this translates into voltage-dependent inhibition is not clear at the moment but will be discussed later.

Not surprisingly, $Ca_V\beta$ subunits influence membrane-delimited inhibition. Using antisense to deplete $Ca_V\beta$ subunits in DRG neurons results in significantly increased membrane-delimited inhibition of currents following activation of $GABA_B$ receptors (Campbell et al., 1995). This finding suggests possible antagonism of membrane-delimited inhibition by $Ca_V\beta$. While co-expression of $Ca_V\beta$ with the channel increases current amplitude, accelerates activation kinetics and shifts the activation curve towards hyperpolarizing potentials, $G\beta\gamma$ causes the reverse: current inhibition, slowed activation kinetics and an activation curve shifted towards more depolarizing potentials. Moreover, during membrane-delimited inhibition, the kinetics of activation slow to different extents, depending on the subtype of $Ca_V\beta$ subunit co-expressed with the channel. For example, when $Ca_V\beta2a$ is co-expressed, modulated currents exhibit the slowest activation kinetics compared to the other $Ca_V\beta$ subunits (Bourinet et al., 1996). In the presence of overexpressed $G\beta\gamma$, relief from membrane-delimited inhibition also varied, depending on the type of $Ca_V\beta$ present (Feng et al., 2001). The binding site of $Ca_V\beta$ on the AID overlaps with a binding site for $G\beta\gamma$ further suggesting a role for $Ca_V\beta$ in membrane-delimited inhibition (Pragnell et al., 1994; Chen et al., 2004; Opatowsky et al., 2004; Van Petegem et al., 2004). Evidence based on work done by numerous labs point towards a role of $Ca_V\beta$ subunits in membrane-delimited inhibition but whether $Ca_V\beta$ subunits antagonize or support membrane-delimited inhibition remains unresolved. In Chapter V, I

present data that provides new information that the orientation $Ca_V\beta$ subunits is critical for prepulse facilitation of currents inhibited by the membrane delimited pathway.

K. Modulation of N-channels by the slow pathway

Another pathway that mediates inhibition of N-current is the slow pathway distinguished from the fast, membrane-delimited pathway by the involvement of PTX-insensitive G-proteins and second messengers (Hille, 1994). Modulation of N-channels by the M_1 muscarinic receptor (M_1R) was originally described as PTX- and voltage-insensitive (Wanke et al., 1987; Beech et al., 1992) and involving the Ca^{2+}-sensitive enzyme phospholipase C (PLC) (Liu and Rittenhouse, 2003a). Slow pathway modulation of N-current is disrupted when high concentrations of bis(O-aminophenoxy)ethane-N, N, N',N'-tetraacetic acid (BAPTA) (Beech et al., 1991; Mathie et al., 1992) is dialyzed into cells. N-channels, isolated in a cell-attached patch, remain sensitive to modulation by the M_1R agonist indicating a diffusible second messenger pathway must mediate inhibition (Bernheim et al., 1991; Mathie et al., 1992; Hille, 1994). Our laboratory has identified arachidonic acid (AA) as a potential diffusible signaling molecule mediating N-current inhibition by M_1Rs (Liu and Rittenhouse, 2003a). However, the identity of the final effector molecule mediating N-current inhibition remains a controversy in the field (Michailidis et al., 2007). Data in Chapters II and III support the notion that a free fatty acid such as AA mediates slow pathway inhibition of N-current.

L. Modulation of N-current by PIP_2

The inhibition of N-current by M_1Rs has been proposed to occur by an analogous pathway that mediates modulation of a voltage-gated potassium current called M-current (Hille, 1994). According to this hypothesis, N-current is modulated by PIP_2, a substrate of the enzyme PLC (Fig. 1.7). Stimulation of G_qPCRs activates PLC, which then catalyzes the release of inositol triphosphate (IP_3) from PIP_2. These observations have been taken to indicate that breakdown of PIP_2 near the activated G_qPCRs causes a local membrane gradient that leads to depletion of PIP_2 from the membrane around the channels thereby inhibiting current (Hille, 1994; Delmas and Brown, 2005; Delmas et al., 2005).

Evidence for involvement of PIP_2 in Ca^{2+} channel modulation was put forward by two groups. The first group observed $Ca_V2.1$ currents by expressing P/Q channels in the *Xenopus* oocyte expression system. Reduction in peak current or "rundown" occurred within minutes after excising a patch from the cell membrane (Wu et al., 2002). Current rundown was slowed by exogenous application of PIP_2 to the cytosolic side of the membrane and accelerated by sequestering PIP_2 with antibodies. Application of PIP_2 caused a positive shift in the activation curve of the channels thereby affecting the voltage-dependence of activation of the channels. This led the authors to propose that PIP_2 binds to two sites on the channel, an S (for stabilization) site that promotes channel availability, stabilizing current and an R (for reluctant and regulatory) site that shifts channels into a reluctant gating mode with characteristics similar to channels inhibited by the membrane-delimited pathway, discussed earlier. The second group measured whole-

cell and perforated-patch N-current in SCG neurons. They recapitulated the finding that exogenous application of PIP_2 prevents current rundown (Gamper et al., 2004). The authors also showed that when SCG neurons were dialyzed with the water-soluble PIP_2 analog, diC8-PIP_2, M_1R activation no longer inhibited Ca^{2+} currents. However, this may not be so surprising since the diC8-PIP_2 does not have an AA moiety that could be released for mediating N-current modulation. Usually, PIP_2 consists of an AA moeity at its *sn*-2-position that is liberated by phospholipase A_2. The released AA not only serves as a precursor for signaling molecules that mediate immune response but also for generating endocannabinoids that play a role in regulating function of ion channels (Sugiura et al., 2002) This study also reported that when re-synthesis of PIP_2 is blocked using high concentrations of wortmannin, modulation by M_1Rs does not reverse. These data support a model for inhibition where PIP_2 is required for N-current inhibition by M_1Rs.

Whether loss of PIP_2 is sufficient for current inhibition remains unresolved since additional metabolites and downstream targets of PIP_2 were only superficially examined for participation in the slow pathway. Moreover, the locations of PIP_2's modulatory sites remain unidentified although it is highly likely that at least one of the sites exists on the channel subunit.

M. Working model for N-current inhibition by G_qPCRs

Modulation of N-current by M_1R requires specific events downstream of phospholipid hydrolysis and is distinct from modulation of M-currents. First, M_1R activation enhances N-current at negative potentials and inhibition of N-current at

positive potentials; this pattern of modulation is remarkably mimicked by exogenous application of AA in SCG neurons (Liu et al., 2001; Liu and Rittenhouse, 2003a). Second, when bovine serum albumin (BSA) is used to sequester free fatty acids liberated upon M_1R activation in the extracellular medium, N-current inhibition by M_1Rs is lost. Third, dialyzing BSA into SCG neurons causes loss of inhibition by AA without affecting N-current enhancement, indicating that inhibition and enhancement are distinct events that occur at two different sites of action (Barrett et al., 2001). Fourth, blocking the enzyme phospholipase A_2 (PLA_2) minimized inhibition by M_1Rs (Liu et al., 2004). Fifth, another by-product of phospholipid metabolism by PLA_2, lyosphosphatidic acid, when exogenously applied did not inhibit whole-cell N-current indicating the specificity of AA as a second messenger (Liu et al., 2004). Sixth, blocking the enzyme diacylgycerol lipase (DAGL) with a pharmacological antagonist minimized inhibition of N-current. In contrast, antagonists to PLA_2, DAGL or the presence of BSA had no effect on modulation of M-current (Liu et al., 2003; Liu et al., 2006; Liu et al., 2008) indicating N-current modulation is mediated by a signaling pathway that diverges from the pathway responsible for M-current modulation. The data support a model where inhibition of N-current requires a specific and probably sequential breakdown of phospholipids to release free AA that inhibits N-channel activity by acting at an inhibitory site.

A role of AA in modulating additional Ca^{2+} currents has also been observed. In the recombinant system AA modulates Ca_V3 currents (Zhang et al., 2000; Talavera et al., 2004; Chemin et al., 2007) as well as native and recombinant Ca_V1 currents (Xiao et al., 1997); Roberts-Crowley and Rittenhouse, submitted). PIP_2 and AA modulate voltage-

gated potassium channel activity where they produce opposite effects on channel inactivation; PIP_2 promotes channel availability whereas AA causes inactivation (Oliver et al., 2004). Thus similar actions of PIP_2 and AA occur across many channel types indicating a fundamental basic relevance of these two molecules for channel function.

Here in my thesis, I present data supporting role of the slow pathway in modulation of N-currents by another G_qPCR, the NK-1R (Chapter II). I have described the signaling components that are necessary for inhibition of N-current when SP activates NK-1Rs. The data support previous observations, reported in separate and unrelated studies, about phospholipid breakdown upon activation of NK-1R and phosphorylation of ERK1/2 in response to noxious stimuli. From a collaboration with Dr. John Heneghan, I present evidence that helps in understanding the mechanism of N-current modulation that was earlier seen by both activation of M_1R and exogenous AA application (Barrett et al., 2001; Liu et al., 2001; Liu and Rittenhouse, 2003a). Specifically, I show results that support a model where the palmitoyl groups of $Ca_V\beta$2a block N-current inhibition possibly by occupying an inhibitory site (Chapter III). That the location of the endogenous palmitoyl groups is important for modulation is supported by data showing that moving the palmitoyl groups of $Ca_V\beta$2a results in the appearance of current inhibition (Chapter IV). Earlier, I discussed that $Ca_V\beta$ is important for membrane-delimited inhibition of N-channel activity. In Chapter V, I present evidence that supports this observation and extends it further by showing that a specific orientation of $Ca_V\beta$ and $G\beta\gamma$ is required for membrane-delimited inhibition and its relief by facilitating prepulses.

In summary, a better understanding of N-current modulation by SP advances the field of pain therapy where discovery of new signaling molecules brings the possibility of developing new drugs to provide analgesia. A better understanding of the role of accessory subunits may help to detect anomalies in N-channel functioning where aberrant modulation may arise not from defects in the channel itself but from changes in expression or modification of accessory subunits. Overall, this study also shows possibility of a new role of protein palmitoylation.

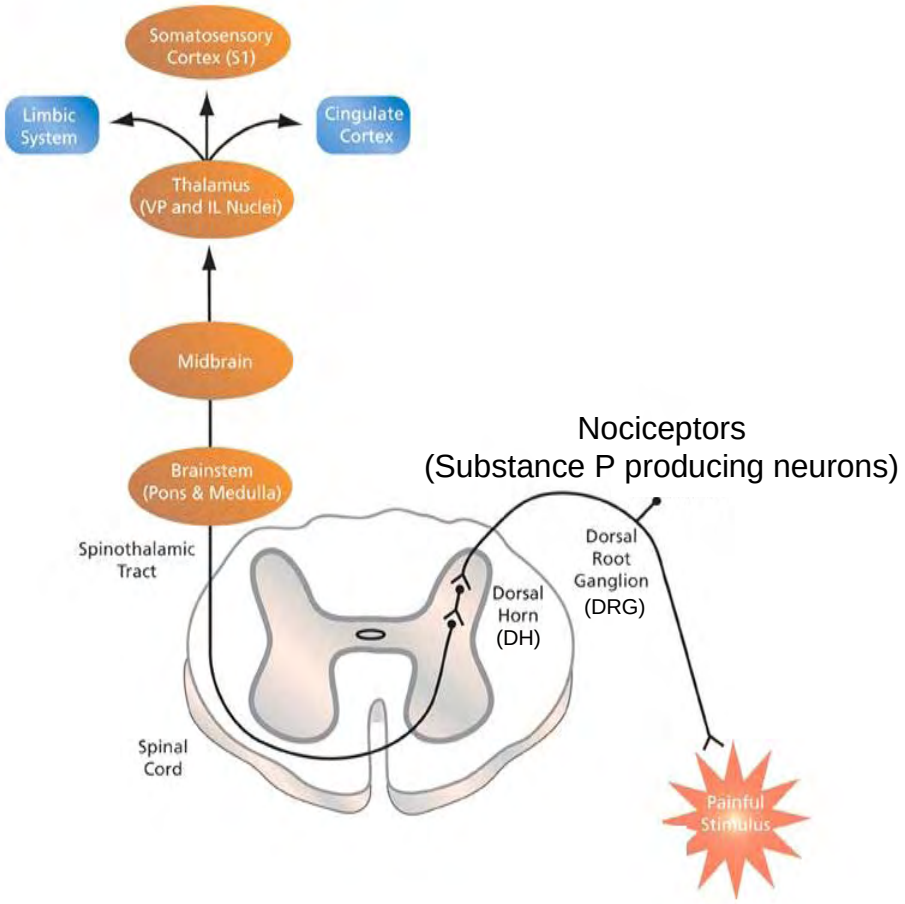

Adapted from:
http://www.sigmaaldrich.com/Area_of_Interest/Life_Science/Cell_Signaling/Key_Resources/Pathway_Slides__Charts/Ascending_Pain_Pathway.html

Figure 1.1 Diagrammatic representation of the ascending pain pathway. Painful signals are transmitted by the specialized nociceptive fibres that synapse onto the dorsal horn of the spinal cord. Efferent neurons carry nociceptive information via the spinothalamic tract to the higher centers for further processing.

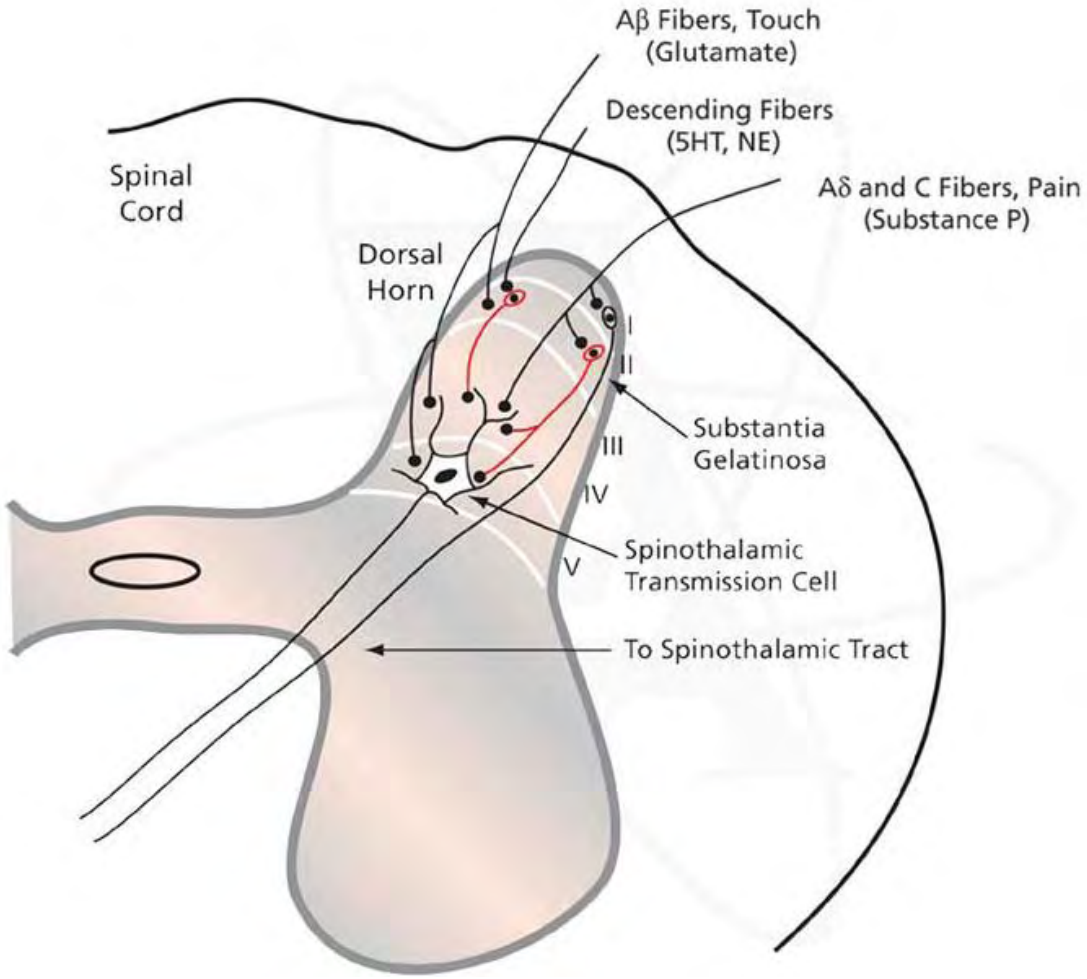

http://www.sigmaaldrich.com/Area_of_Interest/Life_Science/Cell_Signaling/Key_Resources/Pathway_Slides__Charts/Modulation_of_Pain_.html

Figure 1.2 The dorsal horn of the spinal cord receives nociceptive inputs from the Aδ and C-fibres. The nociceptive dorsal horn neurons give rise to efferent fibres which decussate and course upwards in the ascending spinothalamic tract.

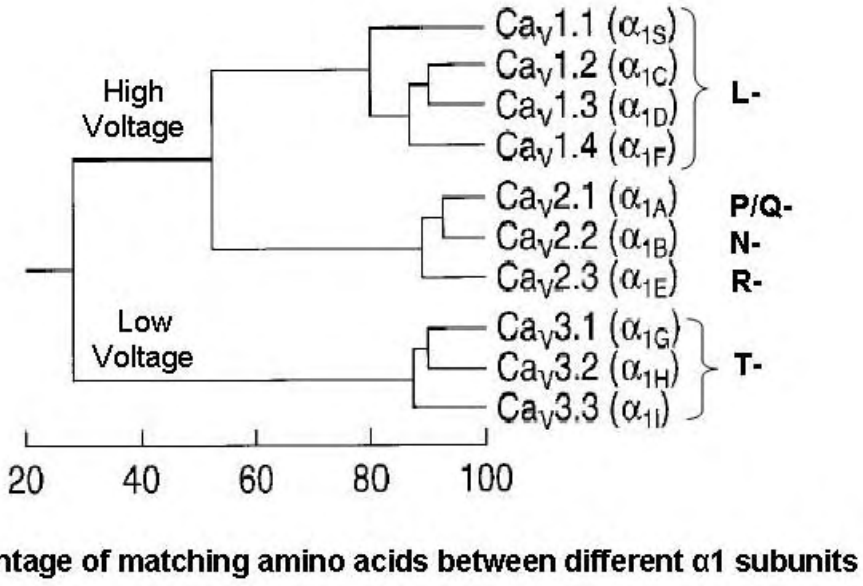

Figure 1.3 Classification of voltage-gated calcium channels based on nomenclature. Comparison of ~350 amino acids from the transmembrane segments and pore loops reveals three subfamilies of calcium channels (Ca_V1, Ca_V2 and Ca_V3) with 80% homology in the sequence of the channels within each family. The high voltage-gated channels are Ca_V1 or L-, $Ca_V2.1$ or P/Q, $Ca_V2.2$ or N- and $Ca_V2.3$ or R-type channels. Ca_V3 channels belong to the low voltage-gated class of channels.

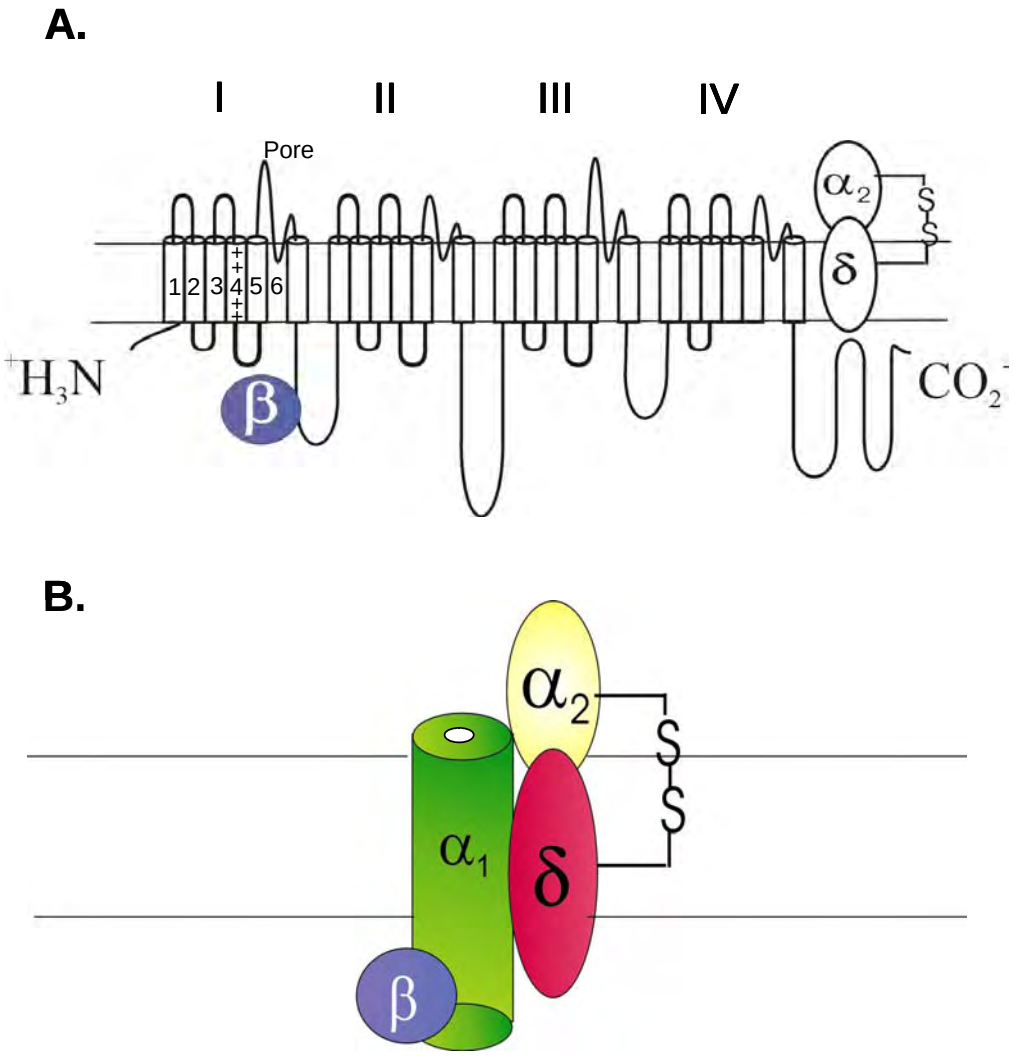

Figure 1.4 The voltage-gated calcium channel is a heteromeric complex of proteins. **(A)** The channel is organized into four domains; each domain consists of six membrane-spanning helices. The transmembrane $\alpha_2\delta$ subunit is linked by two disulfide bonds. The β subunit is cytoplasmic. The γ subunit is not shown. **(B)** An alternative view of the N-type calcium channel is shown in association with the $\alpha_2\delta$ and β subunits.

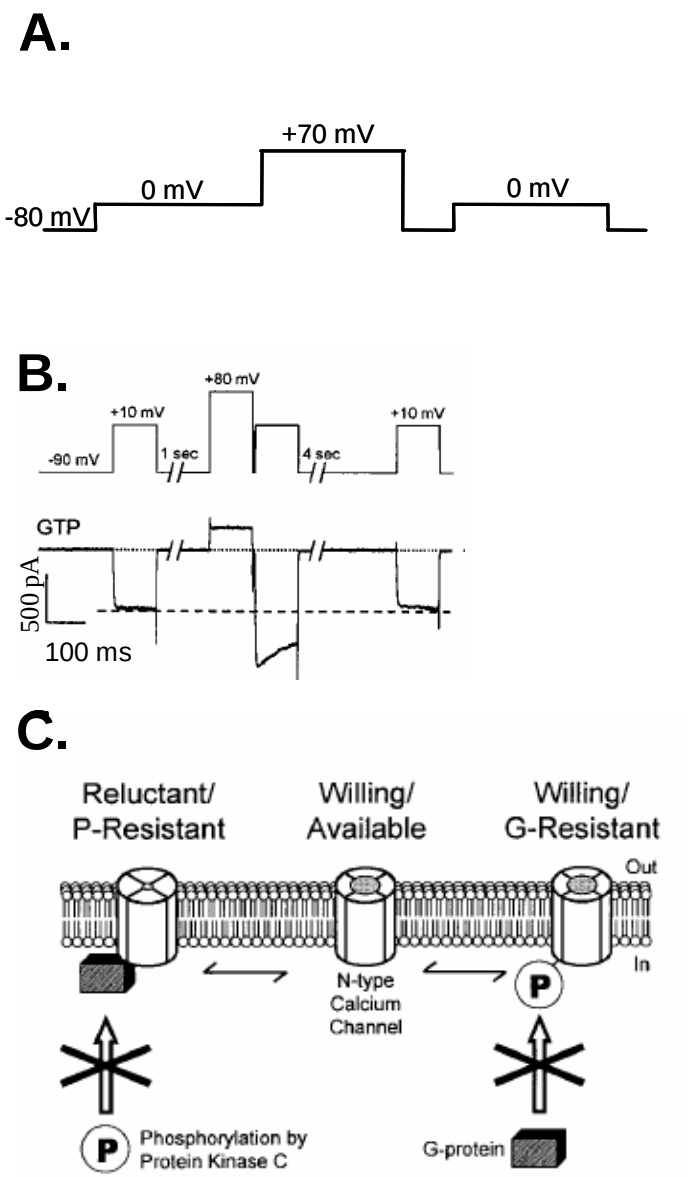

Adapted from Elmslie et al., 1990 and Barrett and Rittenhouse, 2000

Figure 1.5 Membrane-delimited inhibition of N-channel activity. **(A)** Prepulse protocol established by Elmslie et al., 1990 to relieve tonic inhibition of N-current. **(B)** Current traces demonstrating voltage dependent inhibition and its relief by a prepulse. **(C)** Model proposed by Barrett and Rittenhouse (2000) showing that both phosphorylated and dephosphorylated channels are "willing" to open, but only dephosphorylated channels can be bound by G-protein for voltage-dependent modulation.

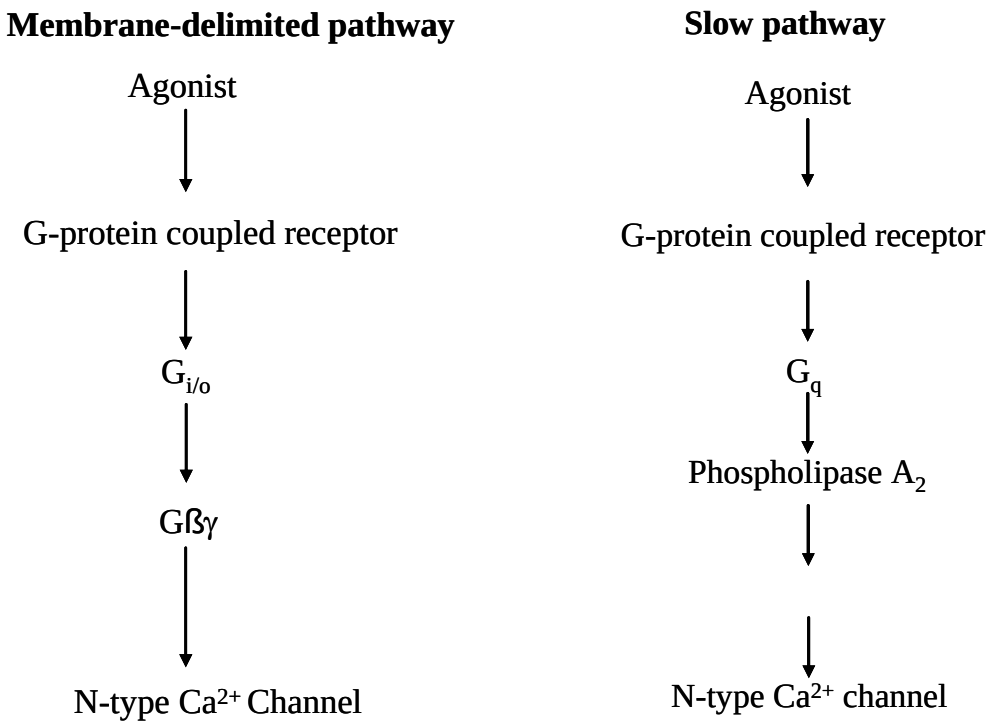

Figure 1.6 Comparison between the membrane delimited and the slow pathway. The membrane-delimited pathway involves inhibition of N type calcium channels by Gi/o-coupled receptors, while the slow pathway involves inhibition by Gq-coupled receptors.

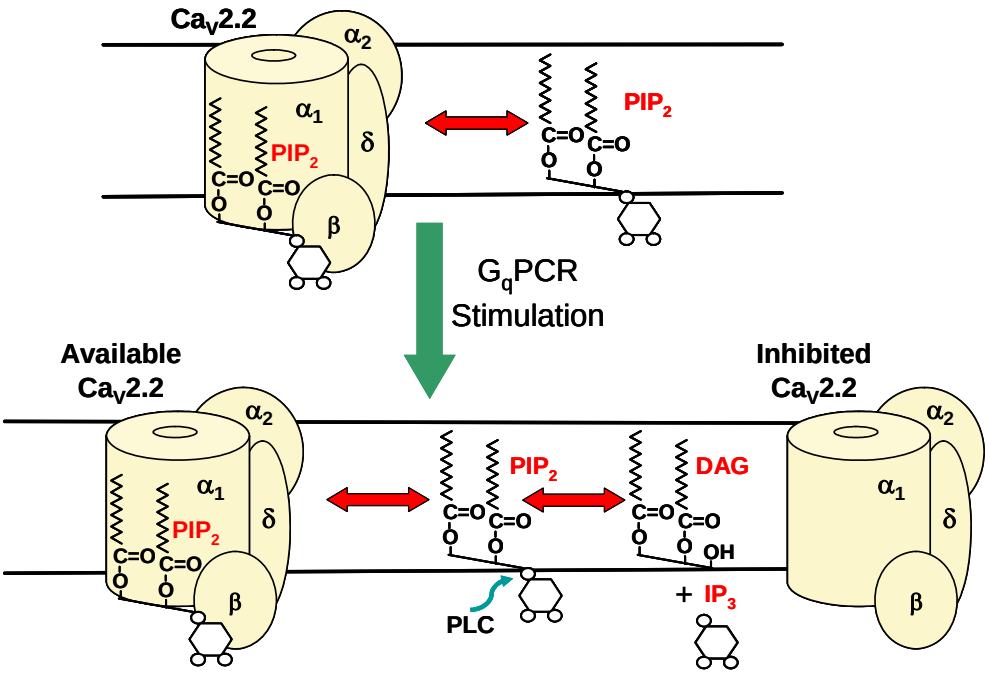

Figure 1.7 The PIP_2 model for inhibition of N-currents. The model proposes that a loss of PIP_2 from the channel causes current inhibition or "rundown".

CHAPTER II:

Modulation of voltage-gated N-type calcium channels by substance P involves lipids and proteins

ABSTRACT

Nociceptive stimulation from the periphery and visceral organs causes dorsal root ganglia neurons to release substance P (SP) onto the soma and dendrites of dorsal horn (DH) neurons. These DH neurons express tachykinin receptors (NK-1R) and N-type calcium channels (N-channels). SP, the principal neuropeptide mediating pain, binds to G_q-coupled NK-1Rs, resulting in N-current inhibition. Pharmacological blockers of N-channels are used as analgesics thus implicating N-channels in pain perception. Yet the complete mechanism by which SP modulates N-channel activity is unknown. G_q-coupled M_1 muscarinic receptors enhance and inhibit native N-current at negative and positive potentials respectively; arachidonic acid (AA) mimics this modulation. Here, by monitoring recombinant channel ($Ca_V2.2$, $\alpha_2\delta$-1 and $\beta3$) activity in HEKM1 cells using whole-cell patch clamp techniques, we show that N-current inhibition by SP is blocked in the presence of a pharmacological antagonist of phospholipase A_2 (PLA_2). This observation is consistent with the need for increased levels of free fatty acid in order to

observe inhibition. When bovine serum albumin (BSA) was used as a fatty acid scavenger to reduce the levels of free fatty acids, SP no longer inhibited N-current. Lastly, in the presence of U0126, a pharmacological blocker for ERK1/2, N-current inhibition by SP was lost. Taken togther, these findings indicate that activation of ERK1/2 and PLA_2 and breakdown of phospholipids are involved in N-current modulation by NK-1R. Thus our present study identifies for the first time the proteins downstream of G_q that mediate modulation of N-current by SP. Phospholipid metabolism involving PLA_2 is a key component mediating pain, inflammation and immune response. Hence, a better understanding of the function of molecules involved in mediating pain will help in designing better pharmacological targets for relieving pain

INTRODUCTION

Pain is caused by intense external stimuli (thermal, mechanical, or chemical) that stimulate sensory nerve activity. This electrical activity transmits the encoded pain sensation through a series of synapses to the brain. Substance P (SP), an 11-amino acid neuropeptide (Carraway and Leeman, 1979) of the tachykinin family, is the principal neurotransmitter that mediates pain. In response to nociceptive stimulation, SP is released from terminals of dorsal root ganglion (DRG) neurons onto dorsal horn (DH) neurons. These latter neurons express the G_q-coupled tachykinin NK-1 receptor (NK-1R) (Cheunsuang et al., 2002). SP is the preferred natural ligand for NK-1Rs (Macdonald et al., 1996).

N-channels appear to be an important target of SP signaling in DH neurons (Westenbroek et al., 1998; Yaksh, 2006). N-channels belong to a family of voltage-dependent Ca^{2+} channels that regulate Ca^{2+} entry into neurons. In animal pain models, loose ligation of the sciatic nerve causes upregulation of the expression of N-channels in the DH (Cizkova et al., 2002). Blockers of N-channel activity inhibit behavioral and neuronal responses to noxious stimuli (Malmberg and Yaksh, 1994; Diaz and Dickenson, 1997). Knockout mice, lacking the gene encoding N-channels, are less sensitive to neuropathic and inflammatory pain compared to wild-type (wt) mice (Hatakeyama et al., 2001; Saegusa et al., 2001). In addition to whole animal studies, SP inhibits N-current in DRG and superior cervical ganglion (SCG) neurons by an incompletely described pathway (Shapiro and Hille, 1993; Sculptoreanu and de Groat, 2003). While the DH is a key area of the spinal cord involved in mediating nociception (Yaksh, 2006), only a limited number of studies have focused on the role of N-channels in this region.

In SCG neurons, N-channels also undergo modulation by another G_q-coupled receptor, the M_1 muscarinic receptor (M_1R). N-current inhibition by M_1Rs involves a lipid-dependent pathway, called the slow pathway (Beech et al., 1992) where inhibition develops over the course of many seconds. This pathway involves phosphatidylinositol-4,5-bisphosphate (PIP_2) breakdown by phospholipase C (PLC) and subsequent release of arachidonic acid (AA) following activation of PLA_2, most likely the Ca^{2+}-dependent cytosolic PLA_2 ($cPLA_2$) (Liu and Rittenhouse, 2003a; Gamper et al., 2004; Liu et al., 2006). AA is found in the *sn*-2 position of membrane phospholipids. $cPLA_2$ preferentially hydrolyzes the *sn*-2 ester bond of arachidonate-containing phospholipids generating free

AA and lysophospholipid (Dennis, 1997; Balsinde et al., 2002). Treatment of cerebral cortical slices with SP produces a significant breakdown of phospholipids (Catalan et al., 1988), indicating possible involvement of these metabolites in downstream signaling following NK-1R activation. Whether phospholipid breakdown, induced by NK-1R activation, can modulate N-channel activity is not known.

Painful stimuli increases phosphorylation of an extracellular-signal-related protein kinase (ERK) (Ji et al., 1999). Phosphorylation by an upstream mitogen-activated protein kinase (MAPK)/ERK kinase (MEK) causes activation of ERK. In turn, ERK phosphorylates $cPLA_2$ at serine-505 (Lin et al., 1993). The MAPK/ERK pathway also appears to directly phosphorylate N-channels in DRG neurons, leading to current enhancement. This increase in current occurs on a time scale of minutes (Fitzgerald, 2000) compared to SP inhibition of N-current that occurs in seconds (Shapiro and Hille, 1993). Whether ERK participates in N-current inhibition by SP has not been tested.

Here we examined whether SP inhibits recombinant N-channels ($Ca_V2.2$) by a pathway similar to inhibition of N-channel activity by M_1Rs (Liu and Rittenhouse, 2003a) We show that activation of NK-1Rs by SP inhibits recombinant N-current in a concentration-dependent manner when $Ca_V2.2$ is co-expressed with the $\alpha_2\delta$-1 and β3 accessory subunits. Using a high concentration of BAPTA, a Ca^{2+} chelator, we show that N-current inhibition by SP is Ca^{2+}-sensitive. The inhibition is also significantly reduced in the presence of U0126 or oleyloxyethyl phosphorylcholine (OPC), pharmacological antagonists of ERK1/2 and PLA_2 respectively. U0126 inhibits the kinase activity of MEK thereby preventing phosphorylation of ERK by MEK. OPC is a competitive antagonist of

PLA_2 thereby blocking phospholipid breakdown by PLA_2. Sequestering free fatty acids by bath applying bovine serum albumin (BSA) during NK-1R activation also diminishes N-current inhibition. These data indicate that NK-1Rs modulate N-channel activity by a "slow" pathway similar to M_1Rs. For the first time, our data implicate ERK1/2 activity in the slow pathway, possibly upstream of PLA_2. This study has important implications for therapeutically manipulating pain transmission since it uncovers key signaling molecules that mediate inhibition of N-channels by NK-1R activation.

MATERIAL AND METHODS

Human embryonic kidney (HEK) cells with a stably transfected M_1R (HEK-M1) were grown at 37°C with 5% CO_2 in Dulbecco's MEM (DMEM)/F12 supplemented with 10% FBS, 1% G418, 0.1% Gentamicin and 1% HT supplement (Gibco Life Technologies, Grand Island, NY). For transfection, cells were plated in 12-well plates at 50-80% confluency. Cells were transiently transfected using Lipofectamine and PLUS reagents (Invitrogen, Carlsbad, CA) as per the manufacturer's instruction. The transfection mixture consisted of plasmids encoding $Ca_v2.2e[^a10$, $\Delta18a$, $\Delta24a$, 31a, 37b, 46] (#AF055477), $\alpha_2\delta$–1 (#AF286488;) and $Ca_V\beta3$ (#M88751) at a 1:1:1 molar ratio. 28ng/well of plasmid encoding NK-1R (#AY462098; UMR cDNA Resource Center, University of Missouri, Rolla, MO) and enhanced green fluorescent protein cDNA at less than 10% of the total cDNA were also included in the transfection medium. After 24-48 hours post transfection, cells were plated on poly-L-lysine coated coverslips for recording currents.

Electrophysiology

Whole-cell Ba^{2+} currents were recorded at room temperature (20-24°C) using a Dagan 3900a patch clamp amplifier (Dagan Instruments Inc., Minneapolis, MN). Currents were filtered at 1-5 kHz using the amplifier's four-pole low-pass Bessel filter and digitized at 20 kHz with a CED micro1401 interface (Cambridge Electronic Design, (CED), Cambridge, UK). Data were collected using Signal 2.16 (CED) and stored on a personal computer. Prior to analysis, capacitive and leak currents were subtracted using a scaled-up hyperpolarizing test pulse to -100 mV. For all recordings, cells were held at -90 mV and given a 100 ms depolarization to the test potential indicated. The protocol was repeated every 4 sec. Electrodes were pulled from borosilicate glass capillary tubes. Each electrode was fire-polished to ~1 μm to yield a pipette resistance of 2-3MΩ. The external solution contained (in mM): 125 NMG-aspartate, 10 HEPES and 5 barium acetate, pH was adjusted to 7.5 with CsOH. When the concentration of Ba^{2+} was lowered from 20 mM to 5 mM for recording $Ca_v2.2$ currents, 135 NMG-aspartate was substituted for Ba^{2+}. The internal solution of the pipette consisted of (in mM): 135 Cs-aspartate, 10 HEPES, 0.1 1,2-bis(O-aminophenoxy)ethane-N,N,N',N'-tetraacetic acid (BAPTA), 5 $MgCl_2$, 4 ATP, 0.4 GTP, adjusted to pH 7.5 with CsOH.

Pharmacology

SP was prepared as a 0.5mM stock solution in 0.05 M acetic acid and stored at -20°C. The stock was serially diluted with bath solution daily to a final working concentration of 5 or 250 nM. BSA (fraction V, heat shock, fatty acid ultra-free; Roche Applied Science,

Indianapolis, IN) was added directly to the bath solution yielding a final concentration of 1 mg/ml. OPC (CalBiochem, La Jolla, California) was prepared as a stock solution made up in 100% ethanol and diluted 1,000 times with bath solution for a final concentration of 10 μM. U0126 (Promega, Madison, Wisconsin) was made up in DMSO and diluted 10,000 times with bath solution to yield a final concentration of 10 μM. All chemicals were obtained from Sigma-Aldrich Inc. (St. Louis, MO) except where noted. Drugs were applied with a gravity-driven bath perfusion system and complete bath exchange was achieved within 10-14 sec.

Data analysis

After the onset of the test pulse, maximal inward current of whole-cell traces was measured using Signal 2.16 (CED) using a trough seeking function. Percent change in current amplitude was measured as [(I-I')/I]*100 where I is the average amplitude of peak current measured from 5 current traces prior to drug application. I' is the average current amplitude measured from 5 current traces at least 2 mins after application of SP, unless otherwise noted.

Statistical Analysis

Summary data are presented as mean ± s.e.m (standard error of the mean). Average current before and after application of SP was compared using a two-tailed paired *t*-test. Differences in inhibition were measured using a two-way Students *t*-test.

Statistical significance was set at *p<0.05 or **p<0.01. Data were analyzed using Excel (Microsoft, Seattle, WA) and Origin (OriginLab, Northampton, MA).

RESULTS

SP inhibits recombinant $Ca_V2.2$ current

In HEK-M1 cells, co-transfection of $Ca_V2.2$, $Ca_V\beta3$ and $\alpha_2\delta$-1 is necessary to elicit peak currents of at least 150 pA (n=3 cells per group; 3 groups were tested where in each group one subunit was absent from the tranfection medium; data not shown) indicating that the recorded currents arise from the transfected channel subunits and not from endogenous channel activity. We hypothesized that NK-1R activation by 250 nM SP will also inhibit $Ca_V2.2$ currents in HEK-M1 cells since SP causes N-current inhibition in SCG neurons via a voltage-independent pathway (Shapiro and Hille, 1993; Kammermeier et al., 2000). M_1R activation also inhibits recombinant N-current (Gamper et al., 2004). Since both M_1Rs and NK-1Rs couple to G_q, Whole-cell currents were recorded by stepping from -90 mV to 0 mV. Following application of SP for three minutes, the maximal inward current decreased to 52 ± 8% of control levels (Fig 2.1A, B; n=6; p<0.05, compared to unstimulated levels). Current inhibition was significantly greater than that observed in cells with no NK-1R transfected (13 ± 12%; n=3; p<0.05 compared to cells transfected with NK-1R); no significant inhibition occurred without receptor expression (Fig 2.1C).

Inhibition of N-currents by SP occurs in a concentration-dependent manner

In the previous experiment we noted that following application of SP, N-current briefly increased in amplitude but then the current reversed resulting in sustained inhibition (Fig 2.2B). A concentration-dependent effect of SP was earlier reported in DRG neurons (Sculptoreanu and de Groat, 2003). We hypothesized that SP may both enhance and inhibit N-current, where enhancement is more sensitive to the SP concentration than inhibition. We predicted that at low concentrations, SP would enhance N-current while at higher concentrations SP would inhibit N-current. Activation of NK-1Rs by different SP concentrations ranging from 1 - 250 nM yielded a range of N-current inhibition. At SP concentrations of 5 nM and above, currents were strongly inhibited (Fig 2.2).

SP inhibits N- currents via the "slow" pathway

N-current inhibition by M_1Rs involves the "slow", BAPTA-sensitive pathway (Beech et al., 1991; Bernheim et al., 1991; Mathie et al., 1992). We hypothesized that the Gq-coupled NK-1R inhibits N-current via the same "slow" pathway. To test this hypothesis, we examined whether inhibition was BAPTA sensitive by comparing the magnitude of inhibition when 0.1 or 20 mM BAPTA was dialyzed into transfected HEK-M1 cells for 2 mins after establishing the whole-cell configuration. Following this control period, application of 5 nM SP inhibited currents of cells dialyzed with 0.1 mM BAPTA (Fig 2.3A-C). In contrast, after dialying cells with 20 mM BAPTA N-current inhibition was lost (Fig 2.3C-E; $p<0.001$ compared to dialysis with 0.1 mM BAPTA). These

findings suggest that NK-1R signaling uses the same “slow” BAPTA-sensitive pathway that was earlier shown to mediate M_1R inhibition of N-current (Beech et al., 1991)

Next, we hypothesized that N-current inhibition by SP involves phospholipid metabolism as part of the signaling cascade. Inhibition of N-current by M_1Rs involves acute activation of $cPLA_2$ (Liu and Rittenhouse, 2003a; Liu et al., 2004). To decrease the availability of free fatty acids such as AA, we used two strategies. First we antagonized the breakdown of membrane phospholipids using OPC, a PLA_2 antagonist. When cells were preincubated in 10 μM OPC for 60 seconds, application of 250 nM SP no longer inhibited N-current. This loss of inhibition is significantly different than inhibition in the absence of OPC (n=5; $p<0.01$; Fig 2.4B and D).

Second, we tested whether the presence of BSA reduced N-current inhibition following stimulation of NK-1R. BSA was earlier shown to reduce N-current inhibition by M_1Rs (Liu and Rittenhouse, 2003a). Following pre-incubation with BSA for 2 mins, SP no longer elicited significant current inhibition (Fig 2.4C and D). However, N-current in the presence of BSA significantly inactivated more rapidly ($\tau = 21 \pm 1.4$ ms) compared to when BSA was not included in the bath ($\tau = 41 \pm 5$ ms; data not shown). The BAPTA sensitivity, the requirement for PLA_2 activity and free fatty acid support the initial hypothesis that activation of NK-1Rs by SP inhibits N-current via the same “slow” pathway used by M_1Rs (Beech et al., 1991; Bernheim et al., 1991; Mathie et al., 1992; Liu and Rittenhouse, 2003a).

ERK1/2 is involved in mediating N-current inhibition by SP

We next tested whether ERK1/2 activity is required for "slow" pathway modulation of N-current by SP. HEK-M1 cells were preincubated with 10 μM U0126 for 15 mins before applying SP. U0126 blocks MEK's activity, thereby preventing phosphorylation of ERK1/2 (Fig 2.5D). While in control conditions, SP inhibited N-currents to 61 ± 9% of unstimulated levels, the presence of U0126 resulted in a loss of inhibition ($p<0.05$; Fig 2.5A-C) as was earlier observed by blocking the release of AA using OPC and reducing AA's availability using BSA . These findings are consistent with a model where following G_q activation, ERK phosphorylates $cPLA_2$ (Fig 2.5D).

We attempted to test whether ERK phosphorylated $cPLA_2$ in HEK-M1 cells upon NK-1R activation. In preliminary experiments HEK-M1 cells were exposed to the muscarinic agonist oxotremorine-M (Oxo-M; 10 μM) for 10 min, then fixed and stained with an antibody (1:5,000) specific to $cPLA_2$, phosphorylated on serine 505 (phospho-$cPLA_2$). However, unstimulated cells exhibited strong staining for constitutive phospho-$cPLA_2$. No detectable increase in fluorescence was observed following Oxo-M since fluorescence appeared to be maximal under control conditions (n=5 expts; data not shown). Antibody concentration was lowered to 1:20,000; however the same result was obtained, suggesting that the HEK-M1 cell line may not be an ideal system to detect changes in phosphorylation of $cPLA_2$ since a high basal level of phosphorylation exists. A similar observation has been reported for Madin-Darby canine kidney (MDCK) cells where pre-incubation with U0126 partially reversed a gel-shift due to phosphorylation of $cPLA_2$ (Evans et al., 2002).

DISCUSSION

Inhibition of N-current by SP was first demonstrated in SCG neurons (Shapiro and Hille, 1993). As with M_1Rs, current inhibition by SP involved PTX-insensitive G proteins and was not relieved by a prepulse, indicating involvement of a voltage-independent pathway (Shapiro and Hille, 1993). As with M_1Rs, inhibition was partially relieved following Ca^{2+} chelation with 20 mM BAPTA (Beech et al., 1991; Bernheim et al., 1991; Mathie et al., 1992). Subsequently, N-current inhibition by SP was shown to involve Gβγ and PLC confirming involvement of a G_q-coupled pathway in N-current modulation (Kammermeier et al., 2000). Here we show that activation of NK-1R by SP inhibits recombinant N-current via the "slow" pathway, a signal transduction cascade involving lipid metabolism that was earlier described for M_1Rs (Delmas et al., 1998; Haley et al., 2000; Liu and Rittenhouse, 2003a; Gamper et al., 2004). We tested whether stimulation of the G_q-coupled NK-1R will activate PLA_2, which releases AA from membrane phospholipids. In the presence of the PLA_2 antagonist OPC, N-current inhibition by SP is lost. When BSA is applied in the bath to reduce the availability of free AA, control currents inactivate faster but the currents are not inhibited by SP. We also predicted that ERK1/2 might also participate in the pathway downstream of receptor activation, since ERK1/2 phosphorylates $cPLA_2$ leading to its acute activation (Houliston et al., 2001). As anticipated, in the presence of UO126, an antagonist of ERK1/2, N-current inhibition by SP was lost. These results identify additional signaling molecules downstream of G_q and PLC that mediate N-current modulation by SP.

Together with our earlier studies we have shown that three different molecules: exogenously applied AA, which is a hydrophobic signaling molecule, Oxo-M, which is a small, hydrophilic molecule and SP, a short neuropeptide all appear to converge on the same pathway where free AA may be the final effector molecule that modulates N-current (Liu and Rittenhouse, 2000; Liu et al., 2001; Liu and Rittenhouse, 2003a). In central and peripheral primary neurons NK-1Rs and M_1Rs stimulate AA release (Catalan et al., 1988; Tence et al., 1994; Liu et al., 2006), further supporting the possibility that either endogenously released AA or bath-applied AA inhibits N-current by the same mechanism.

Modulation of N-current by SP is concentration-dependent

Activation of NK-1R by SP inhibits N-current in a concentration-dependent manner. Inhibition of currents occurs at SP concentrations of 5 nM and above; at very low concentrations (< 5 nM), slight enhancement was observed (Fig 2.2). Such a concentration-dependent response by SP was also observed with N-current, recorded from DRG neurons (Sculptoreanu and de Groat, 2003). Additionally recombinant N-current exhibits both enhancement and inhibition by either M_1R or SP stimulation (Chapter III).

SP inhibits N-currents via the voltage-independent "slow" pathway

M_1R and NK-1R inhibition of native and recombinant N-current is BAPTA-sensitive, indicating calcium-dependent enzymes participate in the pathway (Beech et al.,

1991; Bernheim et al., 1991; Mathie et al., 1992). Consistent with the BAPTA studies, PLC, a calcium-dependent enzyme, participates in N-channel modulation by the slow pathway (Kammermeier et al., 2000; Liu and Rittenhouse, 2003a; Gamper et al., 2004). Additionally in SCG neurons, Ca^{2+}-sensitive $cPLA_2$ is required for N-current modulation by M_1Rs (Liu et al., submitted). We also show that N-current inhibition by SP requires a PLA_2 and downstream release of lipid mediators. In the presence of the PLA_2 antagonist OPC or BSA, which scavenges free fatty acid, inhibition by SP is lost (Fig 2.4). These findings show that both receptors appear to converge on the same signaling pathway to inhibit N-current.

A few studies suggest that a reduction in the level of phosphatidylinositol-4,5-bisphosphate [PIP_2] after G_qPCR stimulation is sufficient for N-current inhibition (Wu et al., 2002; Gamper et al., 2004; Michailidis et al., 2007). However, other studies indicate N-current inhibition by M_1R requires complete breakdown of PIP_2 by PLC, PLA_2 and diacylglycerol lipase (Liu and Rittenhouse, 2003a; Liu et al., 2004; Liu et al., 2008). Antagonizing any of these lipases results in loss of N-current inhibition. These effects appear specific since inhibition of the potassium current, M-current, is only sensitive to antagonism of PLC (Suh and Hille, 2002; Liu et al., 2006; Liu et al., 2008). The characteristics of N-current modulation by exogenously applied AA mimic modulation by M_1Rs (Liu and Rittenhouse, 2003a)- peak current enhancement occurs at negative potentials and inhibition occurs at positive potentials. These findings indicate that not just the loss of PIP_2 but its highly regulated breakdown and liberation of free AA is required

for mediating N-current inhibition by G_qPCRs. Overall, these findings indicate that modulation of N-currents by SP occur via the “slow” pathway.

ERK1/2 is involved in inhibition of N-currents by SP

Antagonism by U0236 of N-current inhibition is consistent with previous identification of ERK1/2 activation in NK-1R signaling. Noxious stimuli from the periphery is sufficient to cause phosphorylation of ERK in DRG (Dai et al., 2002) and DH neurons (Ji et al., 1999). U0126 serves as a highly specific inhibitor by binding to the active forms of MEK1 and MEK2 and preventing activation of the MAPKs (ERK1/2) (DeSilva et al., 1998; Favata et al., 1998). Pre-incubation of cells with 10 μM U0126 for 10-15 mins blocks MAPK activation (Favata et al., 1998). Agonist-induced phosphorylation of $cPLA_2$ by MAPK occurs at serine-505 (Lin et al., 1993). In a separate study, blocking the activation of the ERK pathway blocks agonist-induced AA release as well as partially blocks phosphorylation of $cPLA_2$ (Evans et al., 2002) linking ERK activity with $cPLA_2$ phosphorylation and AA release. Due to issues with current run-down when cells are held in the whole-cell configuration for many minutes, we could not determine the effect of preincubation with U0126 although previous work has shown that preincubation of DRG neurons with U0126 reduces peak current (Fitzgerald, 2000). While ERK1/2 activity causes tonic enhancement of N- and L- currents (Fitzgerald, 2000) by phosphorylating sites on the channel and accessory $Ca_V\beta$ subunits (Martin et al., 2006), receptor-mediated inhibition of P/Q-type currents seemed to be reduced by 50% when the signaling pathway was uncoupled from MAPK (Wu et al., 2002) further suggesting that

modulation of Ca^{2+} channels by ERK1/2 is a mechanism observed across different calcium channel subtypes. Although it is possible that in the presence of U0126, loss of inhibition by SP occurs from a loss of a phosphorylation event either on the channel or on the $Ca_V\beta$ subunit. However the findings would still implicate ERK1/2 as a component in the signaling pathway. Thus we confirmed a role for ERK1/2 in N-current modulation by SP. Whether its role in the inhibitory pathway is only to phosphorylate $cPLA_2$ or whether it serves additional functions in the pathway awaits future investigation. One way to address this would be to test whether mutant $Ca_V2.2$ channels lacking the putative ERK1/2 phosphorylation sites still undergo inhibition by SP. Thus, our present study along with previous studies identifies NK-1R, G_q, PLC, phosphorylation of ERK, PLA_2 and a free fatty acid, most likely AA as signaling components mediating inhibition of N-currents by SP.

Significance of the slow pathway in transmission of nociceptive stimuli

Overall, our present study identifies the signaling components mediating N-current inhibition by SP. So far pharmacological antagonists of calcium channels, most notably N-channels have been used for treatment of chronic pain (Snutch, 2005). Following nerve injury, sensory neurons undergo a progressive increase in excitability due to entry and accumulation of Ca^{2+} and hence cannot be treated by antagonists of neurokinin receptors (Abdulla et al., 2003). N-channels play an important role in regulating membrane excitability by activation of calcium-activated potassium channels (Sah and Faber, 2002; McGivern and McDonough, 2004). Hence, targeting the signaling

pathway that mediates modulation of N-current by SP may be an effective way of reversing aberrant neuronal excitability thus providing relief from pain.

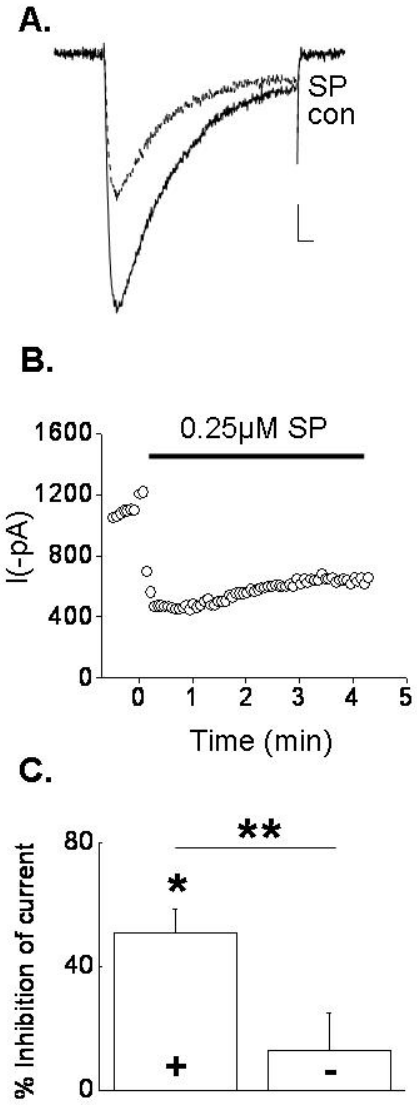

Figure 2.1 SP inhibits recombinant N-current. HEK-M1 cells were transfected with $Ca_V2.2$, β3, α2δ-1 and NK-1R expressing plasmids. **(A)** Representative current traces taken before and 3 mins after application of 0.25 μM SP. **(B)** Time course of currents taken before and after application of 0.25 μM SP. **(C)** Summary of inhibition by SP when NK-1R is co-expressed (+) compared to inhibition of currents when NK-1R is not co-expressed (-) (n=3-7). *$p<0.05$ compared to control currents, **$p<0.05$ compared to cells transfected with NK-1R. The changes in N-current in –NK-1R cells was not significantly different compared to control cells.

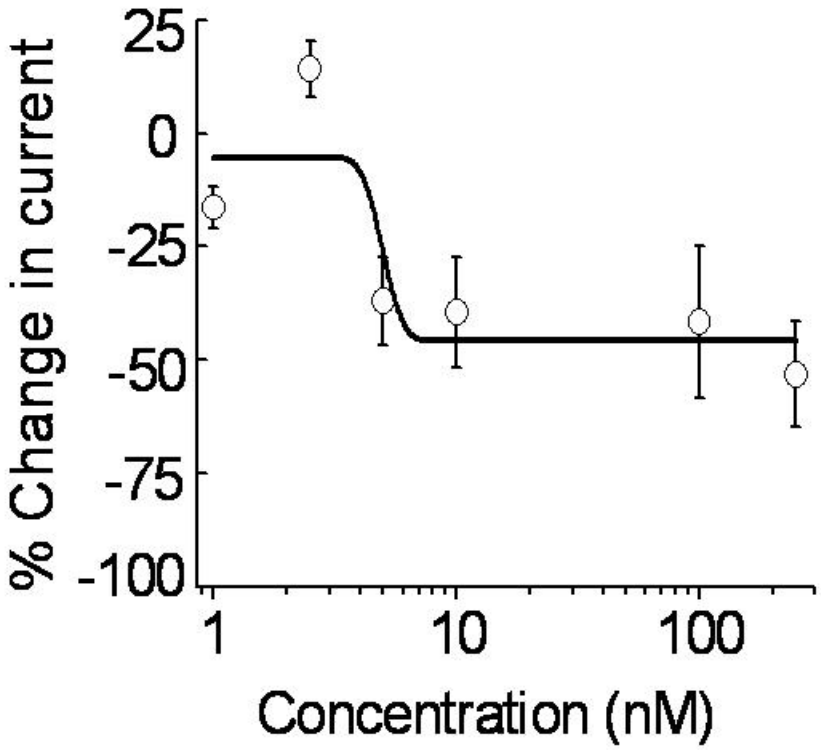

Figure 2.2 Inhibition of N-current by SP is concentration-dependent. Different concentrations of SP ranging from 1 to 250 nM were tested for N-current modulation.

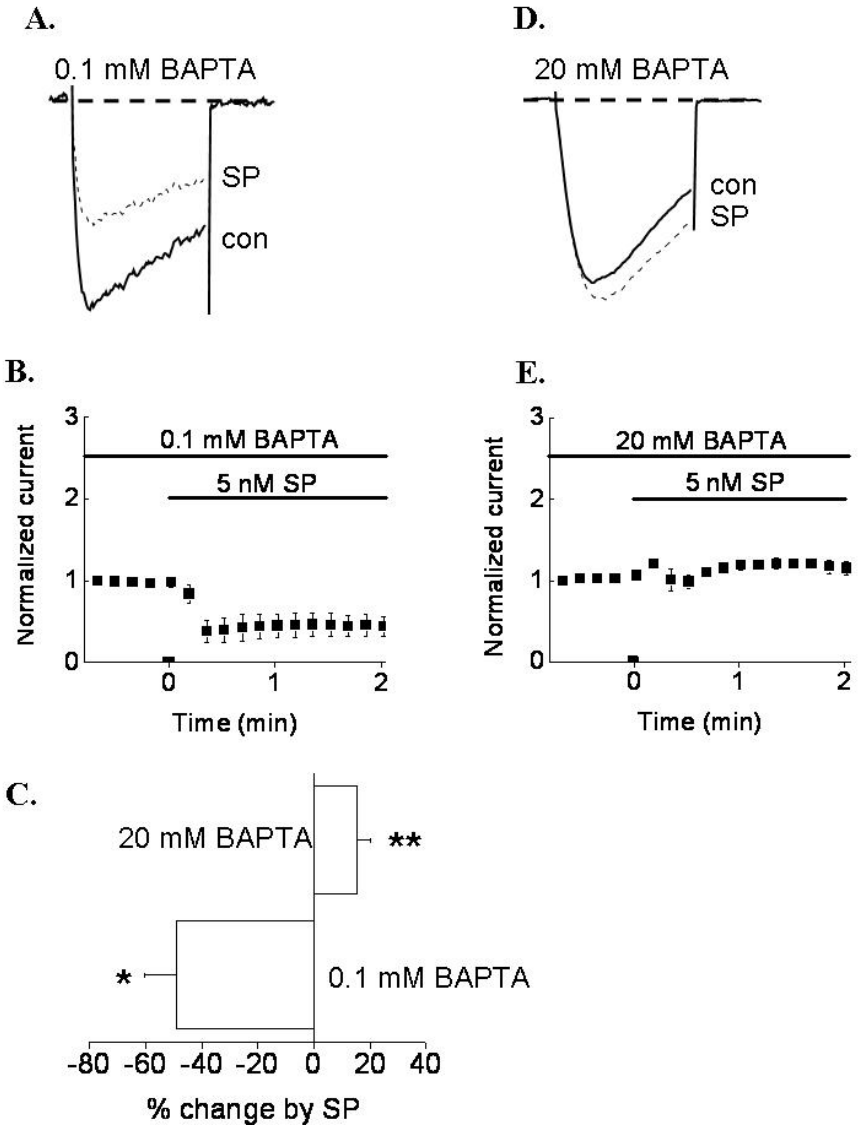

Figure 2.3 N-current inhibition by SP is BAPTA-sensitive. (A) Representative sweeps taken before and 90 seconds after applying 5 nM SP in the presence of 0.1 mM intracellular BAPTA. (B) Averaged time course showing inhibition of currents by 5 nM SP. (C) Summary of inhibition by SP in the presence of 0.1 mM BAPTA compared with inhibition in the presence of 20 mM BAPTA. *$p<0.05$ compared to control currents, **$p<0.01$ compared to currents when 0.1 mM BAPTA was dialysed into the cells. (D) Representative sweeps taken before and 90 seconds after applying 5 nM SP in the presence of 20 mM intracellular BAPTA. (E) Averaged time course showing inhibition of currents by 5 nM SP in the presence of 20 mM BAPTA.

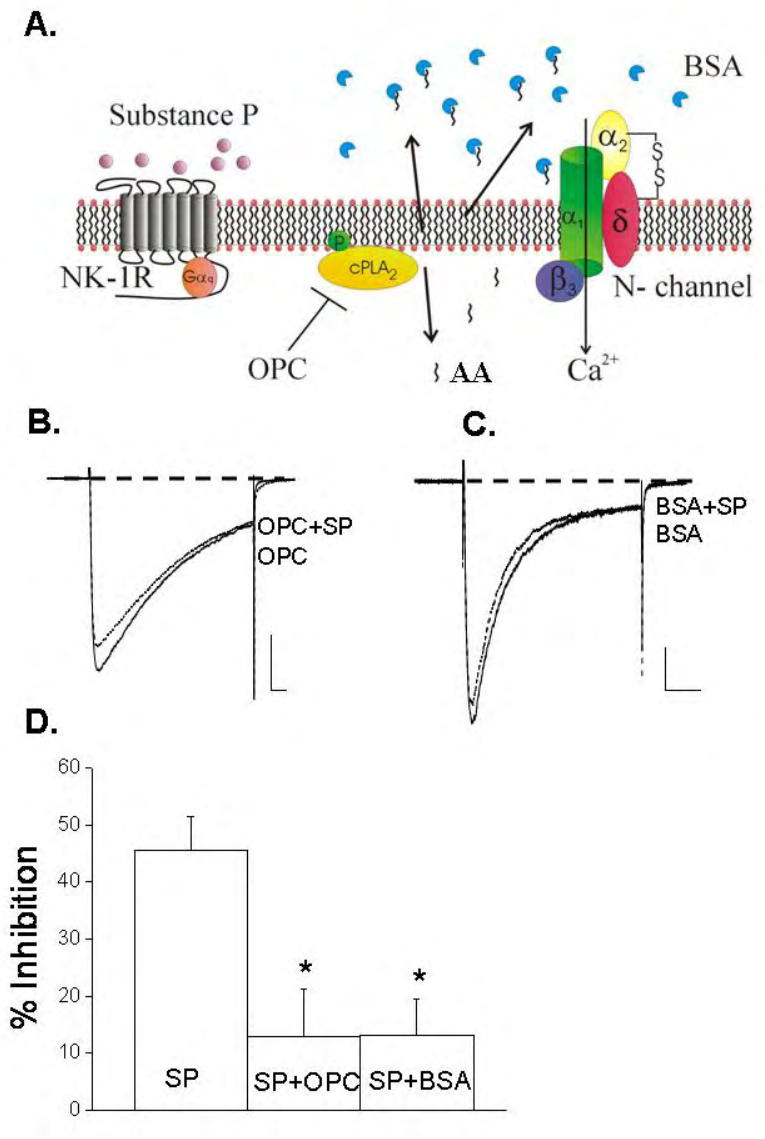

Figure 2.4 PLA2 and downstream release of free AA mediate N-current inhibition by SP. Cells were preincubated in 10 μM OPC or 1 mg/ml BSA for at least 2 mins before application of SP. (A) Model of hypothesized NK-1R signal transduction cascade showing inhibition of N-currents by SP involves cPLA2 and release of free AA. (B) Representative sweeps taken before and after application of 250 nM SP in the presence of 10 μM OPC. (C) Representative sweeps taken before and after application of SP in the presence of 1 mg/ml BSA. (D) Summary of inhibition by SP in the presence of OPC or BSA. n=4-5, *p<0.05 compared to current inhibition by SP alone.

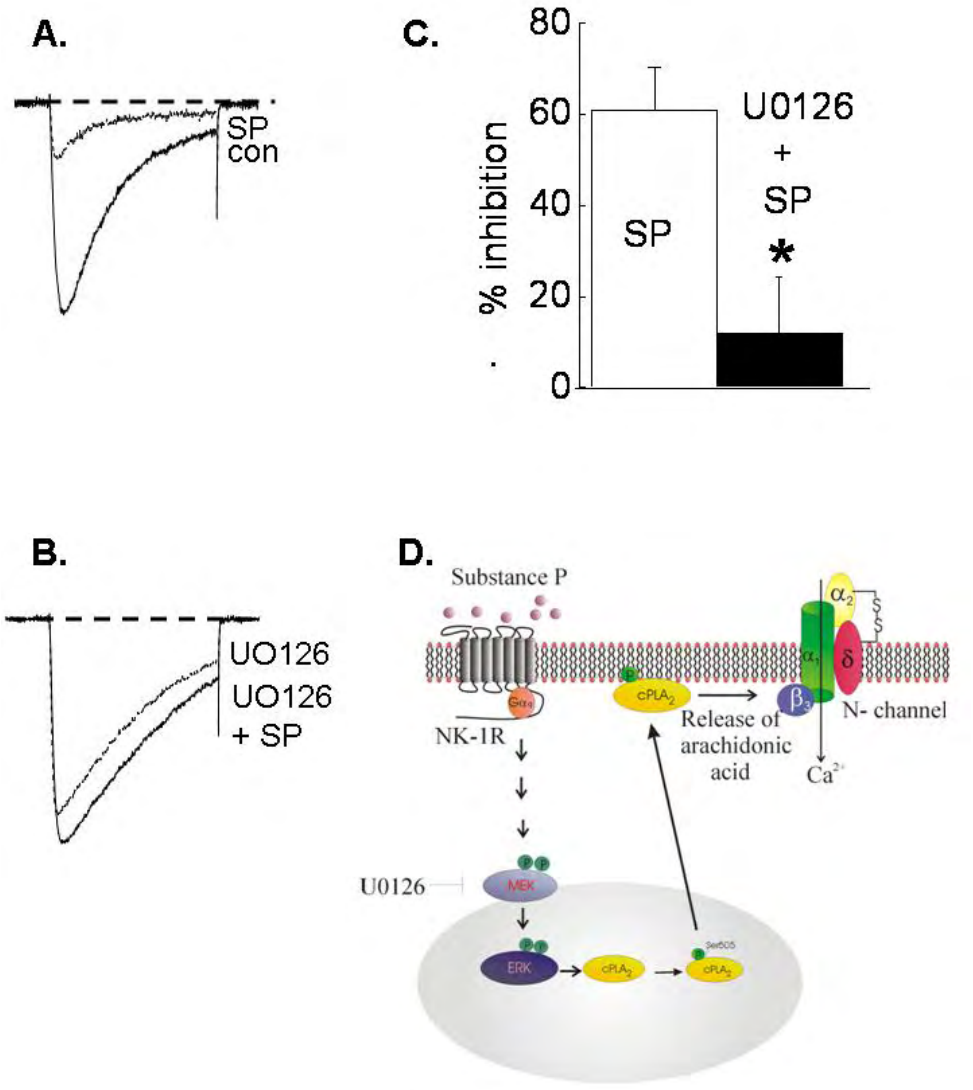

Figure 2.5 ERK1/2 activity is required for N-current inhibition by SP. Cells were preincubated with 10 μM U0126 for atleast 15 mins before application of 5 nM SP. (A) Representative traces taken before and after application of SP. (B) Representative sweeps taken before and after application of SP in the presence of 10 μM U0126. (C) Summary of inhibition by SP alone and in the presence of U0126. (D) Model of hypothesized NK-1R signal transduction cascade representing ERK1/2 phosphorylation occurring downstream of receptor activation.

CHAPTER III:

Palmitoylated $Ca_v\beta2a$ toggles N-current modulation by G_q-coupled receptors from inhibition to enhancement

ABSTRACT

M_1 muscarinic receptors both enhance and inhibit N-type Ca^{2+} channel activity. However, the physiological mechanisms regulating this modulation remain incompletely characterized and controversial. Here we report the N-channel's β-subunit ($Ca_V\beta$) acts as a molecular switch that determines which modulatory effect dominates N-current. In HEK-293 cells, M_1 or neurokinin-1 receptor stimulation inhibited activity of $Ca_V2.2$ coexpressed with $Ca_V\beta1b$, $Ca_V\beta3$ or $Ca_V\beta4$, but enhanced activity when coexpressed with $Ca_V\beta2a$. Arachidonic acid (AA) reproduced this profile of modulation, substantiating its role as the downstream effector. From studies with $Ca_V\beta$ mutants, chimeras and free palmitic acid we ascertained $Ca_V\beta2a$'s mechanism of action and revealed a new role for protein palmitoylation. The two palmitoyl groups of $Ca_V\beta2a$ appear to interact with $Ca_V2.2$ to prevent inhibition by AA, unmasking latent enhancement. Our results predict that N-current modulation by G_q-protein coupled receptors will fluctuate between enhancement and inhibition based on the presence of palmitoylated $Ca_V\beta2a$.

INTRODUCTION

All neural function results from a series of electrical and chemical signals. The two realms of signaling are often bridged within neurons by voltage-gated Ca^{2+} channels, such as N-channels (West et al., 2001). With depolarization of postsynaptic sites, N-channel activity (N-current) triggers biochemical changes including modulation of certain ion channels (Wisgirda and Dryer, 1994), enzyme activation (Rittenhouse and Zigmond, 1999) and gene transcription (Brosenitsch and Katz, 2001; West et al., 2001). In turn, G_qPCRs converge on a number of signal transduction cascades to modulate the N-channel's response to changing membrane potential. Some of these pathways are well described, so that both signaling molecules and sites of modulation on N-channels are known.

A notable exception is the M_1 receptor (M_1R), a G_qPCR that modulates post-synaptic N-current by an incompletely described signaling cascade referred to as the slow pathway (Beech et al., 1992). Other transmitters such as substance P (SP), the natural ligand for the neurokinin-1 receptor (NK-1R), also modulate N-current by a slow pathway (Shapiro and Hille, 1993; Kammermeier et al., 2000) coupled to G_q (Macdonald et al., 1996), suggesting that multiple G_qPCRs converge on this pathway. Recent reports propose a reduction in phosphatidylinositol-4,5-bisphosphate [PtdIns(4,5)P_2] levels during G_qPCR stimulation suffices for inhibition (Wu et al., 2002; Gamper et al., 2004; Michailidis et al., 2007). However, our previous studies with superior cervical ganglion (SCG) neurons indicate that modulation of native N-current by M_1Rs requires events downstream of PtdIns(4,5)P_2 hydrolysis (Liu and Rittenhouse, 2003a). We found that the

muscarinic agonist oxotremorine-M (Oxo-M) and arachidonic acid (AA) elicit the same distinct pattern of modulation (Liu et al., 2001; Liu and Rittenhouse, 2003a), not only inhibiting N-current at positive test potentials, but also enhancing N-current at negative test potentials (Fig. 3.1A). Enhancement and inhibition by AA occur at distinct sites and exhibit different biophysical characteristics (Barrett et al., 2001; Liu et al., 2001). Moreover, M_1R stimulation releases AA in central and SCG neurons (Tence et al., 1994; Liu et al., 2006) suggesting that AA may be a downstream effector of the slow pathway. Consistent with this hypothesis, inhibiting AA release from phospholipids by antagonizing phospholipase A_2 (PLA_2) activity or including bovine serum albumin (BSA), a scavenger of AA, in the bath minimizes N-current modulation by Oxo-M (Liu and Rittenhouse, 2003a). Whether both AA-sensitive sites reside in the same channel, or whether two distinct channel populations mediate enhancement and inhibition, remains untested. Therefore, we attempted to recapitulate N-current enhancement and inhibition in HEK-293 cells.

MATERIAL AND METHODS

Human embryonic kidney (HEK) cells with a stably transfected M_1R [HEK-M1] (Peralta et al., 1988), a generous gift from Emily Liman, were cultured in DMEM/F12 [Gibco (Carlsbad, CA)], supplemented with 10% fetal bovine serum (Gibco), 1% G418 [Geneticin selective antibiotic, non-sterile, Gibco] and 1% HT supplement (Gibco). Cells were transferred into 12-well plates for transfection. Recombinant cells at 60-80% confluence were transfected for 1 hour with $Ca_V2.2$ e[Δ24a, +31a, +37b), the N-channel variant found in SCG neurons (Lin et al., 1997); $\alpha_2\delta$-1, which is also expressed in SCG

(Lin et al., 2004); and various $Ca_V\beta$s at a 1:1:1 or 1:1:2 molar ratio along with enhanced green fluorescent protein (eGFP) at ~10% of the total DNA, using Lipofectamine and PLUS reagent [Invitrogen (Carlsbad, CA)] per the manufacturer's instructions. Where noted, the transfection mixture contained expression plasmids encoding NK-1R (0.028 µg/well; #AY462098; UMR cDNA Resource Center, University of Missouri, Rolla, MO). 500-1000 ng total DNA was transfected per well. 24-48 hours post-transfection, cells were replated on poly-L-lysine coated coverslips and allowed to settle for at least 1 hour prior to recording. TSAA 201 cells stably transfected with $Ca_V2.2$, $\alpha_2\delta$-1, and $Ca_V\beta3$ were generously provided by Diane Lipscombe. Cells were transfected with 500-1000 ng per well of the M_1R cDNA (#J04192; a generous gift from Neil Nathanson) along with eGFP at 10% of the total DNA and processed as above for current recordings.

$Ca_V\beta_{1b}$ (GenBank #X61394), $Ca_V\beta2a$ (#M80545) and $Ca_V\beta4$ (#L02315) were provided by Edward Perez-Reyes; $Ca_V2.2$ (#AF055477), $\alpha_2\delta$-1 (#AF286488), and $Ca_V\beta_3$ (#M88751) provided by Diane Lipscombe; the $Ca_V\beta2a$(C3,4S) mutant was provided by Aaron Fox, $Ca_V\beta2a\beta3$ and $Ca_V\beta2a\beta1b$ chimeras, were provided by Robert Ten Eick, from Marlene Hosey's lab (Chien et al., 1996; Chien et al., 1998; Chien and Hosey, 1998). Recordings from untransfected cells yielded whole-cell currents of 9.0 ± 1.3 pA in 20 mM Ba^{2+} (data provided by Mandy Roberts-Crowley). To avoid spurious results from endogenous currents, any transfected cells having currents less than 150 pA were discarded.

Electrophysiology

Ba^{2+} currents were recorded at room temperature (20-24°C) using the whole-cell configuration of a Dagan 3900a patch-clamp amplifier using methods described previously (Barrett et al., 2001; Liu et al., 2001). Currents were filtered at 5 kHz using the amplifier's four-pole low-pass Bessel filter and then digitized at 20 kHz with a CED micro1401 interface [Cambridge Electronic Design (CED), Cambridge, UK]. Data were collected using Patch 6.4 or Signal 2.15 software suites (CED) and stored on a personal computer. Prior to analysis, capacitive and leak currents were subtracted using a scaled-up current elicited with a test pulse to -100 mV. Pipette resistance ranged from 2.5 to 5 MΩ. Ba^{2+} currents were elicited every 4 sec by stepping from -90 to 0 mV for 100 ms unless otherwise noted. For cells expressing $Ca_V\beta 2a$, 20 mM Ba^{2+} was used as the charge carrier to improve the signal to noise ratio. The internal solution contained (in mM): 135 Cs-aspartate, 10 HEPES, 0.1 1,2-bis(*O*-aminophenoxy)ethane-*N*,*N*,*N*',*N*'-tetraacetic acid (BAPTA), 1 $MgCl_2$, 4 ATP, 0.4 GTP, adjusted to pH 7.5 with CsOH. The external solution contained (in mM): 135 N-methyl glucamine-aspartate (NMG), 10 HEPES, 5 or 20 Ba^{2+} (as indicated), adjusted to pH 7.5 with CsOH. NMG (135 mM) was substituted for Ba^{2+} when its concentration was lowered from 20 to 5 mM.

Pharmacology

Oxotremorine methiodide [Oxo-M; Tocris Biosciences Inc. (Bristol, UK)] was prepared as a stock solution in double-distilled water and then diluted 1,000 times with bath solution. SP was prepared as a stock solution in 0.05 M acetic acid and then diluted

at least 2,000 times with bath solution. AA (Nu Chek Prep, Elysian, MN) and OPC (Calbiochem, La Jolla, CA), were prepared as stock solutions made up in 100% ethanol and diluted 1,000 times with bath solution. All chemicals were obtained from Sigma-Aldrich Inc. (St. Louis, MO) except where noted.

Data Analysis

Patch 6.4 and Signal 2.15 (CED) were used to measure peak inward current of whole-cell traces. The trough seeking function of Patch was used to determine peak current where indicated. Data were further analyzed using EXCEL (Microsoft, Seattle, WA), and ORIGIN 7.0 (Microcal Software, Northampton, MA). Percent inhibition was calculated as: [(I-I')/I]*100, where I is the control current amplitude, determined by an average of five whole-cell current measurements prior to application of a particular agent, and I' is the average of five current measurements at the time specified for the determination. Conductance was calculated from a modified Ohm's Law equation: $G = I/(V_m - V_{rev})$, where I is the peak current at each test potential, V_m is the test potential, and V_{rev} is the apparent reversal potential. Relative conductance (G/G_{max})-voltage (V_m) curves were plotted for whole-cell recordings before and after application of AA. Data were curve fit using the Boltzmann Equation function in Origin 7.0 (MicroCal) yielding a curve fitting the equation: $G/G_{max} = G_{max} + (G_{min}-G_{max})/(1 + \exp[(V_m-V_{m½})/k)]$, where G_{max} is the maximal conductance, G_{min} is the minimal conductance, V_m is the test potential, $V_{m½}$ is the voltage at half maximal conductance and k is the slope factor.

Statistical analyses

Summary data are presented as mean ± standard error of the mean. A two-tailed paired *t*-test was used to determine differences between control and agonist. For comparisons of two different cell groups, data were analyzed by two-tailed Student's *t*-test for two means. For multiple comparisons, statistical significance was determined by a one-way analysis of variance (ANOVA) using Origin followed by a Tukey multiple-comparison post-hoc test. Statistical significance was set at $p \leq 0.05$.

Immunocytochemistry of $Ca_V\beta$ subunits

Adult SCG neurons were plated on chamber slides (Nagle Nune International, Rochester, NY) treated with poly-L-lysine and cultured overnight. Cells were washed with phosphate-buffered saline (PBS; 2 × 5 min) and then fixed with 100% Acetone (10 min). The fixative was washed away with PBS at room temperature (3 × 5 min). Cells were then exposed to PBS containing 10% normal goat serum for 60 min at room temperature, followed by incubation with primary antibody for 60 min at room temperature. Anti-$Ca_V\beta_2$ (mouse; NeuroMap), Anti-$Cav\beta_3$ (rabbit; Sigma), Anti-$Cav\beta_4$ (mouse; NeuroMap) were diluted 1:1,000 in DakoCytomation Antibody Diluent (DakoCytomation, Carpintena, CA). Thereafter, cells were washed with PBS (3 × 5 min) and were incubated for 60 min in the dark at room temperature with Alexa Fluor 488 anti-mouse antibody or Alexa Fluor 488 anti-rabbit antibody (Invitrogen, Carlsbad, CA) diluted 1:200 in DakoCytomation Antibody Diluent. After incubation with secondary antibodies, cells were washed with PBS (3 × 5 min) and a second fixation was performed.

Slides were then washed with distilled water and covered with the aqueous mounting medium Prolong Gold Antifade reagent (Invitrogen). Images of immunofluorescence were obtained at room temperature using a custom-built, video-rate confocal microscope (Sanderson and Parker, 2003) with a 40× objective lens. An excitation wavelength of 488 nm was used and emission spectra collected with long pass filters (OGSIS) at 515 nm (Perez and Sanderson, 2005).

RESULTS

To test whether a homogeneous population of N-channels recapitulates both enhancement and inhibition, N-currents were screened for sensitivity to Oxo-M. Recombinant currents were evoked from HEK-M1 cells transiently transfected with N-channel subunits $Ca_V2.2$, $\alpha_2\delta$-1 and $Ca_V\beta3$, which most commonly associates with $Ca_V2.2$ (Witcher et al., 1993). Oxo-M rapidly inhibited peak inward current, reaching a stable inhibition within 90 seconds (Figs. 3.1C-D). Since N-current enhancement is voltage-sensitive (Liu and Rittenhouse, 2003a), we compared current-voltage (I-V) plots measured before and after Oxo-M expecting to observe current enhancement at negative test potentials. However, Oxo-M inhibited current at virtually all voltages (Fig. 3.3C). tsA 201 cells stably transfected with the same subunits exhibited a similar profile of inhibition following exposure to Oxo-M (Figs. 3.1B, E, F), ruling out a system-specific effect.

$Ca_V\beta$ subunit controls N-current modulation by G_qPCRs.

Lack of enhancement at any potential indicated the recombinant system was fundamentally different from N-current modulation observed in SCG neurons. In addition to incomplete recapitulation of G_qPCR modulation, recombinant N-current exhibited robust, fast inactivation (Figs. 3.1D,F; 3.3C) as previously observed with channels containing $Ca_V\beta3$ (Olcese et al., 1994). In contrast, native N-current in SCG neurons exhibits kinetics with little inactivation (Plummer et al., 1989), similar to recombinant N-current from channels containing $Ca_V\beta2a$ (Hurley et al., 2000; Yasuda et al., 2004). Moreover, AA robustly inhibits noninactivating current in SCG neurons evoked with test pulses ranging in duration from 20 (Fig. 3.2) to 700 ms (Liu et al., 2001). Since SCG neurons express $Ca_V\beta2a$ mRNA (Lin et al., 1997), we hypothesized that the majority of N-current arises from $Ca_V\beta2a$-containing channels. If true, these channels might exhibit both inhibition and enhancement. We found that Oxo-M rapidly inhibited N-current from cells expressing $Ca_V\beta2a$. However, unlike $Ca_V\beta3$, initial inhibition gave way to stable enhancement (Figs. 3.1G-H). Moreover, comparison of I-V plots revealed that Oxo-M no longer inhibited current at any potential, but enhanced current at negative test potentials (Fig. 3.3B). Although we hypothesized expression of $Ca_V\beta2a$ would elicit enhancement at negative potentials, separation of enhancement from inhibition based on $Ca_V\beta$ expression was unanticipated. Therefore, we tested whether other $Ca_V\beta$s would dually modulate N-current by repeating the above experiments with two other neuronal $Ca_V\beta$s: $Ca_V\beta1b$ and $Ca_V\beta4$. As with $Ca_V\beta3$, when either $Ca_V\beta1b$ (Fig. 3.3A) or $Ca_V\beta4$ (Fig.

3.3D) was expressed, Oxo-M inhibited current at all test potentials, indicating that channels containing $Ca_V\beta2a$ exhibit unique N-current modulation by M_1Rs.

To determine whether M_1Rs uniquely influence the profile of modulation, we examined whether N-current modulation by another G_qPCR depends on $Ca_V\beta$. We tested NK-1Rs since in SCG neurons, stimulation of M_1Rs and NK-1Rs inhibit N-current through converging signaling pathways that require $G\alpha_q$ and downstream activation of phospholipase C (PLC) (Shapiro et al., 1994a; Kammermeier et al., 2000). We examined current modulation that occurred following exposure to SP. As with Oxo-M, an initial transient inhibition progressed to a stable current enhancement when $Ca_V\beta2a$ was expressed along with $Ca_V2.2$ and $\alpha_2\delta$-1 (Figs. 3.4A, C). In contrast, SP elicited sustained inhibition with $Ca_V\beta3$ expression (Figs. 3.3E & 3.4B-C). These data indicate that control of modulation by $Ca_V\beta$ is a mechanism used by numerous G_qPCRs, rather than unique to M_1Rs (Fig. 3.1A).

AA elicits a profile of N-current modulation similar to G_qPCR stimulation.

AA mimics N-current modulation by M_1Rs in SCG neurons and may serve as the downstream effector of this pathway (Liu and Rittenhouse, 2003a). If so, AA also should inhibit or enhance recombinant N-current similarly to M_1R or NK-1R stimulation. When this hypothesis was tested, AA's actions recapitulated the pattern of modulation observed with M_1R or NK-1R stimulation; enhancement and inhibition separated based on $Ca_V\beta$ expression (Figs. 3.3F-J). If elevated AA levels mediate enhancement and inhibition, both should reverse following washout of exogenous AA. As with SCG neurons, washing

with copious amounts of bath solution or with 1 mg/ml BSA reversed modulation (Figs. 3.5A-F). Moreover, enhancement recurred with a second application of AA following wash with BSA (Fig. 3.5A). These findings corroborate our assertion that AA mediates N-current modulation by the slow pathway (Liu and Rittenhouse, 2003a; Liu et al., 2004).

As a final test of AA's role in the slow pathway, we antagonized endogenous AA's release from membrane phospholipids using the PLA_2 antagonist oleyloxyethyl phosphorylcholine (OPC) to determine whether OPC minimizes N-current inhibition by Oxo-M. Exposure to Oxo-M for 60 seconds significantly inhibited N-current from $Ca_V\beta3$-containing channels ($P<0.05$ n=16). In contrast, OPC eliminated significant current inhibition by Oxo-M ($P>0.05$ n=7) (Figs. 3.1I-J). A similar profile was observed with SP (Chapter II). The striking recapitulation by AA of G_qPCR-induced N-current enhancement and inhibition, coupled with the loss of modulation when antagonizing AA release or sequestering free AA with BSA advance our previous hypothesis that PLA_2 and AA participate in the slow pathway (Liu and Rittenhouse, 2003a).

Expression of multiple $Ca_V\beta$ isoforms produces heterogeneous N-currents.

Our findings yield a possible explanation for why SCG neurons exhibit both enhancement and inhibition of whole-cell N-current (Barrett et al., 2001; Liu and Rittenhouse, 2003a; Liu et al., 2004). N-current's diverse biophysical properties in different neurons have been attributed to $Ca_V2.2$ coexpression with different $Ca_V\beta$ isoforms within individual neurons (Scott et al., 1996). Similarly, SCG neurons may

exhibit both forms of modulation because $Ca_V2.2$ co-assembles with different $Ca_V\beta$s. If this hypothesis is correct, the pattern of modulation observed in SCG neurons should recapitulate in HEK-M1 cells transfected with multiple $Ca_V\beta$s. When cells were transfected with $Ca_V\beta2a$ and $Ca_V\beta3$, the I-V plots strikingly recapitulated I-V plots from SCG neurons (Liu and Rittenhouse, 2003a), with enhancement occurring at negative potentials and inhibition at positive potentials (Fig. 3.6A). However, unlike activity from SCG neurons (Liu et al., 2001; Liu and Rittenhouse, 2003a), the currents rapidly inactivated. SCG express $Ca_V\beta2a$, $Ca_V\beta3$ and $Ca_V\beta4$ mRNA with trace amounts of $Ca_V\beta1b$ mRNA (Lin et al., 1996). When immunocytochemistry was performed on dissociated SCG neurons to determine which $Ca_V\beta$ proteins are expressed, neurons exhibited immunofluorescence with a rank order density of $Ca_V\beta2a>Ca_V\beta3>Ca_V\beta4$ (Fig. 3.6B). Therefore, we retested the modulatory response in cells transfected with $Ca_V\beta2a$, $Ca_V\beta3$ and $Ca_V\beta4$. In these cells, N-current closely recapitulated both the I-V relationship and current kinetics of native N-current under control conditions and following Oxo-M (Fig. 3.6C). These findings indicate that the characteristic pattern of modulation observed in SCG neurons (Liu and Rittenhouse, 2003a) most likely results from heterogeneous expression of different $Ca_V\beta$ isoforms with $Ca_V2.2$.

A model for dual modulation of N-current

We established a working model for how $Ca_V\beta2a$ controls modulation based on previous studies that examined AA's mechanism of inhibition of different Ca^{2+} channels. Our studies with SCG neurons demonstrated that current inhibition by AA occurs

intracellularly or within the inner leaflet of the membrane. In contrast, enhancement appears located extracellularly or within the outer leaflet of the bilayer (Barrett et al., 2001; Liu et al., 2001). $Ca_V\beta$ subunits bind to cytoplasmic loops of $Ca_V2.2$ (Pragnell et al., 1994). Thus, we hypothesized that the unique interactions of $Ca_V\beta2a$ with $Ca_V2.2$ somehow attenuates inhibition. The observation that in SCG neurons (Barrett et al., 2001; Liu et al., 2001) and with recombinant channels containing either $Ca_V\beta2a$ or $Ca_V\beta3$ (Figs. 3.7A-B), AA induces initial N-current enhancement, which is sustained with $Ca_V\beta2a$, but for $Ca_V\beta3$ is followed by a more slowly progressing inhibition supports this model. Thus, we postulated that N-current modulation first exhibits enhancement that becomes masked by subsequent, more dominant inhibition. Since our previous work indicated enhancement by AA arises from increased voltage sensitivity (Barrett et al., 2001), we compared normalized conductance-voltage (G-V) curves to determine whether increased voltage sensitivity occurs independently of $Ca_V\beta2a$ expression. Both $Ca_V\beta2a$- and $Ca_V\beta3$-containing cells exhibited a negative shift in conductance in response to AA (Figs. 3.7C-D), demonstrating that AA increases N-channel voltage sensitivity independently of $Ca_V\beta$ subunit expression. These data indicate that $Ca_V\beta2a$'s unique ability to attenuate inhibition reveals sustained enhancement. In contrast, inhibition results from increased stability of a closed state (Liu and Rittenhouse, 2000) essentially reducing the number of channels available to open. This type of inhibition should dominate an increase in voltage sensitivity; if channels will not open at any voltage, increasing their voltage sensitivity will have little effect on currents. Thus by blocking a dominating inhibition (Fig. 3.7E), $Ca_V\beta2a$ unmasks latent enhancement.

Loss of $Ca_V\beta2a$ palmitoylation restores partial inhibition of N-current by Oxo-M or AA

Having established that $Ca_V\beta2a$ uniquely blocks N-current inhibition by G_qPCR stimulation or exogenous AA, we investigated the structural aspects of $Ca_V\beta2a$ to determine its mechanism of action. A conspicuous feature of $Ca_V\beta2a$ is its unique palmitoylation of two cysteine residues near the N-terminus (Chien et al., 1996). Our observation that palmitoylated $Ca_V\beta2a$ interferes with a fatty acid-mediated inhibition of $Ca_V2.2$ raises the possibility of direct antagonism between palmitic acid and AA. Therefore, we tested a depalmitoylated mutant to determine whether $Ca_V\beta2a$ must be palmitoylated to minimize inhibition and reveal enhancement. Currents from channels containing depalmitoylated $Ca_V\beta2a$ [$Ca_V\beta2a$(C3,4S)] (Chien et al., 1996) exhibited an initial transient inhibition following Oxo-M that relaxed, yielding a small but insignificant inhibition (Figs. 3.8A, G). AA initially enhanced current amplitude, followed by significant inhibition (Figs. 3.8B, G). The loss of enhancement and appearance of inhibition, though differing in magnitude with Oxo-M or AA, support the idea that palmitoylation blocks inhibition.

If the palmitic acid groups on $Ca_v\beta2a$ are both necessary and sufficient for antagonizing inhibition, then palmitoylating another $Ca_V\beta$ should convert current inhibition to enhancement. Therefore we tested a chimera in which the variable N-terminus of $Ca_V\beta1b$ was replaced with the palmitoylated, 16 amino acid N-terminus of $Ca_V\beta2a$ ($Ca_V\beta2a\beta1b$) (Chien et al., 1998). In cells expressing $Ca_V\beta2a\beta1b$, application of

Oxo-M enhanced current with no inhibition (Fig. 3.8G). AA no longer inhibited these currents significantly compared to $Ca_V\beta1b$ (n=4) (Fig. 3.3J). The difference in modulation by AA and Oxo-M may be attributed to an exaggerated response to exogenous application of AA compared to the response to physiological concentrations of AA released upon M_1R stimulation. I-V plots after either Oxo-M or AA exhibited enhancement of current at negative test potentials and no inhibition at positive test potentials (Figs. 3.8C-D), indicating that the palmitoylated N-terminus is both necessary and sufficient to block inhibition.

However, a second chimera, in which the N-terminus of $Ca_V\beta3$ was replaced with the N-terminus of $Ca_V\beta2a$ ($Ca_V\beta2a\beta3$) (Chien et al., 1998), did not block inhibition as effectively. In cells expressing $Ca_V\beta2a\beta3$, inhibition by Oxo-M was diminished compared to wild-type $Ca_V\beta3$**,** while AA reversibly inhibited currents similarly to wild-type levels (Figs. 3.8E-G). I-V plots taken before and 90 seconds after application of Oxo-M or AA exhibited inhibition at positive test potentials (Figs. 3.8E-F). These results indicate that addition of $Ca_V\beta2a$'s palmitoylated N-terminus to $Ca_V\beta3$ only partially reproduced the stable enhancement by Oxo-M or AA normally observed with wild-type $Ca_V\beta2a$. However, $Ca_V\beta2a$ protein shares highest sequence homology to $Ca_V\beta1b$ (Birnbaumer et al., 1998).

Thus, the simplest interpretation for the varied results with the different chimeras is that $Ca_V\beta2a\beta1b$ binds to $Ca_V2.2$ similarly to wild-type $Ca_V\beta2a$ to minimize N-current inhibition. In contrast, the more divergent $Ca_V\beta2a\beta3$ interacts differently with $Ca_V2.2$

(Fig. 3.8H). In support of this notion, $Ca_V\beta2a\beta3$-containing cells exhibited varied kinetics, from noninactivating currents resembling $Ca_V\beta2a$-containing channel activity (Fig. 3.3B) to rapidly inactivating currents resembling depalmitoylated $Ca_V\beta2a$-containing channel activity (Figs. 3.8A-B). Moreover, the kinetics varied within individual recordings and from cell to cell from a rapidly inactivating to a noninactivating kinetic profile (data not shown). The unstable inactivation kinetics suggests that $Ca_V\beta2a\beta3$ cannot dock properly to $Ca_V2.2$, thus destabilizing and changing the location of $Ca_V\beta2a$'s palmitoyl groups.

Free palmitic acid minimizes N-current inhibition.

If our interpretation that the palmitoyl groups antagonize inhibition is correct, freeing the palmitoyl groups from protein constraints might allow the fatty acids to find and assume their optimal position for interacting with $Ca_V2.2$ and blocking inhibition (Fig. 3.9A). Alternatively, if the palmitic acids do not interact directly with $Ca_V2.2$ then introducing free palmitic acid should not alter N-channel modulation by agonist. We tested this prediction by preincubating cells expressing NK-1Rs and $Ca_V\beta3$-containing channels with free palmitic acid. Under these conditions, the sustained inhibition normally observed with SP (Figs. 3.9B-C) was replaced by an initial enhancement that relaxed resulting in no significant change ($p>0.24$) in current amplitude over time (Figs. 3.9B, D). Moreover compared to control conditions, little inhibition by SP was detected in I-V plots from cells preincubated with palmitic acid (Figs. 3.9C-D). On its own, palmitic acid did not affect N-current when compared to exposure of the cells to bath

solution for 8 mins (Fig 3.9E). Preliminary recordings with a shorter duration of preincubation with palmitic acid did not result in significant reduction in modulation of N-currents by SP. These findings demonstrate that exogenous application of free palmitic acid suffices to block current inhibition of $Ca_V\beta3$-containing N-channels. More importantly, these results support a model where $Ca_V\beta2a$'s palmitic acids interact directly with $Ca_V2.2$ to antagonize N-current inhibition by endogenously released AA (Fig. 3.10).

DISCUSSION

A New Role for Palmitoyl Groups of Palmitoylated Proteins

Our data identify a previously unrecognized role for protein palmitoylation where it serves as the key feature of $Ca_V\beta2a$'s capacity to toggle $Ca_V2.2$ modulation from inhibition to enhancement following stimulation of G_qPCRs. Here and in other systems, palmitoylation serves to target or anchor proteins to specific membrane domains (Chien et al., 1996; Resh, 2006). Once positioned in the membrane, palmitoylation increases stability and efficiency of action, but normally does not alter the functional properties of proteins. One exception to this generalization is retinal epithelial protein 65 (RPE65), a chaperone protein for *all*-trans-retinal esters. In this case, palmitoylation not only targets RPE65 to the membrane, it also reverses RPE65's binding specificity for vitamin A to *all*-trans retinyl ester, consequently affecting how rapidly photoreceptors respond to light (Xue et al., 2004). Thus, palmitoylation qualitatively alters the substrate specificity of the same protein that is reversibly palmitoylated. Here, our data extend the functions of palmitoylation in a new direction by revealing that following stimulation of G_qPCRs, the

palmitoyl groups of one protein, $Ca_V\beta 2a$, block inhibition of a second protein, $Ca_V2.2$. Moreover, we have shown that coexpression of $Ca_V\beta 2a$ with other $Ca_V\beta s$ in a recombinant system recapitulates the dual enhancement and inhibition of N-current observed in SCG neurons. This finding provides an explanation of how stimulation of M_1Rs or exogenous AA elicit both enhancement and inhibition of N-current in individual sympathetic neurons (Liu and Rittenhouse, 2003a).

Our finding that palmitoylation antagonizes an inhibition mediated by PtdIns(4,5)P_2 breakdown and increased free AA (Liu and Rittenhouse, 2003a; Gamper et al., 2004) raises the possibility that dual palmitoyl groups interact directly with $Ca_V2.2$ to antagonize AA's interaction with $Ca_V2.2$ and subsequent inhibition of N-channel activity. The idea that AA directly interacts with Ca^{2+} channels is supported by the finding that M_1R stimulation or application of exogenous AA also inhibits recombinant Ca_V3 currents in whole-cell (Zhang et al., 2000; Talavera et al., 2004; Hildebrand et al., 2007) and ripped-off patch configurations (Chemin et al., 2007). Since Ca_V3 (T-type) channels do not require coexpression of a $Ca_V\beta$ or $\alpha_2\delta$ to open, T-channel modulation must occur at a site on the pore-forming subunit. Moreover, AA inhibits T-current with a Hill coefficient of 1.6, indicating cooperative binding of at least two AA molecules to the T-channels (Talavera et al., 2004). Taken together these findings are consistent with a direct interaction between AA and T-channels. Similarly, AA most likely confers N-current inhibition by acting at a homologous site on $Ca_V2.2$ because both N- and T-channels exhibit similar changes in gating following application of AA (Liu and Rittenhouse, 2000; Talavera et al., 2004).

Palmitoylated $Ca_V\beta2a$ may serve as a phospholipid mimic by competing with PtdIns(4,5)P_2 and free AA for interaction with $Ca_V2.2$.

Under basal conditions AA normally resides in the *sn*-2 position of PtdIns(4,5)P_2. Since palmitoylated $Ca_V\beta2a$ appears to antagonize the actions of free AA on $Ca_V2.2$, it may also compete with PtdIns(4,5)P_2 for interaction with $Ca_V2.2$; the two palmitic acids of $Ca_V\beta2a$ residing in sites normally occupied by the two fatty acid tails of PtdIns(4,5)P_2. Consistent with its ability to block N-current inhibition by free AA, palmitoylated $Ca_V\beta2a$ acts as a "phospholipid mimic" to maintain normal channel activity. This model is attractive in that it incorporates previous findings that PtdIns(4,5)P_2 associates with channels increasing their availability to open (Wu et al., 2002; Gamper et al., 2004). The model also supports our previous findings (Liu and Rittenhouse, 2003a) that increased free AA confers current inhibition either by displacing PtdIns(4,5)P_2 or by remaining associated with channels following phospholipid breakdown. Lastly, our finding that free palmitic acid blocks inhibition by SP of $Ca_V\beta3$-containing channels supports the idea that the palmitic acids occupy the same or overlapping sites recognized by AA.

Whether PtdIns(4,5)P_2 as well as AA compete for the same site of interaction with $Ca_V2.2$ as the palmitoyl groups of $Ca_V\beta2a$ and where the location of that site is awaits future investigation. However, we have observed that whole-cell recombinant current from $Ca_V\beta2a$-containing channels, in contrast to $Ca_V\beta3$-containing channels (Gamper et al., 2004), rundown only minimally over time (data not shown), consistent with palmitoylated $Ca_V\beta2a$ functionally substituting for PtdIns(4,5)P_2. Thus, when taken together, our findings and the results of other laboratories best fit a model where

palmitoylated $Ca_V\beta2a$, PtdIns(4,5)P_2 and free AA compete for an overlapping interaction site on $Ca_V2.2$. Given the extent that lipids such as PtdIns(4,5)P_2 and AA associate with membrane protein complexes, the interference of such interactions by palmitoylated proteins is predicted to occur in other protein complexes, yielding broad importance beyond ion channel functioning.

Expression of palmitoylated $Ca_V\beta2a$ may underlie novel forms of synaptic plasticity

The presence or absence of palmitoylated $Ca_V\beta2a$ may have far-reaching consequences for synaptic plasticity. $Ca_V\beta2a$ expression displays an overlapping distribution with G_qPCRs (Tence et al., 1994; Liu and Rittenhouse, 2003a) throughout the brain and is primarily localized postsynaptically in dendrites and cell bodies (Lie et al., 1999), indicating that enhancement of Ca^{2+} channel activity will affect postsynaptic membrane excitability. In support of this notion, increased current amplitude and/or kinetic changes associated with Ca^{2+} current enhancement (Zhang et al., 2000; Bannister et al., 2004; Guo and Ikeda, 2004; Talavera et al., 2004; Tai et al., 2006; Chemin et al., 2007) occur in different neurons and recombinant channels from the Ca_V2 and Ca_V3 families (Keyser and Alger, 1990; Melliti et al., 2001; Chemin et al., 2007; Meza et al., 2007). In contrast, native or recombinant channels associated with $Ca_V\beta1b$, $Ca_V\beta3$ or $Ca_V\beta4$, exhibit inhibition following similar stimulation (Keyser and Alger, 1990; Liu and Rittenhouse, 2003a; Gamper et al., 2004; Guo and Ikeda, 2004; Meza et al., 2007). Since $Ca_V\beta2$ expression changes developmentally (Tanaka et al., 1995) and with activity (Lie et al., 1999), synaptic output also may change over time. Patients with temporal lobe epilepsy

exhibit increased postsynaptic $Ca_V\beta2$ expression in damaged hippocampal regions. In contrast, hippocampal specimens obtained from patients who underwent surgical lesioning exhibit immunoreactivity for $Ca_V\beta$ that is indistinguishable from control patients (Lie et al., 1999).

Whether upregulation of $Ca_V\beta2$ is a response to counteract hyperexcitability or whether increased $Ca_V\beta2$ levels contribute to excitotoxic neurodegeneration has not been determined. Nevertheless, these findings document in vivo plasticity of $Ca_V\beta2$ expression. In the short term, palmitoyl acyl transferases dynamically regulate protein palmitoylation in hippocampal dendrites and cell bodies to control synaptic function (El-Husseini Ael et al., 2002; Fukata et al., 2004). Thus, expression of $Ca_V\beta2$ in postsynaptic regions should create a previously unrealized level of plasticity where the response to a transmitter, acting on its G_qPCR from moment to moment, may switch from inhibitory to excitatory depending on whether $Ca_V\beta2$a's palmitoyl groups interact with $Ca_V2.2$.

Figure 3.1 M_1R induced inhibition of recombinant N-current is blocked by a PLA_2 antagonist. HEK-M1 cells were transiently transfected with N-channel subunits $Ca_V2.2$, $\alpha_2\delta$-1 and $Ca_V\beta3$. **(A)** Working model of the slow pathway where AA release, catalyzed by PLA_2, is a necessary component to elicit N-current modulation. AA enhances current (green arrow) by acting at a distinct site that may be in the outer leaflet of the membrane (Barrett et al., 2001). AA inhibits current by acting at an intracellular site or a site within the inner leaflet (Barrett et al., 2001; Liu et al., 2001). **(B)** Summary of current inhibition after 1 minute exposure to Oxo-M. **(C)** Time course of peak inward current using 5 mM Ba^{2+} as charge carrier; before, and 3 minutes after bath application of Oxo-M (10 μM). **(D)** Representative whole-cell current traces taken from the respective time course prior to (—) and 1 min after (—) Oxo-M application. Currents were elicited every 4 seconds by stepping to a test potential of 0 mV for 100 ms. Scale bars in **D, F, H, J** correspond to 0.4 nA. **(E, F)** Modulation of N-current from tsA 201 cells stably transfected with $Ca_V2.2$, $\alpha_2\delta$-1 and $Ca_V\beta3$ and transiently transfected with M_1Rs (500-1000 ng/well) and eGFP is shown in the time course and representative sweeps as described above. The charge carrier was increased to 20 mM Ba^{2+} to improve signal to noise ratio, and accordingly the test potential was adjusted to +10 mV. **(G, H)** HEK-M1 cells were transiently transfected with N-channel subunits $Ca_V2.2$, $\alpha_2\delta$-1 and $Ca_V\beta2a$. Modulation of N-current by M_1R stimulation illustrated in a time course (**G**) and current traces (**H**). **(I, J)** N-current modulation from cells expressing HEK-M1 cells transfected as for C. Cells were exposed to the PLA_2 antagonist OPC (10 μM) for at least 3 minutes prior to application of Oxo-M.

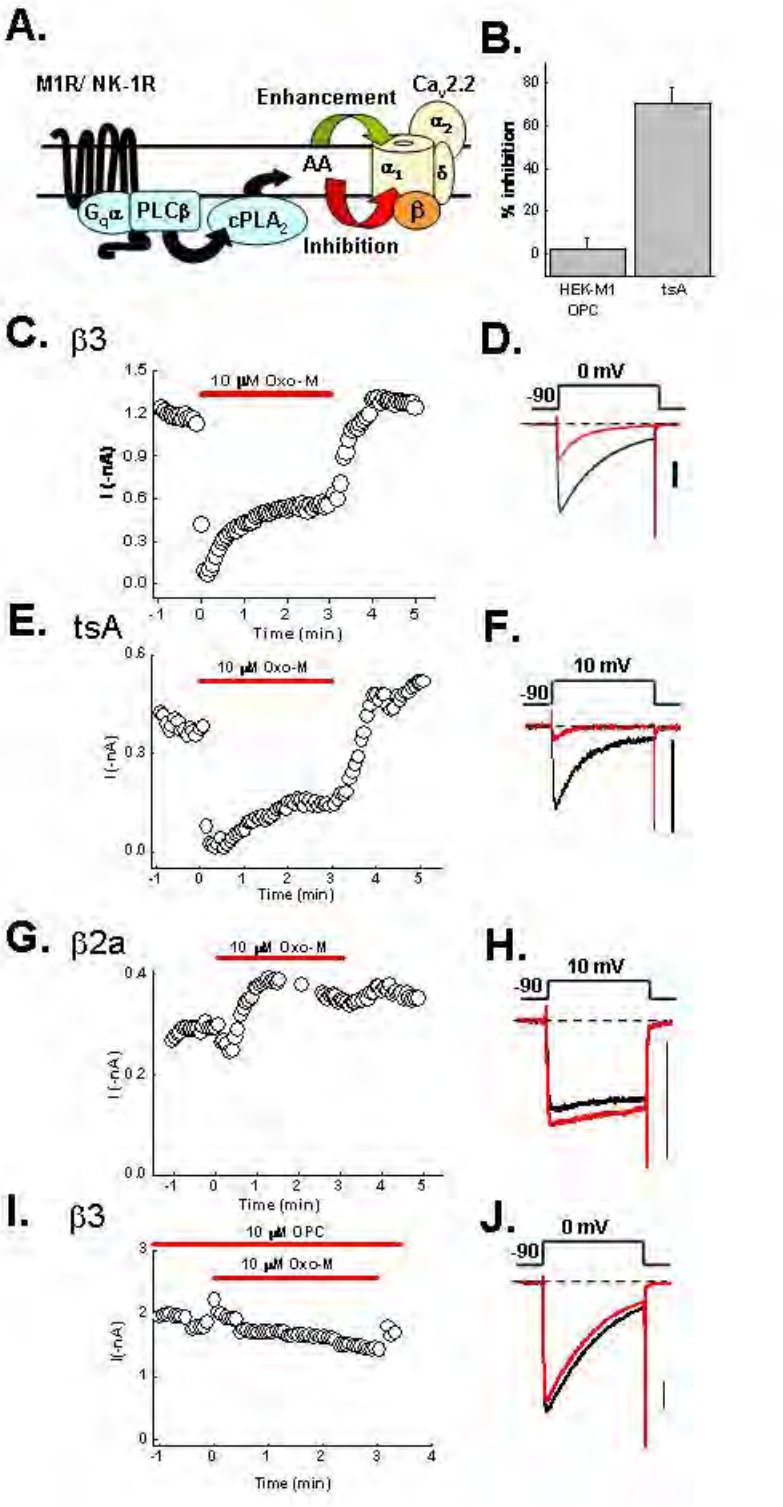
A.
M1R/ NK-1R
Enhancement
$Ca_v2.2$
α_2
AA
α_1
δ
β
$G_q\alpha$
PLCβ
$cPLA_2$
Inhibition
B.
% inhibition
80
60
40
20
0
HEK-M1
OPC
tsA
C. β3
10 μM Oxo-M
I (-nA)
Time (min)
D.
0 mV
-90
I
E. tsA
10 μM Oxo-M
I (-nA)
Time (min)
F.
10 mV
-90
G. β2a
10 μM Oxo-M
I (-nA)
Time (min)
H.
10 mV
-90
I. β3
10 μM OPC
10 μM Oxo-M
I (-nA)
Time (min)
J.
0 mV
-90

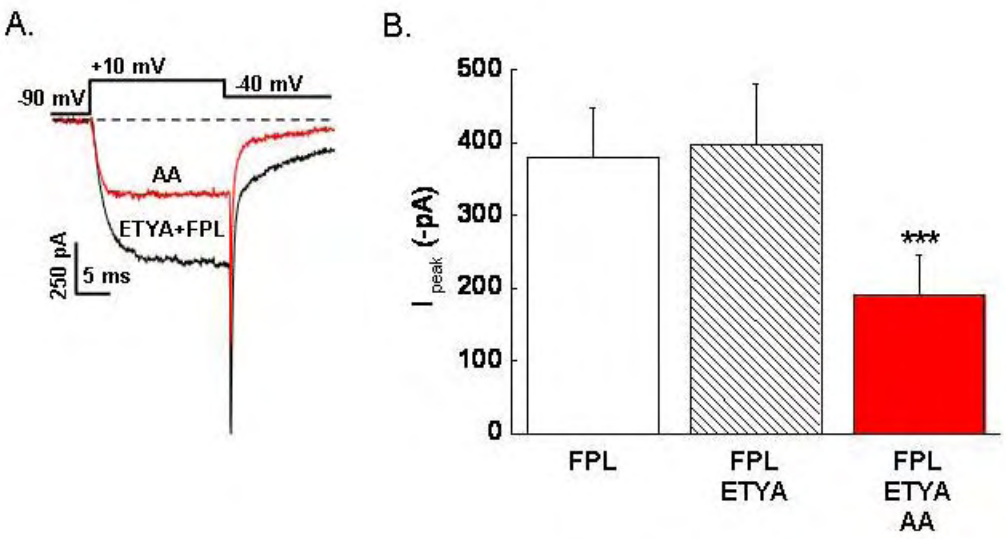

Figure 3.2 AA inhibits whole-cell current in SCG neurons. SCG neurons were acutely dissociated following the methods of Liu et al. (Liu et al., 2006). The whole-cell current is composed primarily of N-current (80-90%) and the remaining component is primarily L-current. Whole-cell currents were recorded using the voltage protocol shown above the current traces. FPL 64175 (FPL; 1 μM) was included in the bath to elicit a long-lasting tail current made up exclusively of L-type Ca2+ channel activity. ETYA (30 μM) was included in the bath to serve two functions. First ETYA will block breakdown of AA, by acting as a competitive substrate for enzymes such as cyclooxygenase and lipooxygenases that metabolize AA. Second, ETYA mimics current enhancement by AA, but not inhibition (Barrett et al., 2001). Thus under these conditions, inhibition by AA can be examined in isolation from enhancement. **(A)** In the presence of FPL and ETYA, SCG currents exhibit noninactivating kinetics. AA inhibits the noninactivating peak current primarily composed of N-current as well as the long-lasting tail current, a measure of L-current. **(B)** Summary data of the effect of AA on whole-cell currents from SCG neurons demonstrating significant inhibition by AA (***$p < 0.002$ using a two-tailed paired t-test; n=6).

Figure 3.3 $Ca_V\beta$ determines N-current modulation by G_qPCRs and AA. **(A-D)** HEK-M1 cells were transiently transfected with $Ca_V2.2$, $\alpha_2\delta$-1 and various $Ca_V\beta$ subunits. Currents, measured in 5 mM Ba^{2+}, were elicited every 4 sec by stepping from -90 to 0 mV for 100 ms unless noted. Representative whole-cell current traces were always taken prior to (▬) and 3 min after (▬) drug application. Scale bars, 0.4 nA. Averaged normalized I-V plots were taken before (●) and 90 seconds after (o) agonist application. (n=3-6 cells per group). For cells expressing $Ca_V\beta2a$, 20 mM Ba^{2+} was used as charge carrier to improve the signal to noise ratio. The test potential was adjusted to +10 mV to correct for the shift in peak inward current. **(E)** Histogram summarizing N-current modulation following 3 minutes of Oxo-M (10 μM; gray bars) and SP (5 nM; black bars). Percent change in current amplitude was highly significant between $Ca_V\beta2a$ and $Ca_V\beta1b$, $Ca_V\beta3$ or $Ca_V\beta4$ irrespective of whether Oxo-M or SP was applied (**p<0.005, one way ANOVA). **(F-I)** Modulation of N-current by 10 μM AA shown as current traces and averaged I-V plots (n=4-5 cells per group). **(J)** Histogram summarizing N-current modulation following 3 minutes of AA (**p<0.005, one way ANOVA).

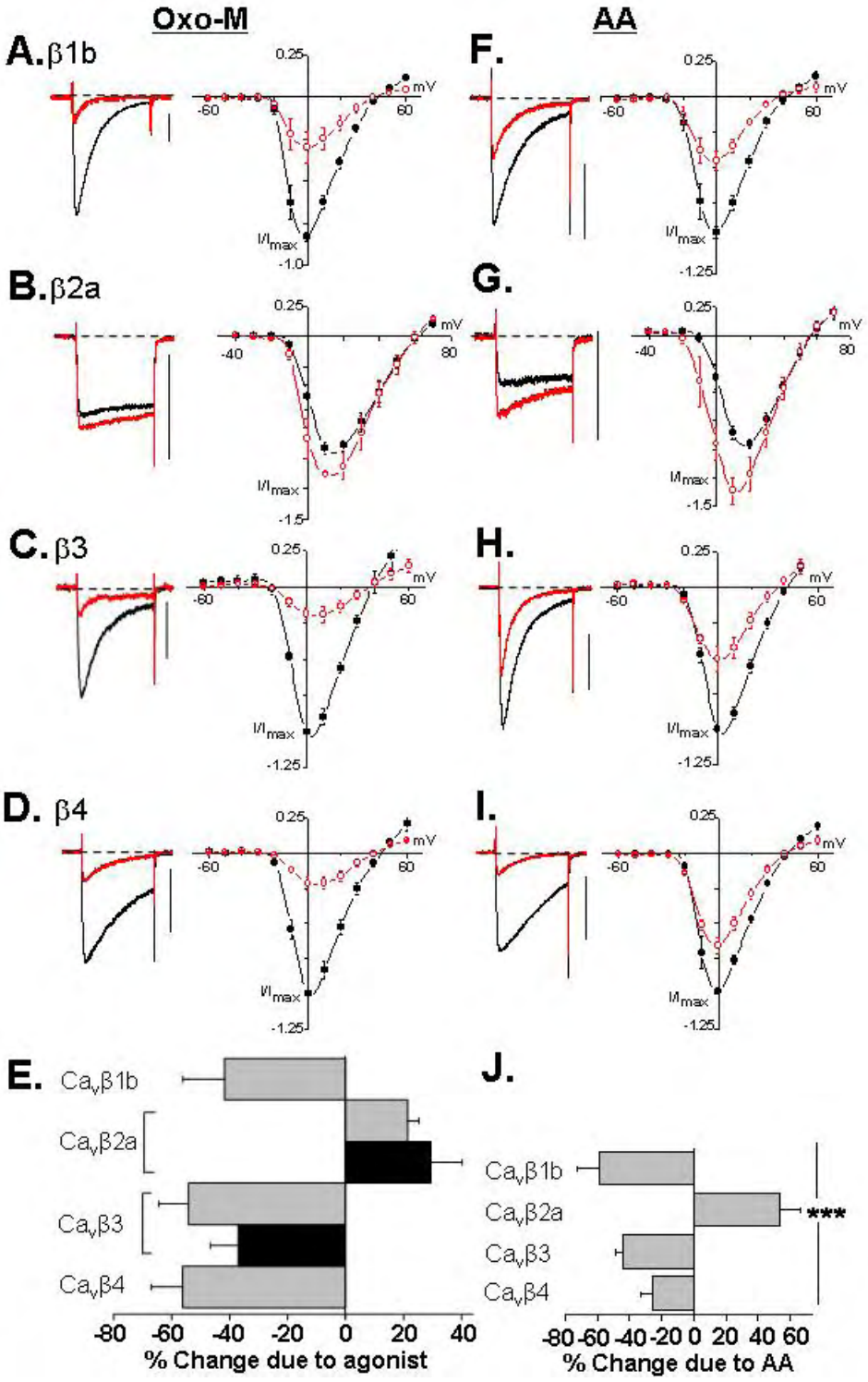
Oxo-M
AA
A. β1b
B. β2a
C. β3
D. β4
F.
G.
H.
I.
E.
J.
mV
I/I max
% Change due to agonist
% Change due to AA
Ca v β1b
Ca v β2a
Ca v β3
Ca v β4
***

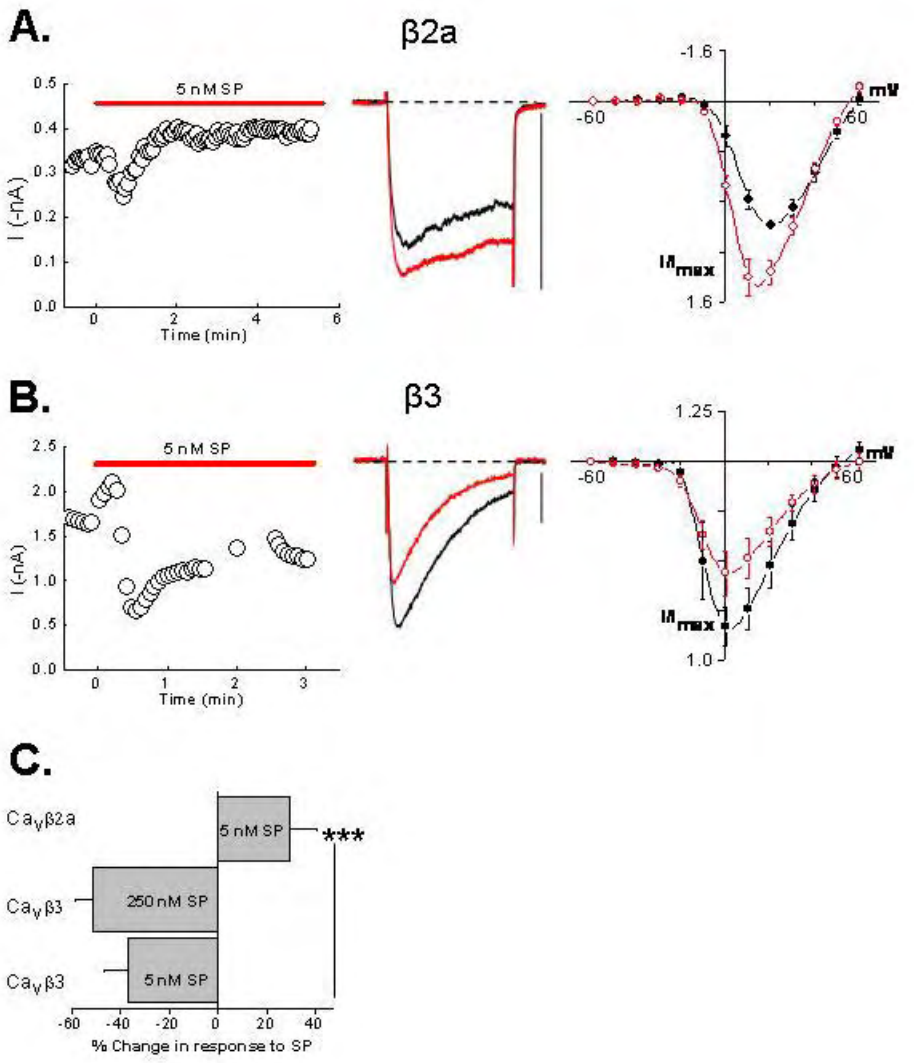

Figure 3.4 NK-1R stimulation elicits a similar profile of N-current modulation as M_1Rs. HEK-M1 cells were transiently transfected with the NK-1R along with $Ca_V2.2$, $\alpha_2\delta$-1 and either **(A)** $Ca_V\beta2a$ or **(B)** $Ca_V\beta3$. Using SP (5 nM) as the agonist, current modulation is shown in *left*, a time course of peak current; *middle*, representative whole-cell current traces; and *right*, averaged I-V plots (n=4). **(C)** Summary of the modulatory effects of SP on currents from cells expressing either $Ca_V\beta2a$ or $Ca_V\beta3$ (***p<0.005, one-way ANOVA). No significant difference in current inhibition was observed from cells expressing $Ca_V\beta3$ with 5 nM and 250 nM SP (p>0.26).

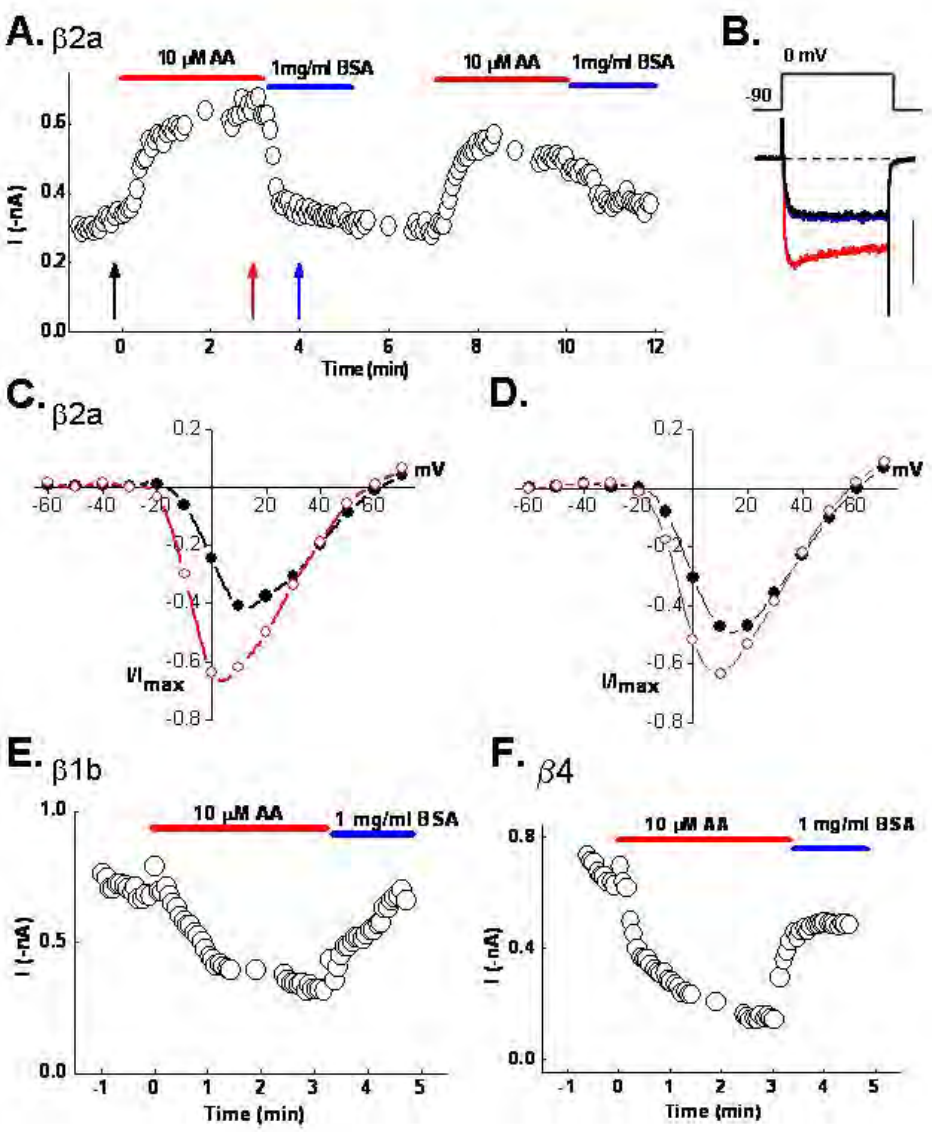

Figure 3.5 Absorption of AA with BSA minimizes N-current enhancement. Modulation of N-current by AA in HEK-M1 cells transiently transfected with $Ca_V2.2$, $\alpha_2\delta$-1, $Ca_V\beta2a$, $Ca_V\beta1b$ or $Ca_V\beta4$ is demonstrated by **(A)** time courses using 20 mM Ba^{2+} as the charge carrier before, during, and after two separate applications of AA (10 μM). Washout of AA was achieved by bath application of 1 mg/ml BSA. **(B)** Representative whole-cell current traces taken at arrows in A. **(C)** Comparison of I-V plots taken from A before (●) and after (o) the first application of AA. **(D)** Comparison of I-V plots taken after washout of AA by BSA (●) and after (o) the second application of AA. **(E, F)** Example time course of reversible inhibition of N-current from **(E)** $Ca_V\beta1b$-containing and **(F)** $Ca_V\beta4$-containing channels.

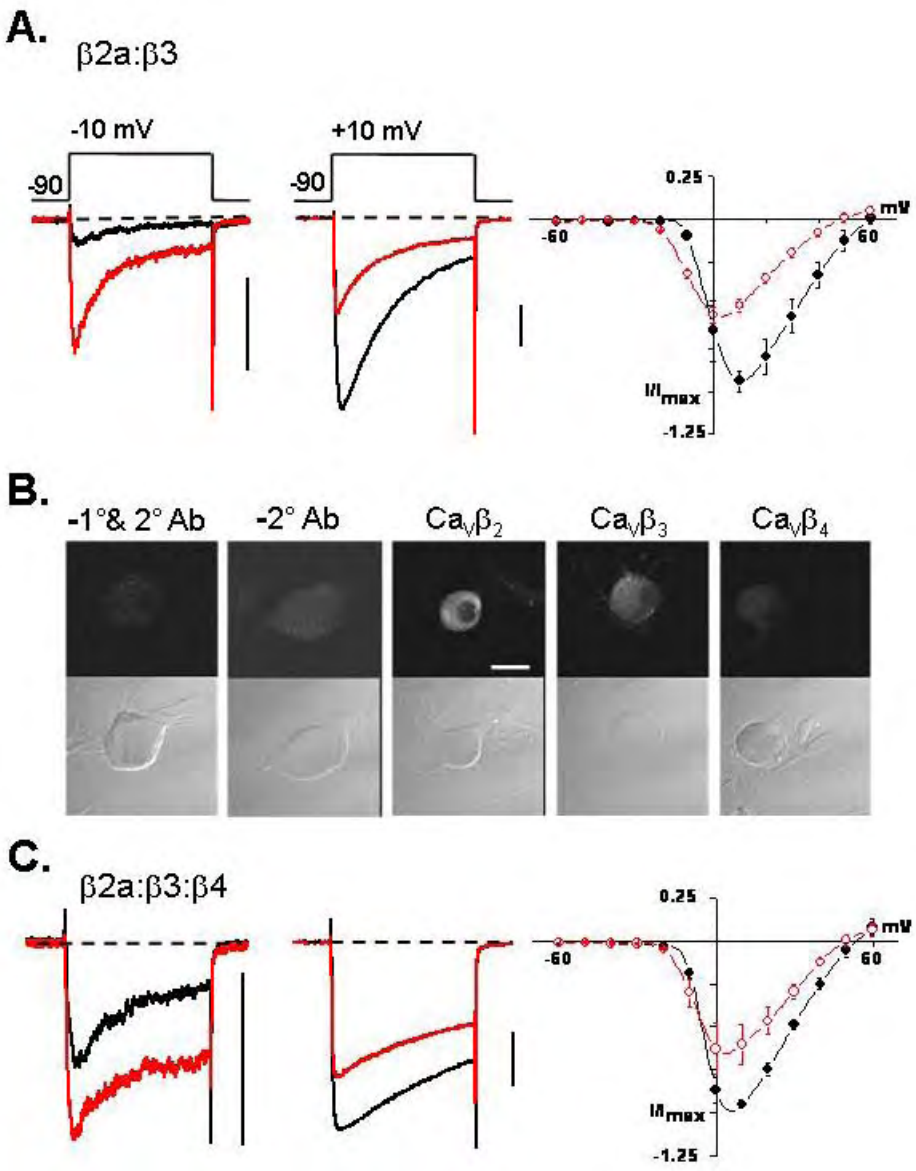

Figure 3.6 Expression of multiple $Ca_V\beta$ subunits recapitulates modulation pattern observed in SCG neurons following M_1R stimulation. Currents were recorded using 20 mM Ba^{2+}. Current traces and average I-V plots from HEK-M1 cells transiently transfected with **(A)** $Ca_V2.2$:α_2-δ-1:$Ca_V\beta2a$:$Ca_V\beta3$ in a 12:12:10:1 ratio; **(B)** *Lower panel*, individual SCG neurons shown in bright field. *Upper panel*, corresponding view when cells were excited with a wavelength of 580 nm. **(C)** $Ca_V2.2$:α_2-δ-1:$Ca_V\beta2a$:$Ca_V\beta3$:$Ca_V\beta4$ in a 12:12:10:1:1 ratio (n=3-4 cells per group).

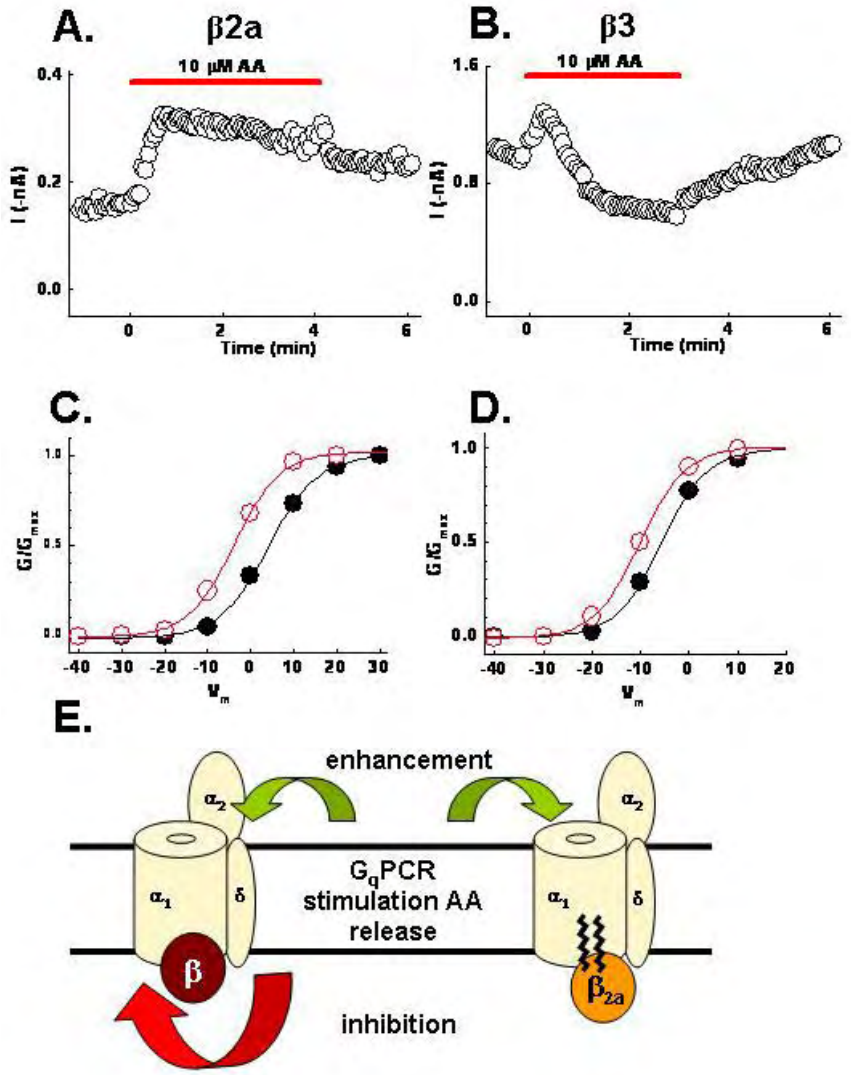

Figure 3.7 $Ca_V\beta2a$ blocks N-current inhibition revealing latent enhancement. **(A, B)** Time courses with AA. AA caused a negative shift in G/Gmax for cells expressing **(C)** $Ca_V\beta2a$ or **(D)** $Ca_V\beta3$. **(E)** Schematic representation of working model. Upon G_qPCR stimulation, the released AA can bind to both inhibitory and enhancement sites on the channel. When $Ca_V\beta3$ is present, both inhibitory and enhancement sites are available for AA to bind. However, since inhibition dominates, the resultant modulation is inhibition of current. When $Ca_V\beta2a$ is present, inhibition no longer occurs probably because the palmitoylated $Ca_V\beta2a$ blocks or occupies the inhibitory site and the resultant modulation is enhancement of current**.**

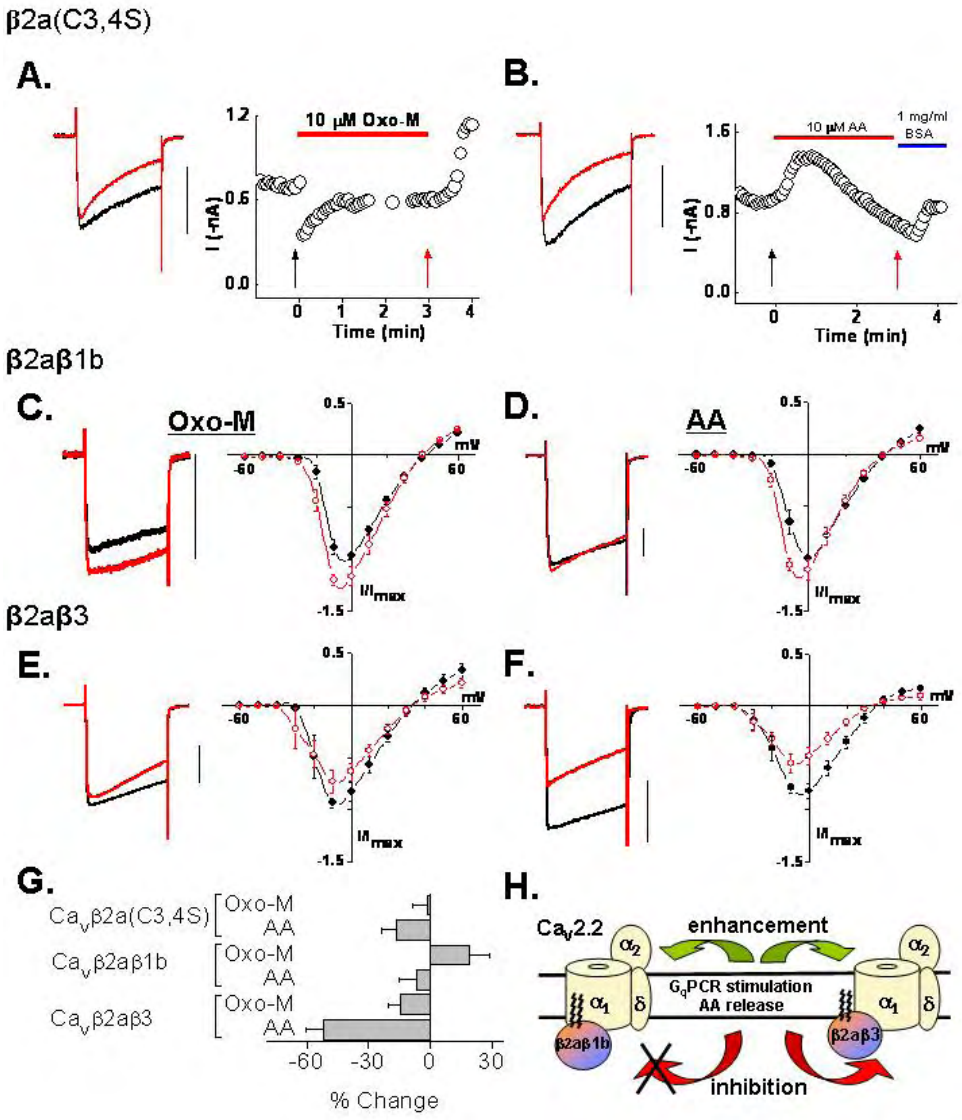

Figure 3.8 Palmitoylation determines which form of modulation is observed. Using 20 mM Ba2+, modulation by Oxo-M or AA of cells expressing **(A, B)** mutant $Ca_V\beta2a(C3,4S)$; **(C,D)** $Ca_V\beta2a\beta1b$; or **(E, F)** $Ca_V\beta2a\beta3$ is shown in current traces and I-V plots. **(G)** Summary of the modulatory effects on currents after application of Oxo-M or AA for 3 minutes (n=4-7). **(H)** Working model for N-current modulation in the presence of $Ca_V\beta2a\beta1b$ and $Ca_V\beta2a\beta3$.

Figure 3.9 Palmitic acid antagonizes inhibition of N-current by NK-1R stimulation. HEK-M1 cells were transiently transfected with NK-1R, $Ca_V2.2$, $\alpha_2\delta$-1 and $Ca_V\beta3$. **(A)** Diagram showing preincubation of HEK-M1 cells with exogenously applied palmitic acid blocks inhibition of N-channels by fatty acids, such as AA, released after NK-1R activation. **(B)** Summary showing preincubation of cells with 10 μM palmitic acid significantly attenuates inhibition by SP (*p<0.05). **(C)** Modulation of N-current by SP from cells expressing $Ca_V\beta3$ is shown in time course, current traces and I-V plots (n=5). **(D)** Preincubation of cells with palmitic acid causes loss of inhibition by SP as shown in time course, current traces and I-V plot (n=6). **(E)** Exposure of cells to either Ba (left) or palmitic acid (middle) for 8 mins has similar effect on amplitude of peak current (right) (n=4-7).

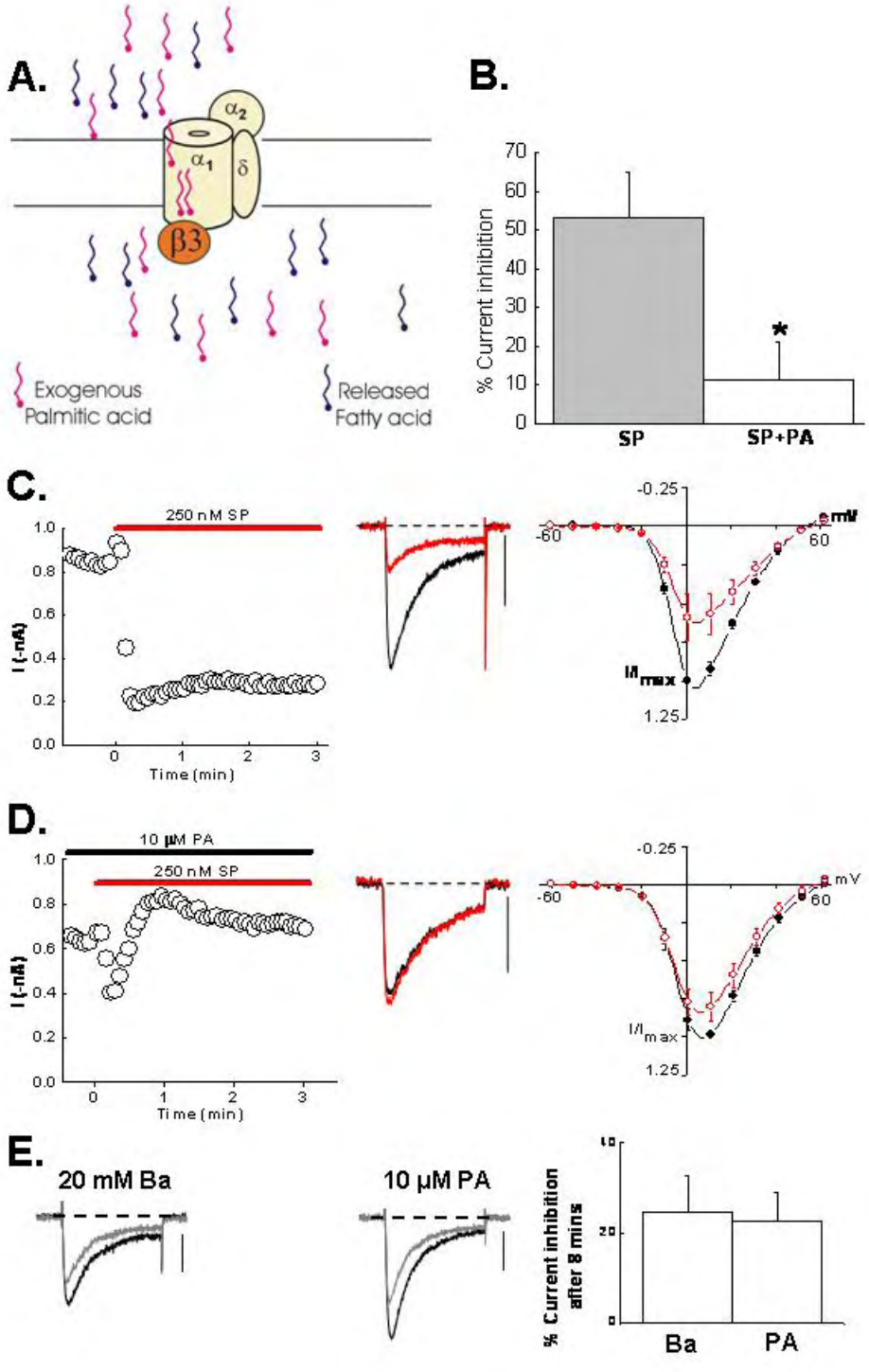
A.
α2
α1
δ
β3
Exogenous
Palmitic acid
Released
Fatty acid
B.
% Current inhibition
70
60
50
40
30
20
10
0
*
SP
SP+PA
C.
250 nM SP
I (-nA)
1.0
0.8
0.6
0.4
0.2
0.0
0
1
2
3
Time (min)
-0.25
-60
60
mV
I/Imax
1.25
D.
10 µM PA
250 nM SP
I (-nA)
Time (min)
-0.25
-60
60
mV
I/Imax
1.25
E.
20 mM Ba
10 µM PA
% Current inhibition
after 8 mins
Ba
PA

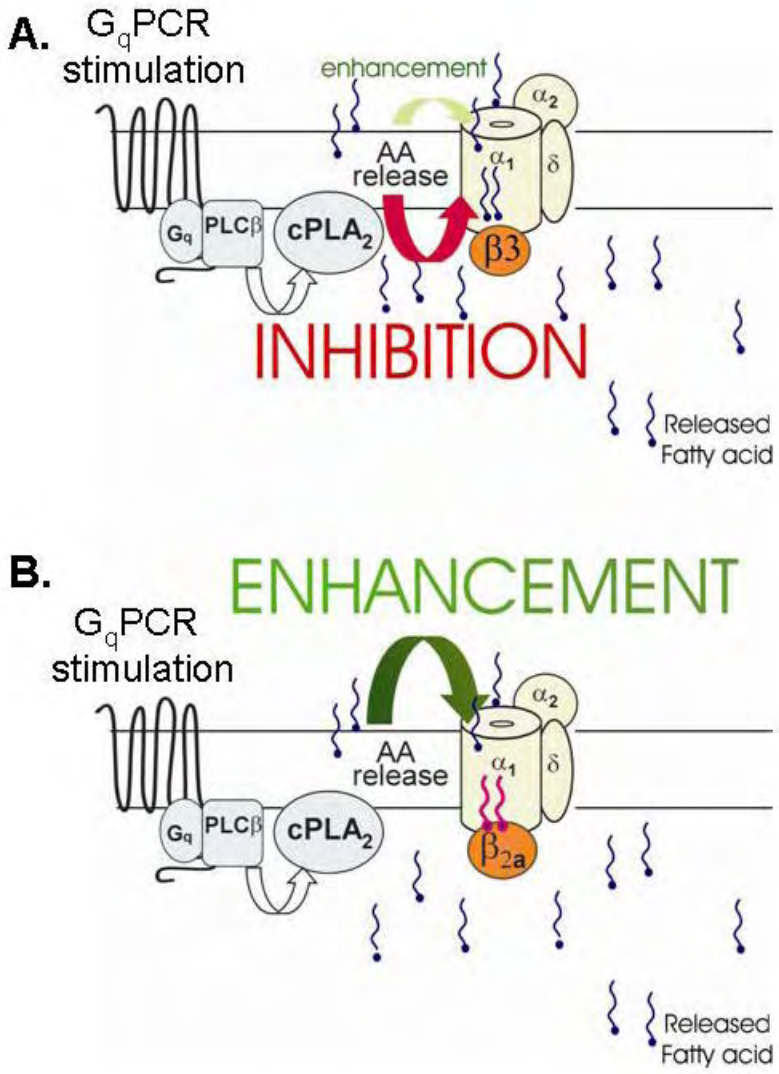

Figure 3.10 Model of interference of inhibition by palmitoylated $Ca_V\beta2a$. **(A)** As presented, our data support a model where upon G_qPCR stimulation, release of AA initially enhances N-current by acting at a site distinct from inhibition. However, N-current inhibition by AA of channels containing $Ca_V\beta1b$, $Ca_V\beta3$, or $Ca_V\beta4$, dominates modulation of $Ca_V2.2$ and obscures enhancement. **(B)** In the presence of $Ca_V\beta2a$, the palmitoylated N-terminus of the $Ca_V\beta$ subunit blocks N-current inhibition by endogenously released AA due to the two palmitic acids competitively interacting with $Ca_V2.2$ thus revealing latent enhancement.

CHAPTER IV:

Orientation of palmitoylated $Ca_v\beta2a$ relative to $Ca_v2.2$ is critical for slow pathway modulation of N-current by the tachykinin receptor NK-1R

ABSTRACT

The G_q-coupled tachykinin receptor (NK-1R) modulates N-type Ca^{2+} channel ($Ca_V2.2$ or N-channel) activity at two distinct sites by a pathway involving a lipid metabolite, most likely arachidonic acid (AA). In the previous study, we found that the form of modulation observed depends on which accessory $Ca_V\beta$ subunit is co-expressed with $Ca_V2.2$. When palmitoylated $Ca_V\beta2a$ is co-expressed, activation of NK-1R by substance P (SP) enhances N-current. In contrast, when $Ca_V\beta3$ is co-expressed, SP inhibits N-current. However, exogenously applied palmitic acid minimizes this inhibition. These findings raise the possibility that the palmitoyl groups of $Ca_V\beta2a$ may occupy an inhibitory site on $Ca_V2.2$, or prevent AA from interacting with that site, thereby minimizing inhibition. If so, changing the orientation of $Ca_V\beta2a$ relative to $Ca_V2.2$ may displace the palmitoyl groups and prevent them from antagonizing AA at the inhibitory site thereby allowing inhibition even in the presence of $Ca_V\beta2a$. Here we tested this hypothesis by deleting one (Bdel1) or two (Bdel2) amino acids proximal to the alpha interacting domain (AID) of $Ca_V2.2$'s I-II linker. $Ca_V\beta$s bind tightly to the AID while the

rigid and helical region proximal to the AID is thought to regulate $Ca_V\beta$'s orientation and consequently its secondary interactions with $Ca_V2.2$. While Bdel1 currents exhibited more variable enhancement by SP, Bdel2 current enhancement was lost at all voltages; instead, inhibition was observed. This inhibition remarkably mimicked the profile of current inhibition elicited from wt $Ca_V2.2$ co-expressed with $Ca_V\beta3$. Moreover, adding back exogenous palmitic acid minimized inhibition of Bdel2 currents. These findings support the hypothesis that $Ca_V\beta2a$'s palmitoyl groups, when appropriately positioned, can minimize N-current inhibition following NK-1R activation by preventing endogenously released AA from binding to the N-channel's inhibitory site.

INTRODUCTION

NK-1R couples to a G_q signal transduction cascade (Macdonald et al., 1996) to release inflammatory products from phospholipid breakdown and mediates nociception (Duffy, 2004). N-type voltage-gated Ca^{2+} (N-channels) appear to be involved in transmission of nociceptive signals to the spinal cord since selectively antagonizing N-current disrupts substance P release from spinal cord slices (Smith et al., 2002). At the level of the whole organism, $Ca_V2.2$ knockout mice display reduced responses to neuropathic and inflammatory pain (Hatakeyama et al., 2001; Saegusa et al., 2001). Pharmacological antagonists of N-channels also effectively relieve pain (Schroeder et al., 2006), suggesting that N-channels may serve as a target of NK-1Rs to transduce pain signals into neuronal activity. Indeed NK-1Rs inhibit N-current using a similar pathway to that which mediates pain. N-current inhibition by SP requires activation of G_q and

Ca^{2+}-dependent phospholipase C (PLC) downstream of NK-1R activation (Shapiro and Hille, 1993; Kammermeier et al., 2000). In sympathetic neurons, M_1 muscarinic receptors (M_1Rs) converge on the same pathway, therefore called the slow pathway. Its stimulation results in voltage-independent, BAPTA-sensitive and phospholipase A_2 (PLA_2)-dependent inhibition of N-current (Beech et al., 1992; Shapiro and Hille, 1993; Kammermeier et al., 2000; Liu and Rittenhouse, 2003a).

Exogenously applied AA or stimulation of M_1Rs or NK-1Rs enhance as well as inhibit N-current (Barrett et al., 2001; Liu et al., 2001; Liu and Rittenhouse, 2003a); Chapter III). As shown in Chapter III, the form of modulation observed depends on which accessory $Ca_V\beta$ subunit is coexpressed with $Ca_V2.2$. When $Ca_V\beta1b$, $Ca_V\beta3$, or $Ca_V\beta4$, is present, AA (or receptor agonist) rapidly enhances N-current; however enhancement quickly progresses to robust inhibition. In contrast, currents from $Ca_V\beta2a$-containing channels exhibit sustained enhancement. Of the known $Ca_V\beta$ subunits, only $Ca_V\beta2a$ is palmitoylated on its two N-terminal cysteine residues (Chien et al., 1996; Takahashi et al., 2003). We hypothesized that persistent enhancement may result from the palmitoyl groups of $Ca_V\beta2a$ assuming a position within the membrane that prevents AA from interacting with the N-channel's inhibitory site(s) (Chapter III). In support of this possibility, we found that AA no longer enhanced but instead inhibited N-current from channels containing a depalmitoylated $Ca_V\beta2a$ [$Ca_V\beta2a$(C3,4S)] (Chien et al., 1996) (Chapter III). Additionally, when $Ca_V\beta2a$'s N-terminus was substituted into $Ca_V\beta1b$ to form a chimeric $Ca_V\beta2a/\beta1b$ (Chien et al., 1998), N-current was no longer inhibited (Chapter III), consistent with the palmitoyl groups preventing inhibition. Lastly,

exogenously applied palmitic acid successfully minimized the inhibition normally observed with $Ca_V\beta3$. Taken together, these findings suggested that the palmitoyl groups are sufficient for preventing N-current inhibition via the slow pathway.

From these findings, we proposed a model in Chapter III whereby the palmitoyl groups of $Ca_V\beta2a$ (Fig. 4.1B) interact with $Ca_V2.2$ at the inhibitory site normally occupied by AA released during phospholipid breakdown that follows stimulation of PLC. For such an interaction to occur, $Ca_V\beta2a$ must reside in a specific orientation so that the palmitoyl groups situate close to or overlap with the channel's inhibitory site (Fig 4.1D). However, while our previous findings suggest that the palmitoyl groups may compete for an inhibitory site on $Ca_V2.2$, they do not rule out the possibility that nonspecific actions of free or tethered palmitic acid disrupt inhibition. Therefore, we tested whether changing $Ca_V\beta2a$'s orientation relative to $Ca_V2.2$ rescues inhibition (Fig. 4.1B).

All $Ca_V\beta$s bind with high affinity to the cytoplasmic linker between domains I and II (Fig. 4.1B) at the alpha-interacting domain (AID) (Pragnell et al., 1994; Chen et al., 2004; Opatowsky et al., 2004; Van Petegem et al., 2004). Their presence tunes the gating properties of channels possibly by modulating the movements of IS6. The region proximal to the AID appears to couple $Ca_V\beta$'s movements to regulate the gating properties of the channel (Vitko et al, submitted). This IS6-AID segment appears to form, in part, a rigid helical structure that regulates the orientation of $Ca_V\beta2a$ and consequently its secondary interactions with $Ca_V2.2$. By deleting one (Bdel1) or two (Bdel2) amino acids in the IS6-AID segment (Fig 4.1C), the orientation of $Ca_V\beta2a$ to $Ca_V2.2$ should

change with each shift in the helix. When the mutated channels were tested for sensitivity to SP, Bdel1 exhibited minimal current enhancement, while Bdel2 rescued current inhibition by the slow pathway. In turn, exogenous palmitic acid reduced Bdel2/β2a current inhibition. This is the first demonstration that the orientation of a palmitoylated cytoplasmic protein alters the regulation of a transmembrane protein: $Ca_V2.2$.

MATERIAL AND METHODS

Site directed mutagenesis

The cDNA encoding the rat brain $Ca_V2.2$ (GenBank entry #AF055477) was cloned into the plasmid vector pcDNA6 (Lin et al., 1997). A 1.5 kb fragment was subcloned into pCR2.1-TOPO (Invitrogen, Carlsbad, CA), then mutated using the Quikchange® protocol and *Pfu* Ultra DNA polymerase (Stratagene, La Jolla, CA). Oligonucleotide primers were obtained from Invitrogen and used without purification. All restriction enzymes were purchased from New England Biolabs (Ipswich, MA). The full-length cDNA was reassembled in the original plasmid vector that was cut with *Asc*I and *Bsi*WI by ligating the following fragments: *Asc*I(32)/*Blp*I(355), *Blp*I/*Sac*I (1407), and *Sac*I/*Bsi*WI (2991). The Bdel1 and Bdel2 amino acid mutations were contained in the *Blp*I/*Sac*I fragment, and the sequence of this fragment was verified for each mutant by automated sequencing at the University of Virginia Biomolecular Research Facility.

Transfection

Human embryonic kidney (HEK) cells with a stably transfected M_1R (HEK-M1) were grown at 37°C with 5% CO_2 in Dulbecco's MEM (DMEM)/F12 supplemented with

10% FBS, 1% G418, 0.1% Gentamicin and 1% HT supplement (Gibco Life Technologies, Grand Island, NY). For transfection, cells were plated in 12-well plates at 50-80% confluency. Cells were transiently transfected using Lipofectamine and PLUS reagents (Invitrogen, Carlsbad, CA) as per the manufacturer's instruction. The transfection mixture consisted of plasmids encoding wt or mutant $Ca_v2.2$ e[^{a}10, Δ18a, Δ24a, 31a, 37b, 46] (#AF055477; Vitko et al., submitted; Fig 1C), $\alpha_2\delta$–1 (#AF286488;) and either $Ca_V\beta$2a (#M80545) or $Ca_V\beta$3 (#M88751) at a 1:1:1 molar ratio. 28 ng/well of plasmid encoding NK-1R (#AY462098; UMR cDNA Resource Center, University of Missouri, Rolla, MO) and enhanced green fluorescent protein cDNA (used at less than 10% of total cDNA), were also included in the transfection medium. Cells were plated on poly-L-lysine coated coverslips 24-72 hours post transfection. However, currents elicited from Bdel1 and Bdel2 mutants were not detectable using the above-mentioned transfection protocol. To boost mutant expression by increasing transcription, 80 ng of plasmid containing the SV40 T antigen was included during transfection. Currents were recorded between 24 and 76 hours post transfection.

Electrophysiology

Whole-cell Ba^{2+} currents were recorded at room temperature (20-24°C) using a Dagan 3900a patch clamp amplifier (Dagan Instruments Inc., Minneapolis, MN). Currents were filtered at 1-5 kHz using the amplifier's four-pole low-pass Bessel filter and digitized at 20 kHz with a CED micro1401 interface [Cambridge Electronic Design, (CED), Cambridge, UK]. Data were collected using Signal 2.16 software (CED) and

stored on a personal computer. Prior to analysis, capacitive and leak currents were subtracted using a scaled-up hyperpolarizing test pulse to -100 mV. For all recordings, cells were held at -90 mV and given either a 24 or 100 ms depolarization to the test pulse indicated. Unless mentioned, the protocol was repeated every 4 sec. For prepulse experiments, a 24 ms depolarization was followed 250 ms later by a step depolarization to +120 mV for 25 ms, then followed 30 ms later by another 24 ms depolarization (see Fig 4.2D) and repeated every 10 sec. Electrodes were pulled from borosilicate glass capillary tubes. Each electrode was fire-polished to ~1 μm to yield a pipette resistance of 2-3 MΩ. The external solution contained (in mM): 125 N-methyl glucamine (NMG)-aspartate, 10 HEPES and 5 or 20 barium (Ba^{2+}) acetate, pH was adjusted to 7.5 with CsOH. When the Ba^{2+} concentration was lowered from 20 mM to 5 mM (for recording wt $Ca_v2.2$ currents), 135 NMG-aspartate was substituted for Ba^{2+}. The internal solution of the pipette consisted of (in mM): 135 Cs-aspartate, 10 HEPES, 0.1 1,2-bis(O-amino-phenoxy)ethane-N,N,N',N'-tetraacetic acid (BAPTA), 5 $MgCl_2$, 4 ATP, and 0.4 GTP; the pH was adjusted to 7.5 with CsOH. When 20 mM BAPTA was included in the pipette solution, the Cs-aspartate concentration was lowered accordingly in the internal solution.

Bimolecular fluorescence Complementation (BiFC)

BiFC imaging was carried out as per methods earlier described (Vitko et al., submitted). Briefly, a small C-terminal (a.a. 159-238) sequence of cyan fluorescent protein (CFP) was fused to the C-terminus of full length β2a. The big N-terminal fragment of CFP (a.a. 1-158) was fused to the N-terminus of $Ca_V2.2$, Bdel1 or Bdel2.

Plasmids encoding $Ca_V2.2$, Bdel1 or Bdel2 (250 ng), $\alpha_2\delta$-1 (1 μg) and full length β2a (1 μg) were transiently transfected into HEK-293 cells. After 18 hrs the cells were plated onto polylysine-treated glass bottom dishes (Fluorodish, World Precision Instruments, Saratoga, FL).BiFC was visualized by cyan fluorescence signals which were collected with IPLab software and a Cooke Sensicam QE (Romulus, MI) mounted on an Olympus BX61WI (100x objective, 2x2 binning) equipped with an Olympus confocal spinning disk unit (Melville, NY). Digital images were background subtracted using a region devoid of cells.

Pharmacology

SP was prepared as a 0.5 mM stock solution in 0.05 M acetic acid and stored at -20°C. To make a working concentration of 5 nM, the stock was serially diluted with bath solution daily. Palmitic acid was dissolved in 100% ethanol to make a stock solution. Working solutions were made by diluting the stock 1:1,000 times with bath solution. Bovine serum album (BSA; fraction V, heat shock, fatty acid ultra-free; Roche Applied Science, Indianapolis, IN) was dissolved in the bath solution and diluted further to make a final concentration of 1mg/ml. All chemicals were obtained from Sigma-Aldrich Inc. (St. Louis, MO) except where noted. Drugs were applied with a gravity-driven bath perfusion system and complete bath exchange was achieved within 10-14 sec.

Data analysis

After the onset of the pulse, maximal inward current of whole-cell traces was measured using Signal 2.16 (CED). Percent change in current amplitude was measured as [(I-I')/I]*100, where I is the average amplitude of peak current measured from 5 current traces prior to drug application and I' is the average current amplitude measured from 5 current traces atleast 2 mins after application of SP, unless otherwise noted. Data were acquired and analyzed using IPLab 4.0 (Scanalytics, Fairfax, VA) as described previously (Vitko et al., 2007).

Statistical Analysis

Summary data are presented as mean ± s.e.m (standard error of the mean). Average current amplitude before and after application of SP was compared using a two-tailed paired t-test. Two means were compared using a two-way Student's *t*-test. Statistical significance was set at $p<0.05$ or $p<0.001$. Data was analyzed using Excel (Microsoft, Seattle, WA) and Origin (OriginLab, Northampton, MA).

RESULTS

SP enhances wt $Ca_v2.2$ current via a BAPTA-sensitive pathway.

To test whether palmitoylated $Ca_V\beta2a$ blocks inhibition to reveal enhancement, we first characterized several biophysical properties of N-current enhancement by NK-1R in a recombinant system. First, we tested whether the enhancement of N-current as with

inhibition occurs via a BAPTA- sensitive pathway. Application of 5 nM SP enhanced currents (Fig 4.2A left, 4.2B). To chelate intracellular Ca^{2+}, 20 mM BAPTA was dialyzed into cells for at least 2 min. Under these conditions, SP no longer enhanced currents (Fig 2A right, 4.2B). Thus enhancement involves a BAPTA-sensitive pathway similar to that shown earlier for M_1R-mediated N-current inhibition (Beech et al., 1991; Bernheim et al., 1991; Mathie et al., 1992; Liu et al., 2001; Liu and Rittenhouse, 2003a).

Second, we tested whether enhancement as with inhibition, is insensitive to prepulses. Similar to our previous studies using exogenously applied AA (Barrett et al., 2001; Liu et al., 2001) or activation of either M_1Rs (Liu and Rittenhouse, 2003a) or NK-1Rs (Chapter III), current enhancement occurs at -10 and 0 mV (Fig 4.2C). The current-voltage (I-V) plot reveals that maximal current enhancement occurs 10 mV negative to the voltage that elicits peak inward current (in this case +10 mV; Fig 4.2C). Hence, we measured whole-cell currents over time by stepping to a test potential 10 mV to the left of where maximal peak current occurs. While a slight relief from tonic prepulse inhibition is observed using this protocol under control conditions, following SP application both P1 and P2 currents exhibit similar significant enhancement (62 ± 18% and 50 ± 11%; $p<0.01$ compared to control currents) (Fig. 4.2D, E).

Third, AA-induced enhancement of N-current coincides with an increased rate of activation, in SCG neurons (Barrett et al., 2001). Therefore, we tested whether enhancement of recombinant N-current by SP involves an increase in activation kinetics, detected as a change in time to peak inward current (TTP). We measured the TTP of $Ca_V2.2$ currents before and after application of SP. As shown in Fig 4.2F, SP significantly

decreased TTP ($p<0.05$; n=6), when $Ca_V\beta2a$ was co-expressed with $Ca_V2.2$. Taken together, these three tests indicate that enhancement involves a similar slow pathway as N-current inhibition by SP.

Modulation of mutant Bdel1 current by SP is disrupted.

Since Bdel1 has a single amino acid deletion in the middle of the helical IS6-AID segment (Vitko et al., submitted; Fig 4.1C), the bound palmitoylated $Ca_V\beta2a$ may reorient to a different position relative to Bdel1. We hypothesized that if $Ca_V\beta2a$ is sufficiently displaced, the palmitoyl groups will move from the inhibitory site and inhibition will occur (Fig 4.3A). Although SP enhanced Bdel1/β2a currents in 7 of 7 cells (Figs 4.3B, C), enhancement varied from as little as 12% to as high as 135% and hence was not significant (Fig 4.3D). To rule out the possibility that inhibition could not be recovered due to a change in $Ca_V2.2$'s inhibitory site, we tested Bdel1 mutants co-expressed with $Ca_V\beta3$ for modulation by SP. Indeed, SP inhibited currents of Bdel1 co-expressed with $Ca_V\beta3$ by 32 ± 10% ($p<0.05$; Figs 4.3E, F). The magnitude of inhibition did not differ significantly from wt $Ca_V2.2/\beta3$ currents indicating that the site of inhibition remained unaffected by the amino acid deletion in the IS6-AID segment.

SP inhibits Bdel2 currents in the presence of palmitoylated β2a.

To determine whether an additional amino acid deletion affects current modulation, we tested the Bdel2 mutant (Fig 4.1C) for modulation. We hypothesized that the additional deletion would further displace $Ca_V\beta2a$ from its normal position resulting in disruption of N-current modulation (Fig 4.4A). After application of SP, robust

inhibition of Bdel2 current was observed rather than enhancement (Figs 4.4B-D). Inhibition was observed at all voltages (Fig 4.4B) and was not relieved following a prepulse (P1: 46 ± 7%; P2: 45 ± 8%; $p<0.05$ compared to control currents before application of SP; Fig 4.4C, D).

To determine whether the amino acid deletions may affect tonic facilitation of control currents, we measured the control prepulse facilitation ratio, measured by the ratio of peak P2 current to peak P1 current. While Bdel1 currents showed a loss of prepulse facilitation, the ratio for Bdel2 was significantly higher than Bdel1; Bdel2 currents were further decreased rather than being enhanced after a prepulse (Figs 4.4E). Overall, current modulation by SP exhibited unique properties with each change in the orientation of $Ca_V\beta2a$: enhancement of N-current normally observed with wt $Ca_V2.2/\beta2a$ channels becomes more variable with Bdel1/β2a channels, while Bdel2/β2a currents exhibit robust inhibition similar to $Ca_V2.2/\beta3$ currents (Fig 4.4F).

To confirm that differences in modulation of the Bdel mutants compared to wt $Ca_v2.2$ does not arise from a difference in their expression levels, we performedBiFC analysis (Kerppola, 2006; Vitko et al., submitted) using wt $Ca_V2.2$, Bdel1 and Bdel2 with Cavβ2a. In this method, CFP is split into two fragments: one fragment is fused to $Ca_V2.2$'s N-terminus and the other fragment is fused to $Ca_V\beta2a$'s C-terminus. Fluorescence occurs when the two non-fluorescent components of CFP associate or reside close enough to each other to bind, forming an intact fluorescing CFP. We found that wt $Ca_V2.2$, Bdel1 and Bdel2 coexpressed with $Ca_V\beta2a$ produced a fluorescent signal at the plasma membrane (Fig 4.5).

Inhibition of Bdel2/β2a currents by SP mimics inhibition of wt $Ca_V2.2/\beta3$ currents.

By deleting amino acids in the IS6-AID segment, N-current modulation changes from robust enhancement to robust inhibition. We wanted to determine whether inhibition of Bdel2/β2a currents occurs via the slow pathway similar to inhibition of $Ca_V2.2/\beta3$ or Bdel1/β3 currents. Since Bdel2/β3 currents inactivate so rapidly that their peak current could not be compared to modulation of other N-channel complexes (Vitko et al., submitted), we did not examine Bdel2/β3 for inhibition by SP. Instead, we took a pharmacological approach to determine whether the same slow pathway used to inhibit wt $Ca_V2.2/\beta3$ currents confers Bdel2/β2a current inhibition. First, we tested whether bovine serum album (BSA) minimizes N-current inhibition by SP. When BSA is included in the bath solution, inhibition of native and recombinant N-current by M_1R stimulation is lost (Liu and Rittenhouse, 2003a; Liu et al., 2006; Chapter III). Since BSA sequesters free AA released from phospholipids following receptor activation (Liu et al., 2006), decreased N-current inhibition is attributed to decreased availability of free AA. When we recorded currents in the presence of BSA, current inhibition by SP normally observed with both $Ca_V2.2/\beta3$ and Bdel2/β2a (Fig. 4.6A, D) was lost (Fig 4.6B, D).

We also tested whether N-current inhibition of $Ca_V2.2/\beta3$ and Bdel2/β2a channels by SP occurs via a BAPTA-sensitive pathway (Beech et al., 1991; Bernheim et al., 1991; Mathie et al., 1992). In the presence of 20 mM BAPTA, N-current inhibition by SP is no longer significant (Figs 4.6C, D) similar to wt $Ca_V2.2/\beta3$. Additionally $Ca_V2.2/\beta3$ current inhibition by SP is not relieved by a prepulse consistent with inhibition occurring via a voltage-independent pathway (Kammermeir et al., 2000, n=6 data not shown).

Comparison of Bdel2/β2a and $Ca_V2.2$/β3 current inhibition (Fig 4.6D) shows that for both currents, inhibition involves a voltage-independent, BAPTA-sensitive pathway that utilizes a free fatty acid, most likely AA as an effector. These findings are consistent with Bdel2/β2a current inhibition by SP occurring by a similar mechanism as $Ca_V2.2$/β3 current inhibition by the slow pathway (Fig 4.1A; Chapter II).

Free palmitic acid blocks inhibition of Bdel2 currents

In Chapter III, we found that exogenous application of palmitic acid blocks inhibition of $Ca_V2.2$/β3 currents by SP. If inhibition of Bdel2/β2a currents involves a similar pathway as inhibition of $Ca_V2.2$/β3 currents, exogenously applied palmitic acid also should minimize inhibition of Bdel2/β2a currents following SP application. To test this hypothesis, cells expressing Bdel2 and Ca_Vβ2a were preincubated with 10 μM palmitic acid for at least 8 min prior to application of SP (Fig 4.7A). Under these conditions, current inhibition by SP (Fig 4.7C, E) was reduced by more than 50% compared to recordings in the absence of palmitic acid (46 ± 7%; $p<0.05$ compared to inhibition by SP in the absence of palmitic acid; Fig 4.7C, D). This finding supports our model where the palmitoyl groups of Ca_Vβ2a (Fig 4.7B) antagonize N-current inhibition by free AA that is released upon SP application.

DISCUSSION

We hypothesized that when $Ca_V\beta2a$ is displaced sufficiently such that its palmitoyl groups can no longer interact with an inhibitory site, the N-current enhancement, normally observed with SP should be replaced by inhibition. Using Bdel1 mutant channels co-expressed with $Ca_V\beta2a$, we found that the single amino acid deletion in the helical IS6-AID segment, predicted to rotate $Ca_V\beta2a$'s position relative to the Bdel1 channel resulted in highly variable N-current enhancement. Furthermore, deleting two amino acids in the IS6-AID segment to form Bdel2 channels resulted in robust N-current inhibition by SP. We found that the same signal transduction pathway involving phospholipid metabolism that mediates inhibition of wt N-current, also mediates both enhancement of wt N-current and inhibition of Bdel2/β2a current. (Figs. 4.2 and 4.6). Inhibition of both $Ca_V2.2/\beta3$ and Bdel2/β2a currents are minimized by exogenous application of 10 μM palmitic acid (Chapter III and Fig. 4.7). These findings support the hypothesis that the palmitoyl groups interact with a site on $Ca_V2.2$ that overlaps with a site that confers inhibition by the slow pathway.

N-current enhancement and inhibition involve a similar voltage-independent slow pathway

Inhibition of native and recombinant N-current by G_q-coupled NK-1R via a voltage-independent pathway was first characterized in SCG neurons (Shapiro and Hille, 1993; Kammermeier et al., 2000). More recently enhancement of native N-current (Liu and Rittenhouse, 2003a) and recombinant $Ca_V2.2$ and $Ca_V2.3$ current by M_1Rs and NK-

1Rs has been described (Meza et al., 2007; Chapter III). In the presence of $Ca_V\beta 2a$, M_1R activation enhances N- but not L-currents (Chapter III; Roberts-Crowley, submitted). These two channels show similar transmembrane organization (Catterall, 2000). Hence, the difference in modulation that is observed cannot arise from any non-specific effect such as changes in the lipid bilayer that might alter gating.

To understand the mechanism for current enhancement, we first show that enhancement occurs via a signaling pathway (Fig 4.1 and 4.2) that is minimized using high concentrations of BAPTA similar to the slow pathway described for inhibition of native N-current in SCG neurons and hippocampal pyramidal neurons by M_1Rs (Beech et al., 1991; Bernheim et al., 1991; Mathie et al., 1992; Shapiro and Hille, 1993; Liu and Rittenhouse, 2003b; Tai et al., 2006) and recombinant R-type ($Ca_V2.3$) current by NK-1R in HEK cells (Meza et al., 2007). Additionally we found that following a strong depolarizing prepulse, current enhancement by SP remained unchanged. N-current inhibition by SP exhibits these same two properties (Chapters II and V). Taken together, these findings suggest that while enhancement and inhibition may occur at different sites on N-channels they are different manifestations of overlapping or the same signaling pathway.

Orientation of $Ca_V\beta 2a$ is important for proper channel modulation

To test our hypothesis that a specific orientation of $Ca_V\beta 2a$ is required, we used two mutants of $Ca_V2.2$ that align the $Ca_V\beta 2a$ subunits differently relative to $Ca_V2.2$. $Ca_V\beta$ does not regulate the the opening probability of Bdel1 channels and also fails to

regulate the kinetics of activation and inactivation of Bdel1 and Bdel2 currents (Vitko et al., submitted). This could be due to a loss of interaction between the α1 subunit and the low affinity interaction sites on $Ca_V\beta$ subunits (He et al., 2007), indicating that altering $Ca_V\beta$'s relative orientation disrupts its ability to regulate channel gating. Whether this change translates into a disruption in channel modulation by the slow pathway was tested here. We found that Bdel1 currents show a variable degree of enhancement by SP. The data supports our model where a slight disruption in the relative orientation of $Ca_V\beta$ moves the palmitoyl groups away from their original site but not enough to prevent the palmitoyl groups from completely blocking the inhibitory sites on all $Ca_V2.2$ channels. Co-expression of $Ca_V\beta3$ with Bdel1 resulted in current inhibition by SP. This finding indicated that the variable enhancement occurring in the presence of $Ca_V\beta2a$ is not due to random disruption of the channel's inhibitory site. Rather, this finding indicates that the low affinity interactions between $Ca_V\beta3$ with Bdel1 play at most a minor role in slow pathway inhibition of N-current.

While deletion of a single amino acid in the Bdel1 mutant channels did not abolish enhancement by SP, deletion of two amino acids in the Bdel2 mutants resulted in modulation changing from enhancement to inhibition. The appearance of current inhibition following receptor activation may occur because the palmitoyl groups are sufficiently displaced from the inhibitory site. This site that is masked by the palmitoyl groups when $Ca_V2.2$ is co-expressed with $Ca_V\beta2a$ now becomes available for binding by released free AA. The inhibited Bdel2/β2a currents did not show voltage-dependent relief from inhibition following a prepulse (Fig 4.3, 4.4). The I-II linker of the N-channel

mediates $Ca_V\beta$-dependent regulation of the channel's voltage-dependent activation and inactivation (Arias et al., 2005). Yet, loss of $Ca_V\beta$-dependent regulation of the channel's current-voltage properties was lost with the Bdel1 mutant, but restored with the Bdel2 mutant (Vitko et al., submitted), indicating a role for the orientation of $Ca_V\beta$2a not just in channel modulation, but also in regulating the channel's kinetic properties.

One possibility remains untested: the disruption in the block of inhibition could be due to changes in the low affinity interactions between $Ca_V\beta$2a and Ca_V2.2. However, the robust inhibition observed with Bdel2 was significantly reduced simply by adding back exogenous palmitic acid. The simplest interpretation of the findings is that though two amino acids are deleted in the IS6-AID segment, N-current inhibition by SP can be minimized by providing palmitic acid to compete with endogenously released AA for a binding site, possibly located on the channel. However, another possibility is that the actions of AA and palmitic acid are indirectly converging on an enzyme, such as a phosphatase that in turn covalently modifies channel proteins.

Previous studies show that in the presence of $Ca_V\beta$2a, Ca^{2+} currents exhibit little inactivation in expression system or in primary cells (Qin et al., 1998; Hurley et al., 2000; Yasuda et al., 2004). Palmitoylation of Cys3 and Cys4 residues of $Ca_V\beta$2a slows the rate of inactivation of Ca^{2+} currents in heterologous expression systems (Chien and Hosey, 1998; Hurley et al., 2000). The I-II linker region is thought to participate in channel inactivation possibly by occluding the mouth of the open channel (Herlitze et al., 1997; Restituito et al., 2000; Stotz and Zamponi, 2001; Hering, 2002). Since the palmitoyl groups serve as an anchor to tether $Ca_V\beta$2a to the membrane, slowed inactivation may

result from restricted movement of the I-II linker being restricted by the anchored $Ca_V\beta2a$ (Restituito et al., 2000). Removing the palmitoyl groups of $Ca_V\beta2a$, either by mutation or by using a depalmitoylating agent, restores inactivation of currents indicating that palmitoylation of $Ca_V\beta2a$ slows voltage-induced inactivation (Chien and Hosey, 1998; Qin et al., 1998; Hurley et al., 2000).

When $Ca_V\beta2a$ is co-expressed with either Bdel1 or Bdel2, channel activity now exhibits more rapid inactivation kinetics similar to channels containing a depalmitoylated $Ca_V\beta2a$ (Vitko et al., submitted), suggesting that the palmitoyl groups no longer reside in their original position relative to $Ca_V2.2$. Consequently, the palmitoyl groups can no longer slow the channel's inactivation kinetics. Thus, the kinetic changes observed with the mutant channels corroborate the findings presented here, that the orientation of the palmityolated $Ca_V\beta2a$ relative to $Ca_V2.2$ is not only critical for regulating N-channel's biophysical properties (Vitko et al., submitted), but also for its modulation by G_qPCRs.

In addition to participating in the slow pathway modulation, $Ca_V\beta$ subunits have earlier been implicated in modifying current kinetics and amplitude as well as in trafficking channel complexes to the plasma membrane (Singer et al., 1991; Olcese et al., 1994; Chien et al., 1996; Brice et al., 1997). Binding of $Ca_V\beta$ to the AID region masks an ER retention site that facilitates channel expression at the plasma membrane (Bichet et al., 2000). Co-expression of a $Ca_V\beta$ subunit is necessary for inhibition of $Ca_V2.2$ currents by a dopamine D2 receptor agonist via $G\beta\gamma$-mediated voltage-dependent pathway (Meir et al., 2000). $G\beta\gamma$ also binds to the channel's I-II linker and elicits a change in the association between the channel and $Ca_V\beta$, probably by changing the orientation of the

$Ca_V\beta$ subunit (Hummer et al., 2003). Compared to other $Ca_V\beta$s, when $Ca_V\beta$2a is co-expressed, channels undergo increased voltage-dependent, membrane-delimited inhibition by $G\beta\gamma$ and slowed prepulse-induced relief from inhibition (Canti et al., 2000; Feng et al., 2001). Our findings suggest that the specific orientation of $Ca_V\beta$2a also is required for channel modulation by the voltage-independent pathway.

Together with the findings in Chapter III, our data provide evidence for a new role of palmitoylation in channel modulation where the palmitoyl groups not only block modulation, but the palmitoylated $Ca_V\beta$2a must be in a specific orientation for this to occur. This idea of a lipid modification of a cytosolic protein interacting with a transmembrane protein is quite novel and extends the role of palmitoylation beyond its known functions of targeting or tethering proteins to the membrane (Resh, 2006). An exception exists in the visual system where besides ensuring membrane targeting, palmitoylation of a membrane-associated form of retinal epithelial protein 65 (RPE65) not only enhances its targeting to membranes but most importantly enhances its selectivity for binding to all-trans-*retinyl*-esters. or even in one case, changing the binding affinity of one protein for another (Xue et al., 2004). However, a change in the function of a palmitoylated protein arising from a change in its position has never been shown.

Inhibition of Bdel2/β2a current occurs via the slow pathway

We found that the inhibition of Bdel2 currents by SP in the presence of Ca_Vβ2a occurs via the same slow pathway that mediates inhibition of wt Ca_V2.2/ Ca_Vβ3 currents by SP. This finding raises the question that if the palmitoyl groups of Ca_Vβ2a are unable to block inhibition of Bdel2 currents, would adding back palmitic acid be sufficient to block Bdel2/β2a inhibition? Previously we showed that exogenous application of palmitic acid blocked SP-mediated inhibition of Ca_V2.2/β3 currents (Chapter III). Here we show that palmitic acid also minimizes inhibition of Bdel2/β2a currents (Fig 4.6). It is possible that due to a loss of low-affinity interactions of Ca_Vβ2a arising from the deletions in the I-II linker, Bdel2 currents are no longer enhanced but become inhibited instead. However, we can rule out this possibility because exogenous palmitic acid is sufficient to reduce Bdel2/β2a current inhibition. This piece of evidence taken together with the rest of the data presented here indicates that inhibition of Bdel2/β2a currents occurs due to a loss of interaction of the palmitoyl groups with the inhibitory site.

Overall, our finding provides an insight into the coupling of G_qPCR activation with modulation of Ca_V2.2 involving the Ca_Vβ subunit. Ca_Vβ not only determines the modulation of Ca_V2.2 by the subtype that is co-expressed with the channel but also by its relative orientation with the channel. Mutations in the IS6-AID segment have the potential to disrupt critical protein-lipid interactions between the palmitoyl moities of Ca_Vβ2a and Ca_V2.2 that in turn uncouples the otherwise tight regulation of Ca_V2.2 by G_qPCRs. Entry of Ca^{2+} ions through voltage-gated Ca^{2+} channels regulates opening of

small-conductance potassium channels during afterhyperpolarization (Stocker, 2004). N-channels expressed post-synaptically on the dorsal horn affect neuronal excitability during and following transmission of nociceptive stimuli (Yaksh, 2006). It is not known if up- or down-regulation of the different Cavβ subunits can occur as an adaptation to a nociceptive stimulus; however both increases and decreases in calcium currents have been observed in different neuronal subtypes following nerve injury (McGivern and McDonough, 2004). Thus any disruption in modulation of N-current by SP, for example, during transmission of nociceptive stimulation in the spinal cord may alter the frequency of action potential firing that conveys nociceptive information to the brain for further processing.

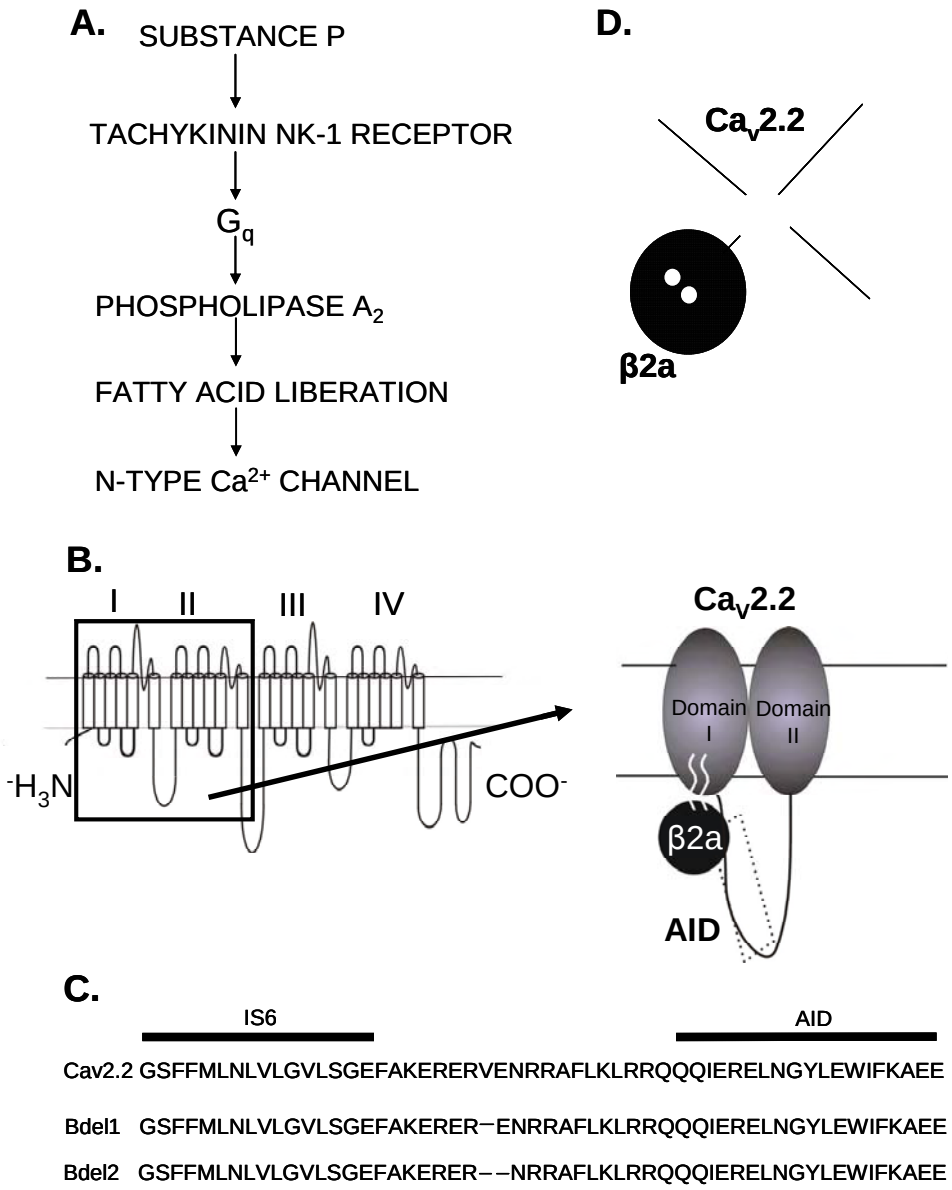

Figure 4.1 Schematic representation of $Ca_V2.2$ by NK-1R activation. **(A)** Flowchart representing the signaling cascade used by substance P to modulate N-current. **(B)** N-channels consist of a pore-forming $Ca_V2.2$ α1 subunit complexed with one cytoplasmic $Ca_V\beta$ and one transmembrane α_2-δ (not shown) subunit. $Ca_V2.2$ consists of four homologous domains (I-IV) that serve as four pseudo-subunits tethered to the subsequent domain by intracellular linkers. Shown here, the I-II linker connects domains I and II. $Ca_V\beta$ binds to the AID region (delineated by the dotted line) on the I-II linker at a site that overlaps with the binding site for Gβγ. **(C)** The amino acid deletions in the region proximal to the AID result in Bdel1 and Bdel2 mutant channels.

Figure 4.2 NK-1R activation enhances wt $Ca_v2.2$ current in the presence of a β2a subunit. HEK cells were transiently transfected with wt $Ca_V2.2$, α2δ–1, β2a and NK-1R. **(A)** Individual sweeps taken before (con) and 2 mins after application of 5 nM SP *left*, in the presence of 0.1 mM BAPTA and *right*, in the presence of 20 mM BAPTA. **(B)** Comparison of the average inhibition in the presence of 0.1 mM and 20 mM BAPTA (n=4-9); **p*<0.05 compared to inhibition in the presence of 0.1 mM BAPTA. **(C)** Averaged current-voltage plots measured before (■) and after (□) application of SP. **(D)** Individual sweeps taken before and 2 min after application of SP. P1 and P2 represent current measured before (P1) after (P2) a prepulse. **(E)** Summary of enhancement at 0 mV before and after a prepulse (n=9); ***p*<0.01 compared to P1 and P2 control currents prior to SP application. **(F)** Summary of time to peak (TTP) before and after application of SP (n=6), **p*<0.05 compared to control.

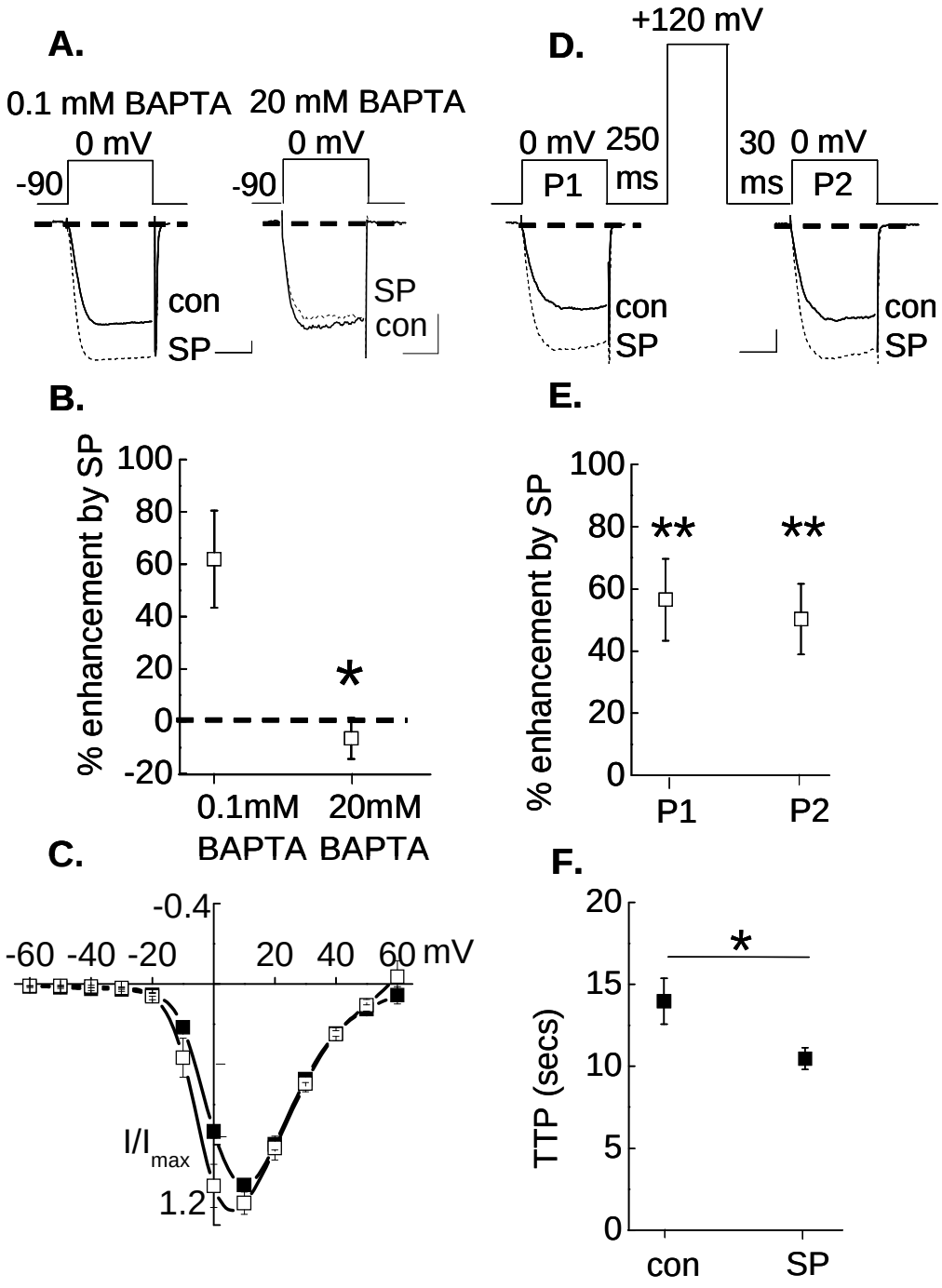
A.
0.1 mM BAPTA
20 mM BAPTA
0 mV
-90
con
SP
SP
con
D.
+120 mV
0 mV
250 ms
P1
30 ms
0 mV
P2
con
SP
B.
% enhancement by SP
100
80
60
40
20
0
-20
*
0.1mM BAPTA
20mM BAPTA
E.
% enhancement by SP
**
**
P1
P2
C.
-0.4
-60 -40 -20
20 40 60 mV
I/I max
1.2
F.
TTP (secs)
20
15
10
5
0
*
con
SP

Figure 4.3 Modulation of Bdel1 current by 5 nM SP is modestly disrupted. HEK cells were transiently transfected with NK-1R, Bdel1, α2δ−1, β2a **(B-D)** or β3 **(E, F). (A)** Working model of the Bdel1 channel with an associated β2a subunit. **(B)** Individual sweeps taken before (con) and 2 min after application of SP. **(C)** Summary of enhancement at +20 mV due to SP before and after a prepulse (n=7). **(D)** Averaged current-voltage plot measured before (■) and after (□) application of SP. **(E)** Representative sweeps taken before (con) and 2 min after application of SP. **(F)** Summary of the inhibition at +20 mV due to SP before and after a prepulse (n=4); **p*<0.05 compared to currents before SP was applied.

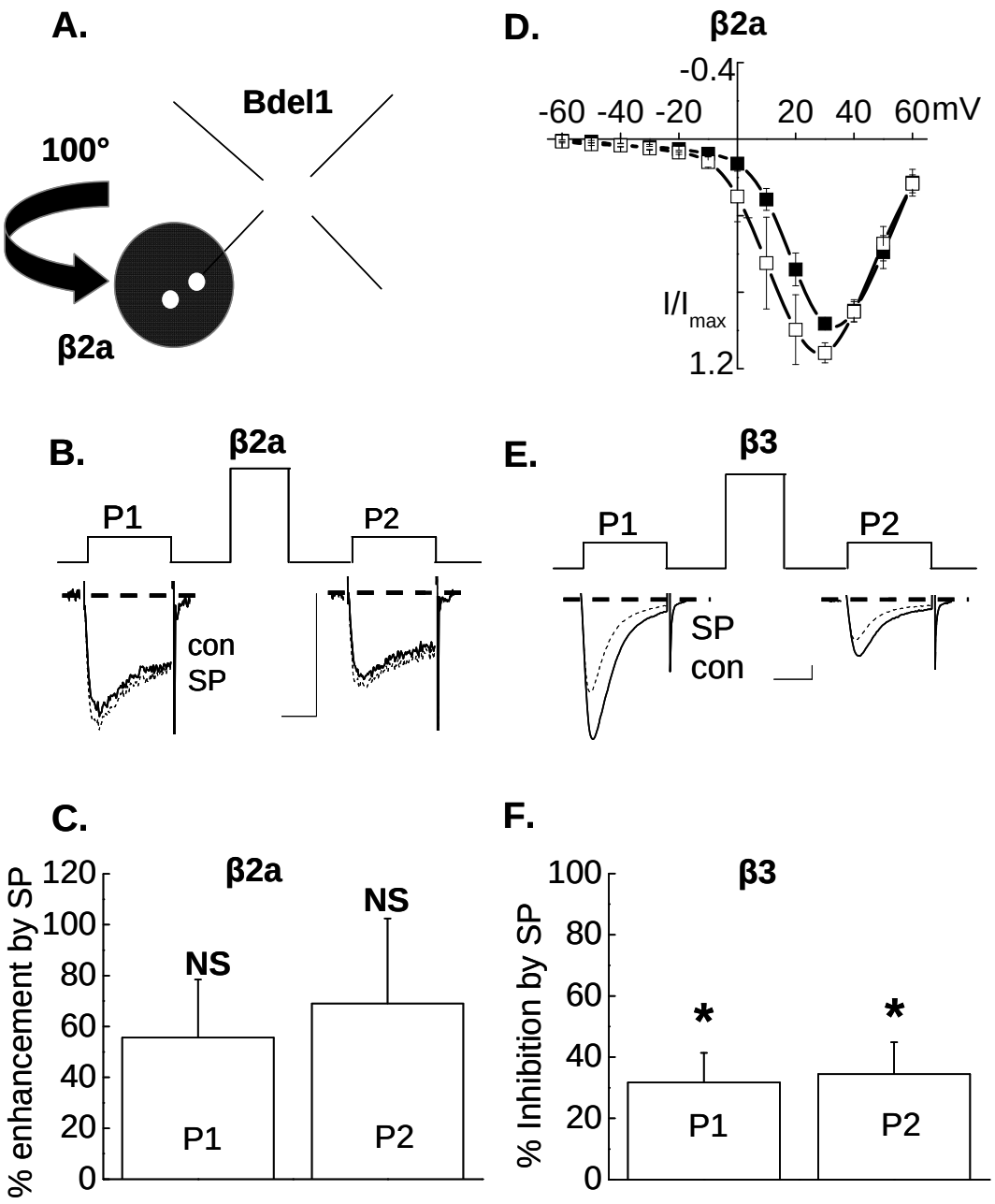
A.
Bdel1
100°
β2a
D.
β2a
-0.4
-60 -40 -20 20 40 60mV
I/I max
1.2
B.
β2a
P1
P2
con
SP
E.
β3
P1
P2
SP
con
C.
β2a
% enhancement by SP
120
100
80
60
40
20
0
NS
NS
P1
P2
F.
β3
% Inhibition by SP
100
80
60
40
20
0
*
*
P1
P2

Figure 4.4 NK-1R activation inhibits Bdel2 currents. HEK cells were transiently transfected with Bdel2, α2δ−1, β2a and NK-1R. **(A)** Working model of the mutant Bdel2 channel associated with β2a. **(B)** Averaged current-voltage plot measured before and after application of 5 nM SP. **(C)** Individual sweeps taken before (con) and 2 min after application of SP. **(D)** Summary of modulation of wt Cav2.2 (■), Bdel1 (●) and Bdel2 (▲) by SP before (filled) and after (open) a prepulse; **p*<0.05 compared to control currents (n=4-9). **(E)** Prepulse facilitation (ratio of P2/P1) for wt Cav2.2 (■), Bdel1 (●) and Bdel2 (▲); **p*<0.05 compared to Bdel1. **(F)** Individual sweeps taken before (con) and 2 min after application of SP.

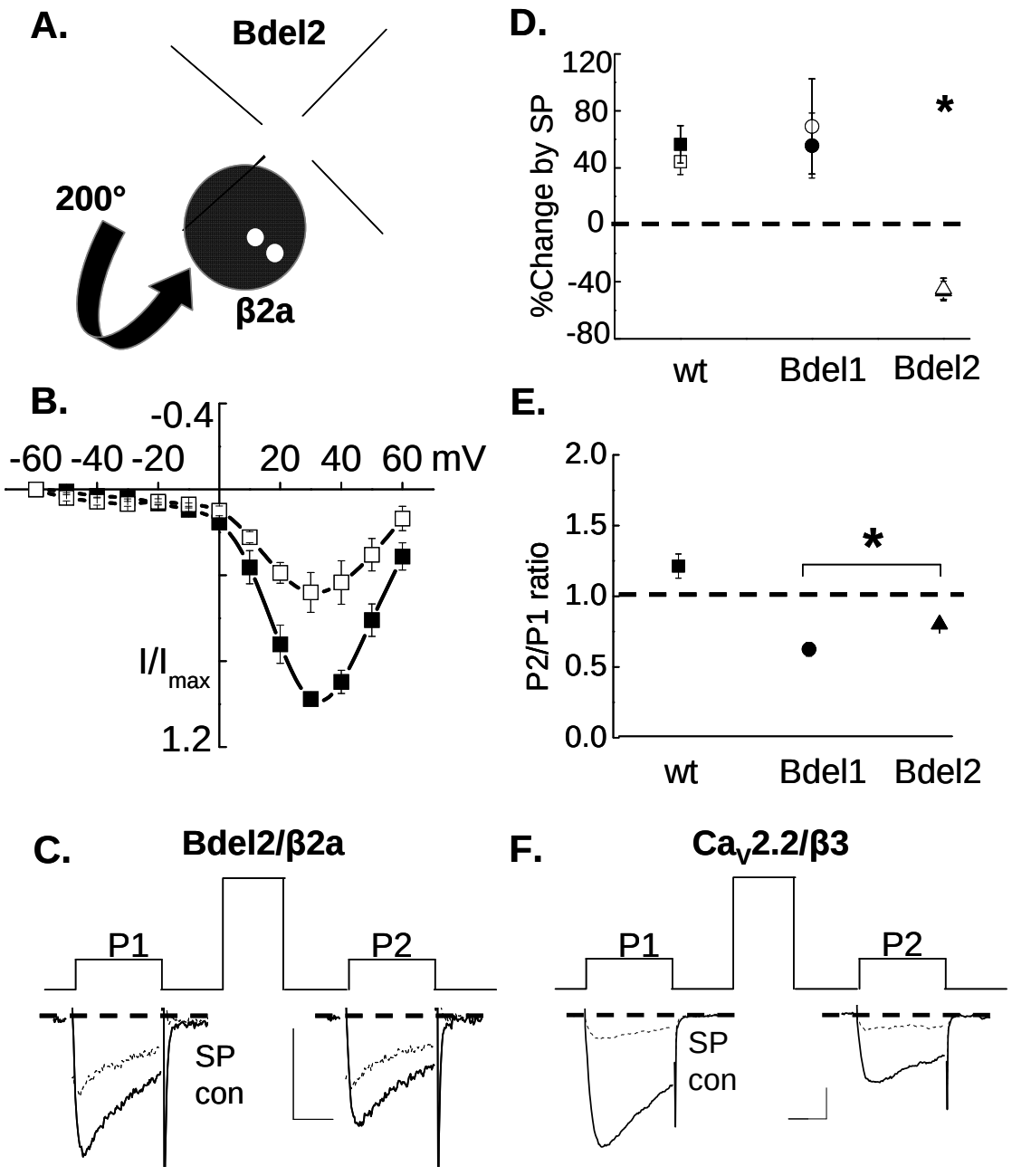
A.
Bdel2
200°
β2a
D.
%Change by SP
120
80
40
0
-40
-80
*
wt
Bdel1
Bdel2
B.
-0.4
-60 -40 -20
20 40 60 mV
I/I max
1.2
E.
P2/P1 ratio
2.0
1.5
1.0
0.5
0.0
*
wt
Bdel1
Bdel2
C.
Bdel2/β2a
P1
P2
SP
con
F.
Ca V 2.2/β3
P1
P2
SP
con

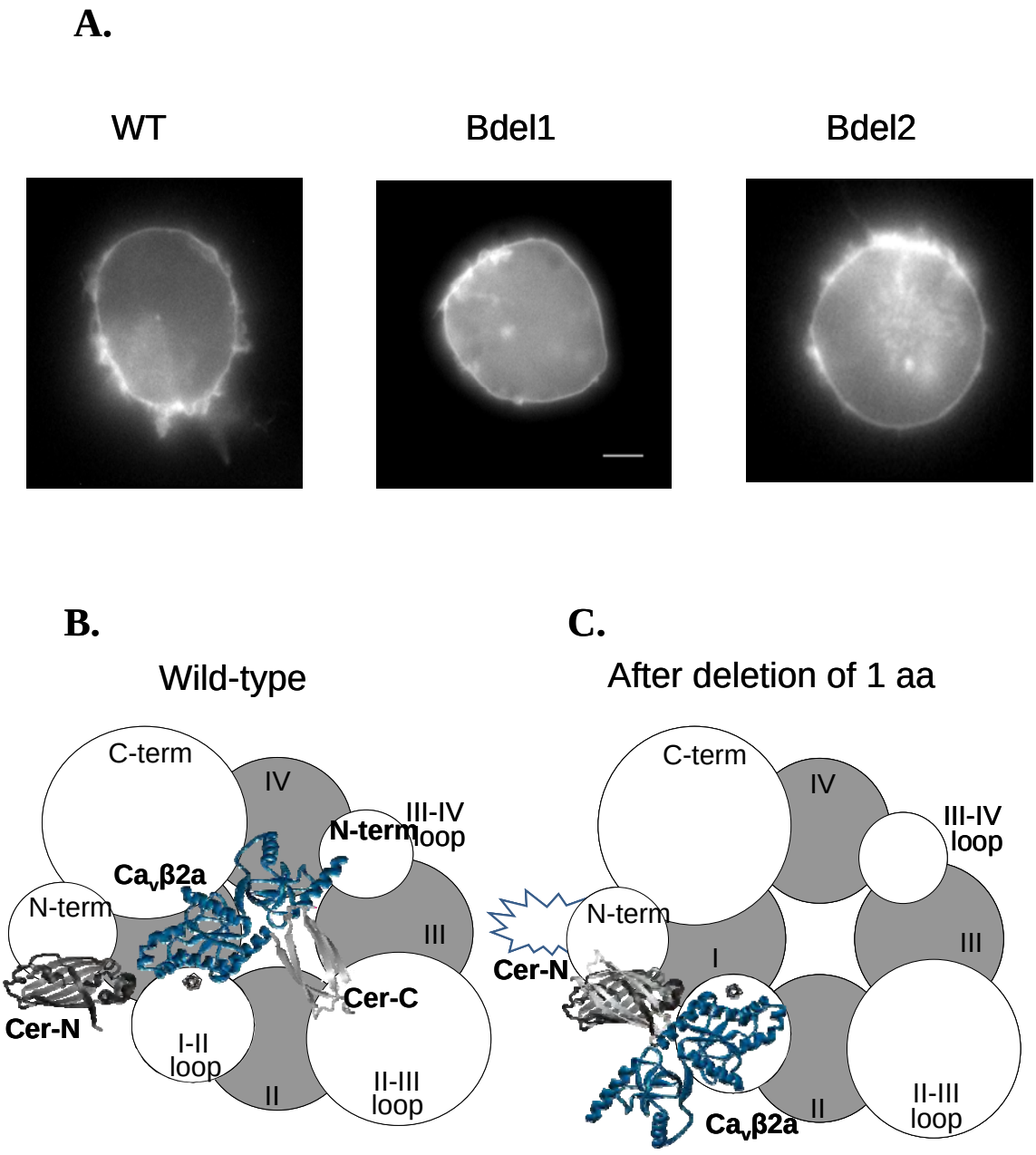

Figure 4.5 Bdel1 and Bdel2 channels both localize to the plasma membrane with $Ca_V\beta 2a$. **(A)** Images of representative HEK cells transfected with wt $Ca_V2.2$ (left), Bdel1 (middle) and Bdel2 (right) obtained after bimolecular fluorescence complementation (BIFC). Scale bar in A, 5 μm. Schematic representation ofBiFC imaging using **(B)** wt $Ca_V2.2$ and **(C)** Bdel1.

Figure 4.6 Inhibition of Bdel2 currents by SP is voltage-independent and occurs via a similar slow pathway as wt $Ca_V2.2$. HEK cells were transiently transfected with NK-1R, either Bdel2 or wt $Ca_V2.2$; $\alpha_2\delta$-1, and either β2a or β3. Individual traces from left wt $Ca_V2.2$/β3 and right Bdel2/β2a currents taken before and 90 secs following application of 5 nM SP **(A)** alone, **(B)** in the presence of 1mg/ml BSA and **(C)** in the presence of 20 mM BAPTA. **(D)** Summary of loss of inhibition of $Ca_V2.2$/β3 and Bdel2/β2a currents by SP; *$p<0.05$ compared to control currents (n=5-6).

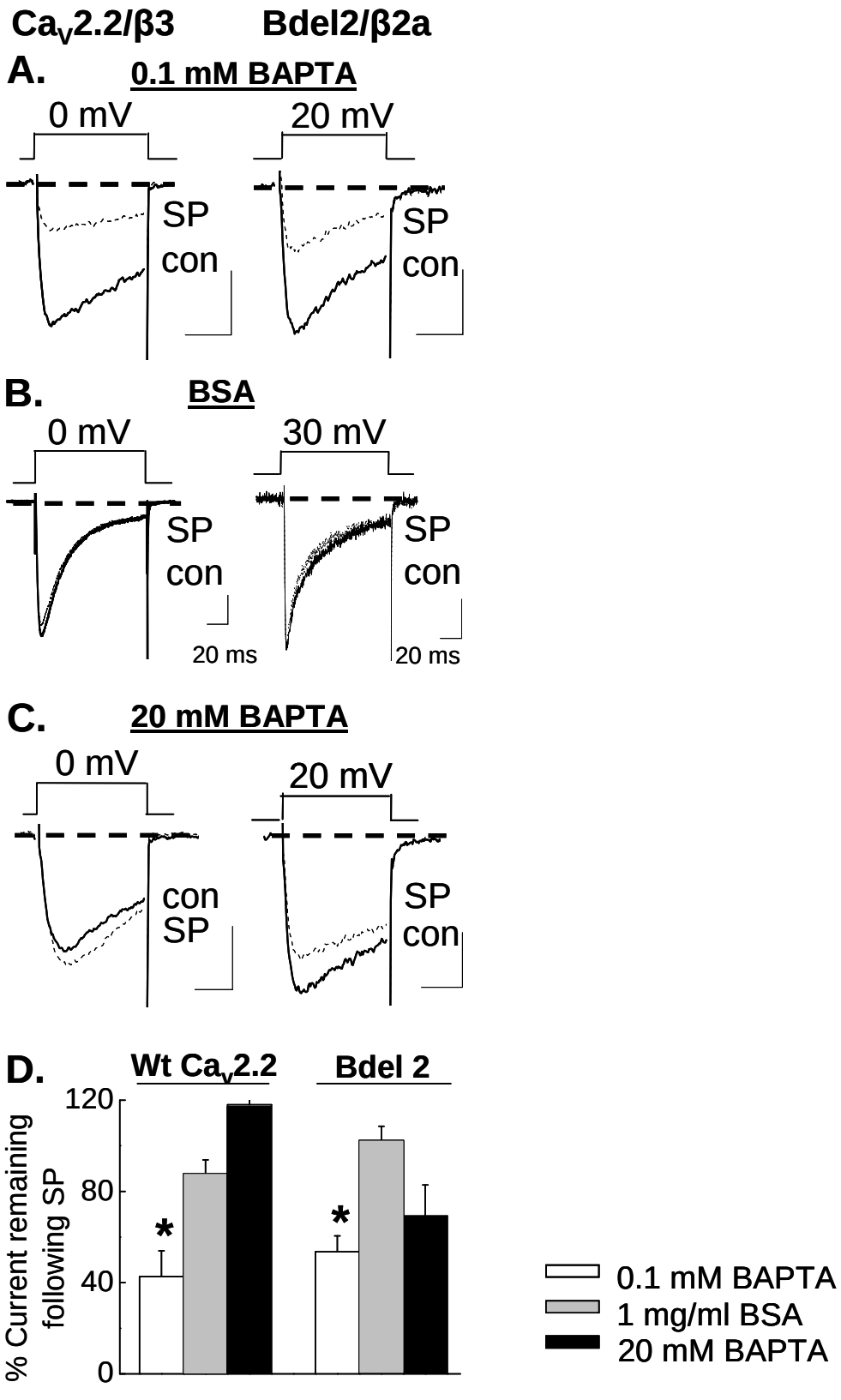
Ca$_V$2.2/β3
Bdel2/β2a
A.
0.1 mM BAPTA
0 mV
20 mV
SP
con
SP
con
B.
BSA
0 mV
30 mV
SP
con
SP
con
20 ms
20 ms
C.
20 mM BAPTA
0 mV
20 mV
con
SP
SP
con
D.
Wt Ca$_V$2.2
Bdel 2
% Current remaining following SP
120
80
40
0
*
*
0.1 mM BAPTA
1 mg/ml BSA
20 mM BAPTA

Figure 4.7 Palmitic acid blocks inhibition of Bdel2 currents by 5 nM SP. HEK cells were transiently transfected with Bdel2, $\alpha_2\delta$-1, $Ca_V\beta$2a, and NK-1R. **(A)** Schematic representing preincubation of cells with palmitic acid blocks free AA, released after stimulation of NK-1R, from occupying the inhibitory site **(B)** Cross sectional model of the channel representing the palmitoyl groups (white dots) oriented away from the inhibitory site on the Bdel2 subunit. The inhibitory site is occupied by exogenous palmitic acid (purple dots). **(C)** Summary of inhibition by SP in the presence of 10 μM palmitic acid *p<0.05 compared to current amplitude prior to SP (n=7) or compared to the presence of palmitic acid alone (n=6). **p<0.05 % inhibition by SP compared to % inhibition by PA+SP. Individual traces taken before and 2 mins following application of 5 nM SP **(D)** alone or **(E)** in the presence of 10 μM palmitic acid.

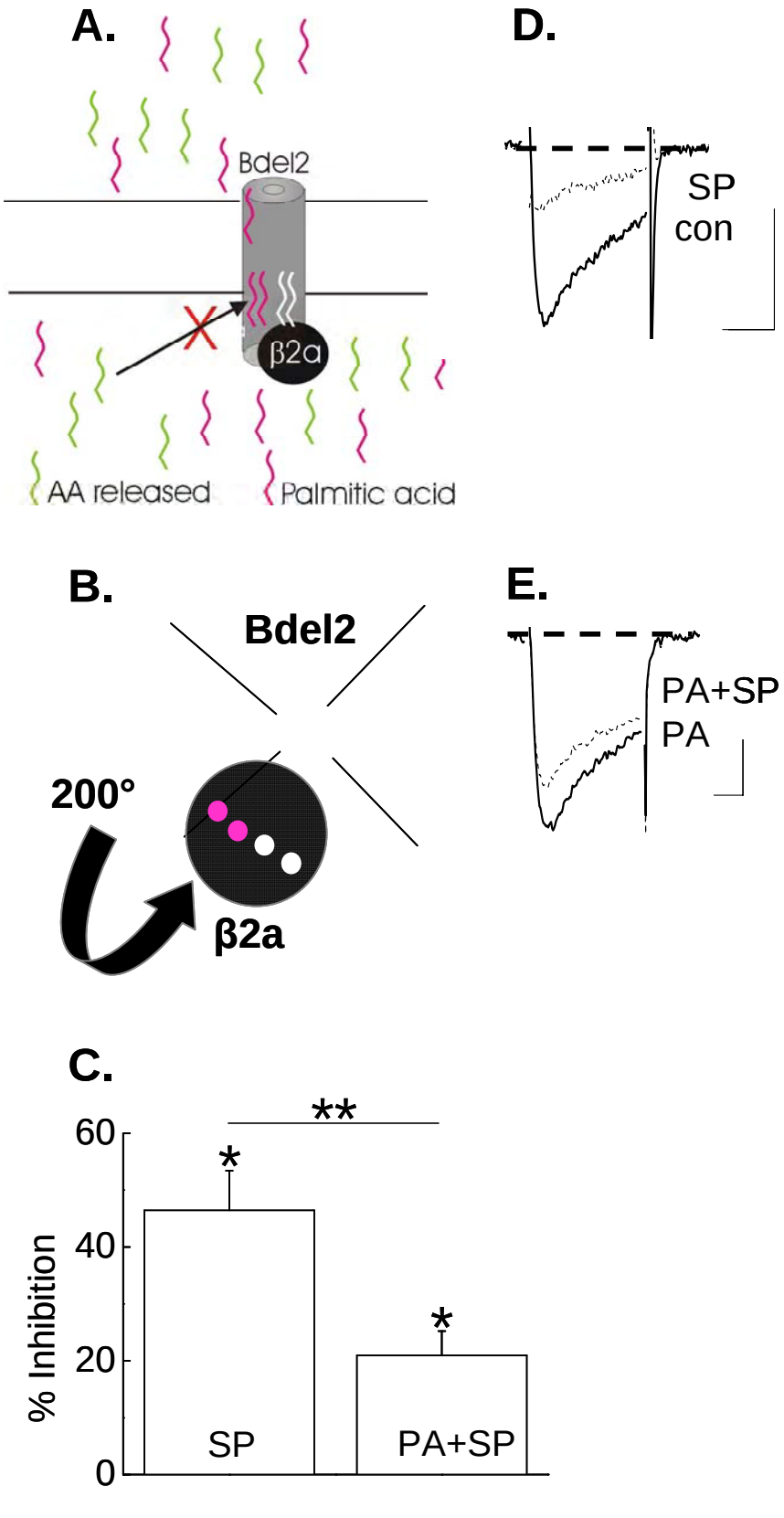
A.
Bdel2
β2a
AA released
Palmitic acid
B.
Bdel2
200°
β2a
C.
**
*
*
60
40
20
0
% Inhibition
SP
PA+SP
D.
SP
con
E.
PA+SP
PA

CHAPTER V:

Orientation of $Ca_v\beta$ to $G\beta\gamma$ is critical for membrane-delimited inhibition of $Ca_v2.2$ by dopamine D2 receptors

Abstract

Voltage-dependent $Ca_V2.2$ (N-) channels undergo inhibition by different G-protein coupled receptors via a membrane-delimited, voltage-dependent pathway. This type of modulation involves interaction of $G\beta\gamma$ with multiple regions of $Ca_V2.2$. $Ca_V\beta$ acts as a competitive antagonist of $G\beta\gamma$ for binding to the N-channel's I-II linker. While $G\beta\gamma$ displaces $Ca_V\beta$ to inhibit N-channel activity, $Ca_V\beta$ in turn displaces $G\beta\gamma$ during a depolarizing pulse to relieve inhibition. As with $G\beta\gamma$, $Ca_V\beta$ interacts with multiple sites on $Ca_V2.2$; however its interaction with the I-II linker controls the "off rate" of $G\beta\gamma$ during a depolarization. Previously, we examined the gating properties of $Ca_V2.2$ mutants lacking one or two amino acids in the IS6-AID segment, a rigid, region distal to IS6 and proximal to $Ca_V\beta$'s AID binding site on the I-II linker, and found that a specific orientation of $Ca_V\beta2a$ is required for normal gating. The mutations result in inefficient coupling between voltage sensor movement and channel opening, apparently by altering $Ca_V\beta$'s orientation relative to $Ca_V2.2$. Here we tested whether the mutant N-channels

support voltage-dependent inhibition following D2 dopamine receptor activation by quinpirole. A single amino acid deletion abolished N-current inhibition. In contrast, deletion of two amino acids restored inhibition; however, inhibition now was voltage-independent. Gβγ maintained a close association with $Ca_V\beta$ in mutant channels, as confirmed by bimolecular fluorescence complementation measurements. We conclude that the relative orientation of $Ca_V\beta$ to $Ca_V2.2$ is critical for relief of voltage-dependent inhibition. These findings are consistent with the IS6-AID segment serving a role in coordinating $Ca_V\beta$ movements to promote channel opening.

INTRODUCTION

N-channels affect numerous physiological processes by regulating the influx of calcium ions. G-protein coupled receptors (GPCRs) modulate N-channels by both voltage-dependent and voltage-independent mechanisms (Hille, 1994). Voltage-dependent inhibition, also referred to as membrane-delimited inhibition, occurs when activated G_α release Gβγ dimers that then bind N-channels (Herlitze et al., 1996; Ikeda, 1996; De Waard et al., 1997; Zamponi et al., 1997). Gβγ binding delays the opening of N-channels in response to positive voltages, resulting in decreased current amplitude and slowed activation kinetics, termed reluctant gating (Bean, 1989). During voltage steps to depolarizing potentials, N-current inhibition is relieved due to apparent dissociation of Gβγ. Reversal is transient; upon repolarization to negative potentials Gβγ rebinds so that N-current exhibits reluctant gating during a subsequent depolarizing voltage step (Elmslie et al., 1990; Ikeda, 1991). In certain primary neurons under basal conditions (Barrett and

Rittenhouse, 2000) or conditions that favor high tonic G protein activity (Ikeda, 1991, 1996), prepulses also relieve tonic inhibition, i.e., reluctant gating in the absence of transmitter.

Prepulse facilitation of transmitter-stimulated or tonic reluctant gating requires the presence of the $Ca_V\beta$ subunit (Meir et al., 2000). In $Ca_V\beta$'s presence, slowed activation kinetics, a rightward shift in voltage-dependence of activation and changes in inactivation are more pronounced. These findings suggested that $Ca_V\beta$'s and $G\beta\gamma$'s interactions at the I-II linker reversibly shift channel activity between two biophysical profiles. When $Ca_V2.2$ is coexpressed with a $Ca_V\beta$, its voltage sensitivity increases compared to expression of $Ca_V2.2$ alone; both activation and inactivation profiles shift in the negative direction. Mean open time also increases (Dolphin, 2003). In contrast, following membrane-delimited inhibition currents exhibit the reverse trend, similar to N-channel gating in the absence of a $Ca_V\beta$. These findings suggest that inhibition by $G\beta\gamma$ is due to the displacement of $Ca_V\beta$ binding (De Waard et al., 2005).

Their molecular interactions support this possibility. N-channels consist of the pore-forming $Ca_V2.2$ subunit, which is organized in four transmembrane domains (I-IV) interconnected by intracellular linkers. $Ca_V\beta$ binds $Ca_V2.2$ with high affinity at the alpha-interacting domain (AID) of the I-II linker (Fig 5.1A) (Pragnell et al., 1994) while $G\beta\gamma$ binding partially overlaps with the AID region (Chen et al., 2004; Opatowsky et al., 2004; Van Petegem et al., 2004). The overlap results in competition such that $G\beta\gamma$ displaces $Ca_V\beta$ for binding to the AID region (Hummer et al., 2003; Sandoz et al., 2004).

In turn, positive voltages allow $Ca_V\beta$ to displace $G\beta\gamma$ (Canti et al., 2000; Sandoz et al., 2004). Thus it is the dynamic nature of their competition at the I-II linker that gives rise to voltage-dependent inhibition (Lopez and Brown, 1991; Bourinet et al., 1996; Zamponi and Snutch, 1998; Sandoz et al., 2004). However, how $Ca_V\beta$ disturbs $G\beta\gamma$ binding during prepulses and prolonged depolarization remains poorly understood.

Therefore, in the present study we have tested $Ca_V\beta$'s role in relieving voltage-dependent membrane-delimited inhibition of N-current by one such GPCR, the dopamine D2 receptor (D2R). D2Rs belong to the D2-like subfamily that couples to pertussis toxin (PTX)-sensitive $G_{i/o}$, and can stimulate membrane-delimited inhibition of recombinant N-current (Senogles et al., 1987; Page et al., 1998; Stephens et al., 1998; Canti et al., 1999). Other studies show that D2Rs activate PLA_2 at least partially via a PTX-insensitive G protein and its activation releases free AA (Kanterman et al., 1991; Caccavelli et al., 1992; Schinelli et al., 1994). Moreover, exogenous AA modulates N-current by a different mechanism than membrane-delimited inhibition (Liu et al., 2001). Here we first show that with coexpression of $Ca_V\beta2a$, inhibition of $Ca_V2.2$ by the D2R agonist quinpirole (quin) occurs via a BAPTA-insensitive, voltage-dependent pathway (Fig 5.1B), confirming D2Rs mediate N-current inhibition by the membrane-delimited pathway.

Second, we asked whether a specific orientation of $Ca_V\beta$ and $G\beta\gamma$ relative to $Ca_V2.2$ confers prepulse facilitation. We used mutant N-channels with one or two amino acids deleted in the region between the last transmembrane segment (S6) of domain I (IS6) and the AID, termed the IS6-AID segment (Vitko et al., submitted; Fig 5.1C). Since

the IS6-AID segment is a rigid helical region (Arias et al., 2005), one or two amino acid deletions should orient $Ca_V\beta2a$ and $G\beta\gamma$ to a different face of the helix, thus positioning them differently relative to $Ca_V2.2$ (Vitko et al., submitted). We show that mere association of $Ca_V\beta$ with $Ca_V2.2$ is insufficient for the voltage-dependence of membrane-delimited inhibition, but rather a specific orientation of $Ca_V\beta2a$ is required to relieve reluctant gating and facilitate current amplitude.

MATERIAL AND METHODS

Site directed mutagenesis

The cDNA encoding the rat brain $Ca_V2.2$ (GenBank entry #AF055477) was cloned into the plasmid vector pcDNA6 (Lin et al., 1997). A 1.5 kb fragment was subcloned into pCR2.1-TOPO (Invitrogen, Carlsbad, CA), then mutated using the Quikchange® protocol and *Pfu* Ultra DNA polymerase (Stratagene, La Jolla, CA). Oligonucleotide primers were obtained from Invitrogen and used without purification. All restriction enzymes were purchased from New England Biolabs (Ipswich, MA). The full-length cDNA was reassembled in the original plasmid vector that was cut with *Asc*I and *Bsi*WI by ligating the following fragments: *Asc*I(32)/*Blp*I(355), *Blp*I/*Sac*I (1407), and *Sac*I/*Bsi*WI (2991). The Bdel1 and Bdel2 amino acid mutations were contained in the *Blp*I/*Sac*I fragment, and the sequence of this fragment was verified for each mutant by automated sequencing at the University of Virginia Biomolecular Research Facility.

Transfection

Human embryonic kidney (HEK) cells with a stably transfected M_1R (HEK-M1) were grown at 37°C with 5% CO_2 in Dulbecco's MEM (DMEM)/F12 supplemented with 10% FBS, 1% G418, 0.1% Gentamicin and 1% HT supplement (Gibco Life Technologies, Grand Island, NY). For transfection, cells were plated in 12-well plates at 50-80% confluency. Cells were transiently transfected using Lipofectamine and PLUS reagents (Invitrogen, Carlsbad, CA) as per the manufacturer's instruction. The transfection mixture consisted of plasmids encoding wt or mutant $Ca_v2.2$ e[^{a}10, Δ18a,

Δ24a, 31a, 37b, 46] (#AF055477; Vitko et al., submitted; Fig 5.1C), $\alpha_2\delta$–1 (#AF286488) and either $Ca_V\beta$2a (#M80545) or $Ca_V\beta$3 (#M88751) at a 1:1:1 molar ratio. 32 ng/well of D2R (#NM_000795; UMR cDNA Resource Center, University of Missouri, Rolla, MO) and enhanced green fluorescent protein cDNA (used at less than 10% of total cDNA), were also included in the transfection medium. Cells were plated on poly-L-lysine coated coverslips 24-72 hours post transfection. However, currents elicited from Bdel1 and Bdel2 mutants were not detectable using the above-mentioned transfection protocol. To boost mutant expression by increasing transcription, 80 ng of plasmid containing the SV40 T antigen was included during transfection. Currents were recorded between 24 and 76 hours post transfection.

Electrophysiology

Whole-cell Ba^{2+} currents were recorded at room temperature (20-24°C) using a Dagan 3900a patch clamp amplifier (Dagan Instruments Inc., Minneapolis, MN). Currents were filtered at 1-5 kHz using the amplifier's four-pole low-pass Bessel filter and digitized at 20 kHz with a CED micro1401 interface [Cambridge Electronic Design, (CED) Cambridge, UK]. Data were collected using the Signal 2.16 software (CED) and stored on a personal computer. Prior to analysis, capacitive and leak currents were subtracted using a scaled-up hyperpolarizing test pulse to -100 mV. For all recordings, cells were held at -90 mV and given either a 24 or 100 ms depolarization to the test pulse indicated. Unless mentioned, the protocol was repeated every 4 sec. For prepulse experiments, a 24 ms depolarization was followed 250 ms later by a step depolarization

to +120 mV for 25 ms, then followed 30 ms later by another 24 ms depolarization (see Fig 5.2B) and repeated every 10 sec. Electrodes were pulled from borosilicate glass capillary tubes. Each electrode was fire-polished to ~1μm to yield a pipette resistance of 2-3 MΩ. The external solution contained (in mM): 125 N-methyl glucamine (NMG)-aspartate, 10 HEPES and 5 or 20 barium (Ba^{2+}) acetate; the pH was adjusted to 7.5 with CsOH. When the Ba^{2+} concentration was lowered from 20 mM to 5 mM (for recording wt $Ca_v2.2$ currents), 135 NMG-aspartate was substituted for Ba^{2+}. The internal solution of the pipette consisted of (in mM): 135 Cs-aspartate, 10 HEPES, 0.1 1, 2-bis(O-amino-phenoxy)ethane-N,N,N',N'-tetraacetic acid (BAPTA), 5 $MgCl_2$, 4 ATP, and 0.4 GTP; the pH was adjusted to 7.5 with CsOH. When 20 mM BAPTA was included in the pipette solution, the Cs-aspartate concentration was lowered accordingly in the internal solution.

Pharmacology

Quin was prepared as a 3 mM stock solution in double-distilled water and stored at -20°C. To make a working concentration of 300 nM, the stock solution was serially diluted with bath solution daily. Bovine serum album (BSA; fraction V, heat shock, fatty acid ultra-free; Roche Applied Science, Indianapolis, IN) was dissolved directly in the bath solution and diluted further to make a final concentration of 1mg/ml. All chemicals were obtained from Sigma-Aldrich Inc. (St. Louis, MO) except where noted. Drugs were applied with a gravity-driven bath perfusion system and complete bath exchange was achieved within 10-14 s.

Bimolecular fluorescence complementation (BIFC)

BIFC imaging was carried out as per methods earlier described (Vitko et al., submitted). Briefly, a small C-terminal (a.a. 159-238) sequence of cyan fluorescent protein (CFP) was fused to the C-terminus of full length β3 or β3 core (Chen et al., 2004). The big N-terminal fragment of CFP (a.a. 1-158) was fused to the N-terminus of G protein gamma 2 (Gγ2). Gγ2 plasmid was bicistronic with mCherry using the internal ribosome entry signal from IRES-2 (Clontech). This red signal was used for both selection of transfected cells and calculation of the cyan BiFC to red ratio. Plasmids encoding $Ca_V2.2$, Bdel1 or Bdel2 (250 ng), $\alpha_2\delta$-1 (250 ng), full length β3 or β3 core (100 ng), Gβ2 (250 ng) and Gγ2-mCherry (100 ng) were transiently transfected into HEK-293 cells. After 18 hrs the cells were plated onto polylysine-treated glass bottom dishes (Fluorodish, World Precision Instruments, Saratoga, FL). Transfected cells were identified by their red fluorescence. Their red and cyan fluorescence signals were collected using the Olympus microscope (40x objective, 2x2 binning) described below. Digital images were background subtracted using a region devoid of cells, and the ratio of cyan to red signal for each cell was calculated. Following the method of Shyu et al. (Shyu et al., 2006), BiFC specificity was determined using the median of the CFP/RFP signal for each condition. Images of live cells were collected using a Cooke Sensicam QE (Romulus, MI) mounted on an Olympus BX61WI equipped with an Olympus confocal spinning disk unit (Melville, NY).

Data analysis

After the onset of the test pulse, maximal whole-cell inward current amplitude was measured using Signal 2.16 (CED). Percent change in current amplitude was measured as [(I-I')/I]*100 where I is the average amplitude of peak current measured from 5 current traces prior to drug application and I' is the average current amplitude measured from 5 current traces at least 90 s after application of quin. BiFC data were acquired and analyzed using IPLab 4.0 (Scanalytics, Fairfax, VA) as described previously (Vitko et al., 2007).

Statistical Analysis

Summary data are presented as mean ± s.e.m (standard error of the mean). Average current amplitude before and after application of quin was compared using a two-tailed paired *t*-test. Two means were compared using a two-way Student's *t*-test. Statistical significance was set at $p<0.05$ or $p<0.01$. Data were analyzed using Excel (Microsoft, Seattle, WA) and Origin (OriginLab, Northampton, MA). Statistical analysis of fluorescent images was performed using one-way ANOVA with the Kruskal-Wallis post test using GraphPad Prism.

RESULTS

Quin inhibits wt $Ca_V2.2$ current via a voltage-dependent pathway.

We hypothesized that a specific orientation of $Ca_V\beta2a$ relative to $Ca_V2.2$ (Fig 5.2A) is critical not only for regulating the channel's gating properties (Vitko et al., submitted) but also for voltage-dependent modulation of N-current. To first recapitulate voltage-dependent inhibition of N-current by D2R activation, we applied 300 nM quin to HEK-M1 cells transfected with $Ca_V2.2$, $\alpha2\delta$-1and $Ca_V\beta2a$. Application of quin inhibited the $Ca_V2.2/\beta2a$ currents by 53 ± 12% (n=4; $p<0.05$; Fig 5.2B & C). Inhibition was significantly relieved following a depolarizing prepulse ($p<0.01$). To rule out any possibility of a Ca^{2+}-sensitive diffusible second messenger pathway mediating inhibition of $Ca_V2.2/\beta2a$ currents, we dialyzed cells with a high concentration of BAPTA (20 mM) to chelate intracellular Ca^{2+} (Beech et al., 1991). In the presence of 20 mM BAPTA, quin still inhibited currents by 60 ± 4% (n=4; $p<0.05$; Fig 5.2E & F). Moreover, with 20 mM BAPTA, inhibition was significantly relieved following a prepulse ($p<0.05$).

One of the hallmarks of N-current inhibition by the membrane-delimited pathway is a slowed rate of current activation. As with membrane-delimited inhibition, the slowed activation kinetics are abolished with a strong depolarization (Bean, 1989). To confirm that N-current inhibition by quin occurs via a membrane-delimited pathway similar to previous observations (Page et al., 1998; Stephens et al., 1998; Canti et al., 1999), we tested whether N-current inhibition involves a decrease in activation kinetics, detected as a change in time to peak inward current (TTP). As shown in Fig 5.2D, following

application of quin, there is an upward trend for TTP. However, with a strong depolarizing pulse, TTP significantly decreased (p<0.05; n=6). The above properties of N-current modulation are consistent with D2Rs inhibiting $Ca_V2.2$/β2a currents via a membrane-delimited, voltage-dependent pathway.

Relief of tonic inhibition is disrupted with deletions in the IS6-AID segment.

The orientation of $Ca_V\beta$ relative to $Ca_V2.2$ subunit was earlier shown to be critical for $Ca_V\beta$ to regulate activity of $Ca_V2.2$ channels (Vitko et al., submitted). They found that with one or two amino acid deletions in the IS6-AID segment, $Ca_V\beta$'s ability to increase the open probability of the channels was lost; so was the ability to regulate the channel's activation and inactivation kinetics. While $Ca_V\beta$ is thought to regulate the movement of the IS6 with voltage thereby regulating the channel's inactivation (Hering, 2002), an altered orientation of $Ca_V\beta$ was proposed to affect the coupling between movements of the voltage sensor of IS4 to movements of IS6 thereby affecting how $Ca_V\beta$ modulates the channel's voltage sensitivity (Vitko et al., submitted). Since Gβγ increases the latency to N-channel opening (Dolphin, 2003), we wondered whether the relative orientation of $Ca_V\beta$ is also critical for voltage-dependent relief of tonic Gβγ-mediated inhibition of $Ca_V2.2$. To determine the optimal relation between prepulse voltage and facilitation, we measured $Ca_V2.2$/β2a currents after varying the prepulse voltage from -40 mV to +120 mV in 20 mV increments (Fig 5.3A). We compared the profile of $Ca_V2.2$ with Bdel1 and Bdel2 mutants, each co-expressed with $Ca_V\beta$2a and α2δ-1. A depolarizing step to 0 mV

(P2) produced facilitation of wt $Ca_V2.2$ currents (P1) that steadily increased with voltage before reaching a maximum prepulse value of +120 mV. In contrast, Bdel1 and Bdel2 currents showed no prepulse facilitation (Fig 5.3B). We also tested the dependence of facilitation on test pulse voltage by varying the test pulse voltage from -20 to +20 mV in 10 mV increments (Fig 5.3C). Facilitation of wt $Ca_V2.2$ currents was apparent over the voltage range -20 to +20 mV. In contrast, the dependence of facilitation on test pulse potential was lost for both Bdel1 and Bdel2 currents (Fig 5.3D, 5.4).

Deletion mutants retain Gβγ binding to the Ca_Vβ subunit.

To determine whether the loss in facilitation was due to a loss of the close association of Gβγ and Ca_Vβ at the AID in Bdel mutants, we used bimolecular fluorescence complementation (BiFC) analysis to detect interactions between Gβγ and either Ca_Vβ3 core or the full length Ca_Vβ3. Our results show that significant fluorescence occurs when wt $Ca_V2.2$, Bdel1 or Bdel2 is present while little fluorescence occurs in the absence of an α1 subunit (Fig 5.5). Experiments where either Ca_Vβ3 core or full length Ca_Vβ3 are expressed with different α1 subunits show similar fluorescence profiles, consistent with our observation that the close association between Gβγ and Ca_Vβ is retained in the deletion mutants.

Deletion mutants disrupt voltage-dependent modulation by D2 receptors.

Since Bdel1 and Bdel2 exhibited disruption in relief from tonic inhibition, we tested whether voltage-dependent modulation by quin was similarly disrupted. We

predicted that by disrupting the relative orientation of the $Ca_V\beta$ subunit, Bdel1 and Bdel2 would no longer show voltage-dependent inhibition by quin, matching the profile observed with tonic prepulse facilitation. We found that Bdel1 and Bdel2 show disrupted current modulation as well as disrupted relief of tonic Gβγ inhibition (Fig 5.6 and 5.7). Co-expression of Bdel1 with $Ca_V\beta2a$ (Bdel1/β2a) yielded currents that rapidly inactivated and showed no prepulse facilitation (Figs 5.6A, B & F). Application of quin elicited no current inhibition (Fig 5.6A & B). To confirm that the loss of inhibition was not due to disruption in the interaction of Bdel1 specifically with $Ca_V\beta2a$, we co-expressed Bdel1 with $Ca_V\beta3$. Again, application of quin caused little prepulse facilitation (Fig 5.6D-F) or inhibition (Fig 5.6D, E) of N-current.

To determine whether a further change in the orientation of $Ca_V\beta$ (Fig 5.7A) would recover current modulation, we tested the Bdel2 mutant. Application of quin strongly inhibited the current (Fig 5.7B, C); however, depolarizing prepulses did not relive the inhibition (Fig 5.7C, D).

Inhibition of Bdel2 currents by quin is voltage-independent and not mediated by the slow, diffusible second messenger pathway.

Inhibition of native or recombinant N-current by two other GPCRs, the tachykinin NK-1 and M_1 muscarinic receptor involves a voltage-independent, lipid-dependent pathway often referred to as the slow pathway (Chapters II, III and IV; (Shapiro and Hille, 1993; Liu and Rittenhouse, 2003b, 2003a; Bannister et al., 2004). We hypothesized that the voltage-independent inhibition of Bdel2 currents described in Fig 5.7 might

involve a similar lipid-dependent pathway. To test this possibility, we employed two different strategies. First, we applied quin in the presence of BSA, which will scavenge any free fatty acid that may be released after receptor activation (Liu and Rittenhouse, 2003a). Second, we dialyzed 20 mM BAPTA into cells to chelate intracellular Ca^{2+} and minimize N-current modulation by the slow pathway. In the presence of BSA or 20 mM BAPTA, application of quin still inhibited Bdel2 currents (59 ± 5% and 54 ± 3% respectively (Fig 5.8).

DISCUSSION

Inhibition of $Ca_V2.2$ channels by D2R involves a membrane-delimited pathway

Here using a mammalian cell line, we show that in HEKM1 cells, inhibition of $Ca_V2.2/\beta2a$ currents by D2R stimulation occurs via a voltage-dependent pathway that does not involve a Ca^{2+}-sensitive diffusible second messenger pathway. These findings are similar to previous studies performed by the Dolphin lab where they found that co-expression of $Ca_V2.2$ with $Ca_V\beta2a$ along with $\alpha_2\delta$ and D2R resulted in inhibition of N-currents by quin in Xenopus oocytes. Inhibition was voltage-dependent and relieved by a large depolarizing prepulse (Page et al., 1998; Stephens et al., 1998; Canti et al., 1999). In contrast, D2R activation by quin inhibits N-currents in neostriatal neurons via a membrane-delimited pathway; this inhibition is voltage-independent and not relieved by a depolarizing prepulse (Yan et al., 1997). D2R activation causes release of AA in neurons (Kanterman et al., 1991; Caccavelli et al., 1992; Schinelli et al., 1994). These observations suggest that D2Rs may also couple to G_q proteins and their activation stimulates a lipid-dependent pathway similar to other G_qPCRs such as M_1 muscarinic and

NK-1Rs (Chapters II, III; Liu and Rittenhouse, 2003a). However modulation of recombinant $Ca_V2.2$ channel activity by D2Rs does not appear to involve a BAPTA-sensitive, lipid signaling pathway (Page et al., 1998; Stephens et al., 1998; Canti et al., 1999) (unpublished data from Mandy Roberts-Crowley). Consistent with recombinant data dialyzing a high concentration of BAPTA (20 mM) into striatal neurons to chelate intracellular Ca^{2+} did not affect inhibition of peak currents elicited from non-L-type channels (Hernandez-Lopez et al., 2000). These findings suggest that different Gβγ subunits may interact with native N-channels to mediate a BAPTA-insensitive, membrane-delimited pathway since earlier studies demonstrated that the amount of N-current facilitation observed is dependent on not only the $Ca_V\beta$ subunit expressed but also which Gβγ subunits were present (Meir et al., 2000; Feng et al., 2001).

Changing the relative orientation of $Ca_V\beta$ affects Gβγ-mediated inhibition as well as prepulse relief of the inhibition

Having shown that D2R modulation of N-current is membrane-delimited, we tested the role of $Ca_V\beta2a$ in regulating the properties of membrane-delimited inhibition. Previous studies have shown that $Ca_V\beta$ and Gβγ compete with each other for binding to α1 subunits (Tedford and Zamponi, 2006). The presence of a $Ca_V\beta$ subunit increases the peak current as well as causes a hyperpolarizing shift both in channel activation and inactivation. On the contrary, the presence of a Gβγ subunit decreases peak current and causes a depolarizing shift in the activation curve (De Waard et al., 2005; Tedford and Zamponi, 2006). In the absence of $Ca_V\beta$, channels undergo increased G-protein mediated

inhibition as if the absence of a competing $Ca_V\beta$ facilitates $G\beta\gamma$ binding to the AID (Campbell et al., 1995; Roche et al., 1995; Bourinet et al., 1996). However, conflicting evidence also showed that the presence of $Ca_V\beta$, in fact, promotes $G\beta\gamma$-mediated inhibition (Meir et al., 2000). Because this study was done in a different expression system as compared to the other studies, it is difficult to reconcile the latter data with previous evidence. While a number of possibilities, such as displacement or steric hindrance of $Ca_V\beta$ by $G\beta\gamma$, could account for the observation it is clear that a competition exists between $Ca_V\beta$ and $G\beta\gamma$ for binding to the AID region (De Waard et al., 2005; Tedford and Zamponi, 2006).

Additionally, the role of $Ca_V\beta$ in prepulse-induced relief of $G\beta\gamma$-mediated inhibition is well documented (Tedford and Zamponi, 2006) where with depolarization, $Ca_V\beta$ seems to compete with $G\beta\gamma$ and regain its binding to the AID. The presence of $Ca_V\beta$ subunits not only increases the rate of prepulse facilitation, but depending on the subtype of $Ca_V\beta$ and $G\beta\gamma$ subunits that are co-expressed, the "off" rate for $G\beta\gamma$ also varies (Roche and Treistman, 1998; Canti et al., 2000; Meir et al., 2000; Feng et al., 2001). These data further support the theory of competition between $Ca_V\beta$ and $G\beta\gamma$ in prepulse relief of membrane-delimited inhibition.

Our data support that a model where competition existing between $G\beta\gamma$ and $Ca_V\beta2a$ for binding to the AID region may underlie voltage-dependent modulation of N-current by GPCRs. Specifically, the disruption in the relative orientation of $Ca_V\beta2a$ to $Ca_V2.2$ disrupts the competitive relationship between $G\beta\gamma$ and $Ca_V\beta$. In the presence of quinpirole, currents elicited from wt $Ca_V2.2/\beta2a$ channels show inhibition that can be

relieved by a prepulse, while Bdel2/β2a currents show inhibition which is not relieved by a prepulse. Imaging data in Chapter IV indicate that $Ca_V\beta$ maintains close proximity to both Bdel2 and Gβγ at the plasma membrane. This finding rules out the possibility that the loss of prepulse facilitation arises from dissociation of $Ca_V\beta$ from Bdel2. It is possible that with a change in orientation, $Ca_V\beta$ loses a key interaction site with Bdel2 and is thus incapable of sensing the electric field and displacing Gβγ during a depolarizing prepulse. Alternatively, it is also possible that new constraints imposed upon $Ca_V\beta$ from its palmitoyl groups tethered to the plasma membrane, while assuming a different orientation relative to Bdel2, restricts $Ca_V\beta$ from displacing Gβγ.

The palmitoyl groups of $Ca_V\beta$2a contribute to the slowed inactivation kinetics of wt Ca_V2.2 currents (Olcese et al., 1994; Qin et al., 1998) possibly by interacting with the inactivation machinery (Hering, 2002). This interaction appears disrupted in Bdel1 and Bdel2 since the currents inactivate more rapidly than Ca_V2.2/β2a currents (Vitko et al., submitted). The palmitoyl groups require a specific orientation for modulating N-channel activity (Chapter IV) and possibly also for regulating channel inactivation (Vitko et al., submitted). Thus, the mutations in Bdel1 and Bdel2 cause $Ca_V\beta$2a's palmitoyl groups to orient differently and hence the profiles of fast inactivation are also strongly affected.

With the Bdel1 mutant channels, the lack of inhibition that accompanies changes in inactivation may be another manifestation of competition between $Ca_V\beta$ and Gβγ. Imaging data in Fig 5.5 confirm that $Ca_V\beta$ and Gβγ are in close proximity. This proximity depends on the presence of Ca_V2.2 thereby ruling out the possibility that inhibition does not occur because Gβγ cannot come in close proximity with Bdel1 or $Ca_V\beta$ due to the

changed orientation arising from the mutation. There could be multiple explanations for the lack of inhibition of Bdel1/Ca_Vβ2a currents. First, the amino acid deletion in Bdel1 may cause a reorganization of the helical structure of the AID that disrupts Ca_Vβ's ability to couple with AID and increase channel open probability (P_o) (Vitko et al. submitted). Hence, with low P_o, N-channels are already effectively "inhibited" and Gβγ can no longer confer inhibition when quinpirole is applied. Second, it is possible that due to a change in the orientation of Ca_Vβ2a, it no longer competes with Gβγ for binding to the AID. Hence tonic inhibition is never relieved with a prepulse and because it is not relieved, no further inhibition occurs. Third, due to the mutation in the IS6-AID segment, the Gβγ that binds to the AID may reside in closer proximity to its higher affinity interaction sites such as the carboxy terminus (De Waard et al., 2005). As a consequence, the increased strength of interaction between Gβγ and Bdel2 no longer allows Gβγ to be displaced by Ca_Vβ2a during a prepulse.

Voltage-independent inhibition of Bdel2/β2a currents does not involve the slow pathway

Inhibition of Bdel2/β2a currents is BAPTA-insensitive and was unaffected by the presence of BSA, indicating that this form of inhibition is distinct from the slow pathway inhibition that was earlier characterized for N-current in neurons (Beech et al., 1991; Bernheim et al., 1991; Mathie et al., 1992; Liu and Rittenhouse, 2003a). Voltage-independent inhibition of N-channel activity by GPCRs couple to PTX-insensitive G proteins such as G_q (Hille et al., 1995), G_{13} (Wilk-Blaszczak et al., 1994), G_s or G_{olf}

(Surmeier et al., 1995). This rules out the possiblity that keeping all other conditions unchanged, by deleting the two amino acids in the AID region, there is a switch to a different G-protein isoform, such as G_q, that mediates the inhibition. Thus, we conclude that the resulting change in orientation of $Ca_V\beta2a$ that arises from the mutations in Bdel2 is sufficient to place $Ca_V\beta2a$ out of the electric field and render it incapable of participating in prepulse-relief of inhibition.

Previously we showed that $Ca_V\beta2a$ assumes a specific orientation relative to $Ca_V2.2$ so that the palmitoyl groups may interact with an inhibitory site on the channel to block voltage-independent inhibition by the slow pathway (Chapter IV). The orientation of the palmitoyl groups may also be critical for enabling $Ca_V\beta2a$ to interact with regions of the N-channel that slow inactivation (Qin et al., 1998). Moreover, palmitoylation may orient low-affinity interaction sites of $Ca_V\beta2a$ to facilitate their interaction with the channel; these low-affinity interaction sites may facilitate movement of $Ca_V\beta$ during depolarization (He et al., 2007). By deleting one or two amino acids, as in Bdel1 and Bdel2, the disruption in voltage-dependent modulation could disrupt a) the interaction of the palmitoyl groups of $Ca_V\beta2a$ with the $\alpha1$ subunit b) interaction of the low affinity sites on $Ca_V\beta2a$ with the $\alpha1$ subunit c) the competitive relationship between $G\beta\gamma$ and $Ca_V\beta2a$ for binding to the AID.

In summary, our data support previous observations that $Ca_V\beta$ is necessary for voltage-dependent inhibition of N-current. Although, the exact role of $Ca_V\beta$ in voltage-dependent inhibition remains incompletely elucidated, we conclude that the precise orientation of $Ca_V\beta$ at the AID region allows rapid voltage-dependent inhibition and its

relief by a prepulse. Voltage-dependent, membrane-delimited inhibition of presynaptic N-channels by GPCRs, such as the opioid receptor, regulates Ca^{2+} entry into nerve terminals thus providing relief from pain (Altier et al., 2006). While channel subtypes, accessory subunit composition and membrane potential contribute to regulating membrane-delimited inhibition (Tedford and Zamponi, 2006), our study raises the possibility that N-channel mutations may underlie disrupted structural and functional properties of voltage-dependent modulation when no other discrepancy in receptor, ligand or signaling pathway is clinically obvious. Dysfunction of Ca^{2+} channels underlies several neuronal diseases such as migraine and epilepsy. It is possible that mutations that change the structure of key regions of the Ca^{2+} channels, such as in the AID, may cause more subtle changes in channel function, but could severely impact the channel's response to agonists released during neural activity.

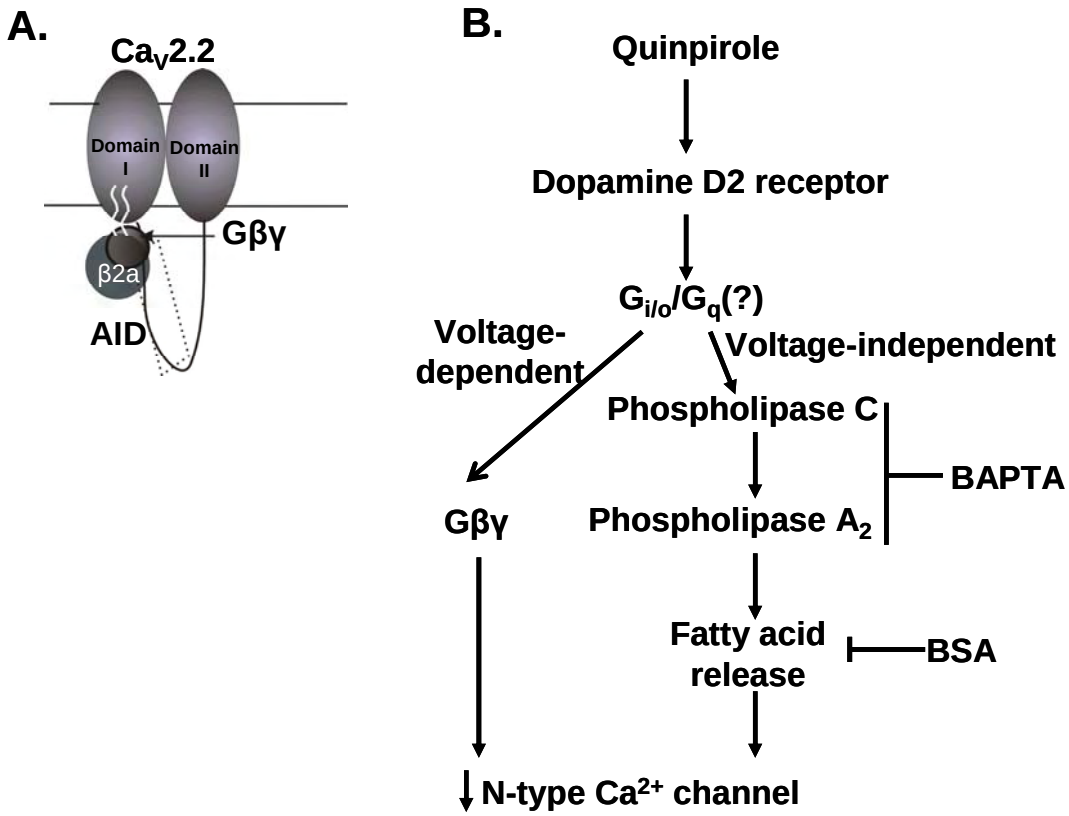

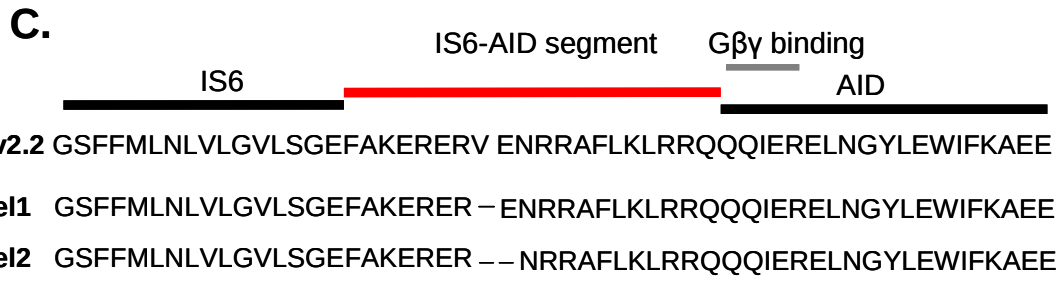

Figure 5.1 Membrane-delimited modulation involves Gβγ binding to $Ca_V2.2$ **(A)** Schematic representation of Gβγ binding to $Ca_V2.2$ following D2R activation. The I-II linker connects domain I and II of the N-channel. The $Ca_V\beta$ and Gβγ bind to overlapping sites at the AID region. **(B)** Flowchart showing the signaling cascades by which quinpirole may modulate $Ca_V2.2$. **(C)** I-II linker sequences for wt $Ca_V2.2$, Bdel 1 and Bdel 2 show where the amino acid deletions were made within the IS6-AID segment.

Figure 5.2 D2R inhibits recombinant $Ca_V2.2$ currents via a voltage-dependent pathway. HEK cells were transiently transfected with wt $Ca_V2.2$, α2δ–1, β2a and D2R. **(A)** Working model of the $Ca_v2.2$ channel with an associated β2a subunit. β2a's palmitoyl groups are shown as two white dots. **(B, E)** Individual traces taken before (con) and after application of 300 nM quin using **(B)** 0.1 mM or **(E)** 20 mM BAPTA. P1 represents current before a prepulse and P2 represents current measured after a prepulse. Scale bars always represent 200 pA on the Y-axis and 0.024 s on the X-axis. **(C, F)** Summary of the inhibition due to quin before and after prepulse in the presence of **(C)** 0.1 mM BAPTA (n=4; $^{**}p<0.01$) and **(F)** 20 mM BAPTA (n=4; $^{**}p<0.01$). **(D)** Summary of TTP before and after application of quinpirole (n=6, $^{*}p<0.05$).

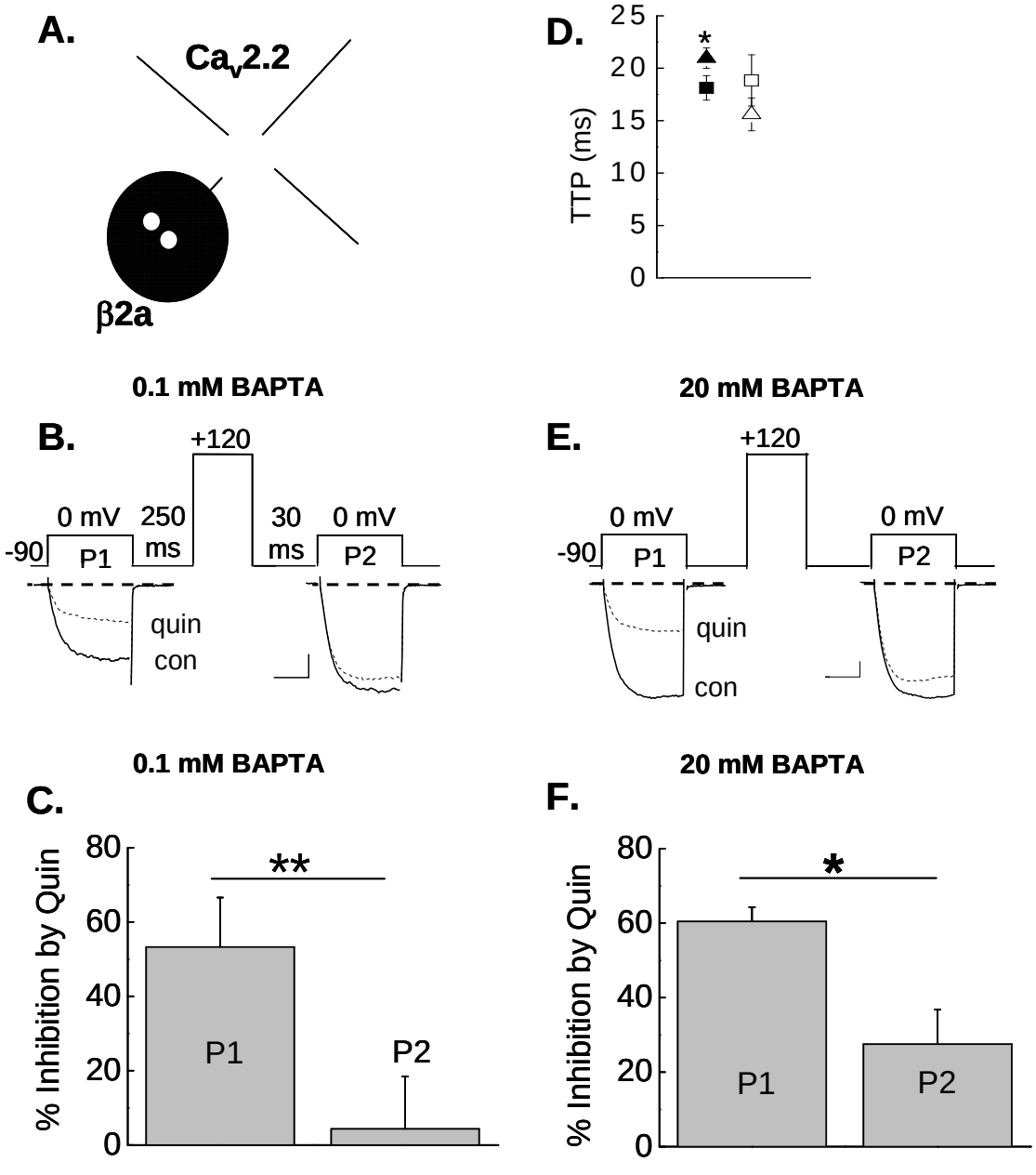
A.
Ca$_V$2.2
β2a
D.
TTP (ms)
25
20
15
10
5
0
*
0.1 mM BAPTA
20 mM BAPTA
B.
E.
+120
0 mV
250 ms
30 ms
0 mV
-90
P1
P2
quin
con
0.1 mM BAPTA
20 mM BAPTA
C.
F.
% Inhibition by Quin
80
60
40
20
0
**
*
P1
P2

Figure 5.3 Deletions in the IS6-AID segment disrupt voltage-dependence of current facilitation. **(A)** Voltage protocol to determine dependence of facilitation on prepulse potential. The depolarizing pulse was increased from -40 mV to +120 mV with 20 mV increments. Individual sweeps representing P1 and P2 obtained by stepping to indicated test potentials. Dashed line represents sweep following a prepulse to -40 mV; solid line represents sweep following a prepulse to +120 mV. **(B)** Facilitation ratio (P2/P1) was plotted against prepulse potential for wt (○), Bdel1 (◊) and Bdel2 (▲). **(C)** Voltage protocol to determine dependence of facilitation on test potential. The test potential was increased from -20 mV to +40 mV with 10 mV increments. **(D)** Facilitation ratio for each prepulse was plotted against test pulse potential for wt (○), Bdel1 (◊) and Bdel2 (▲).

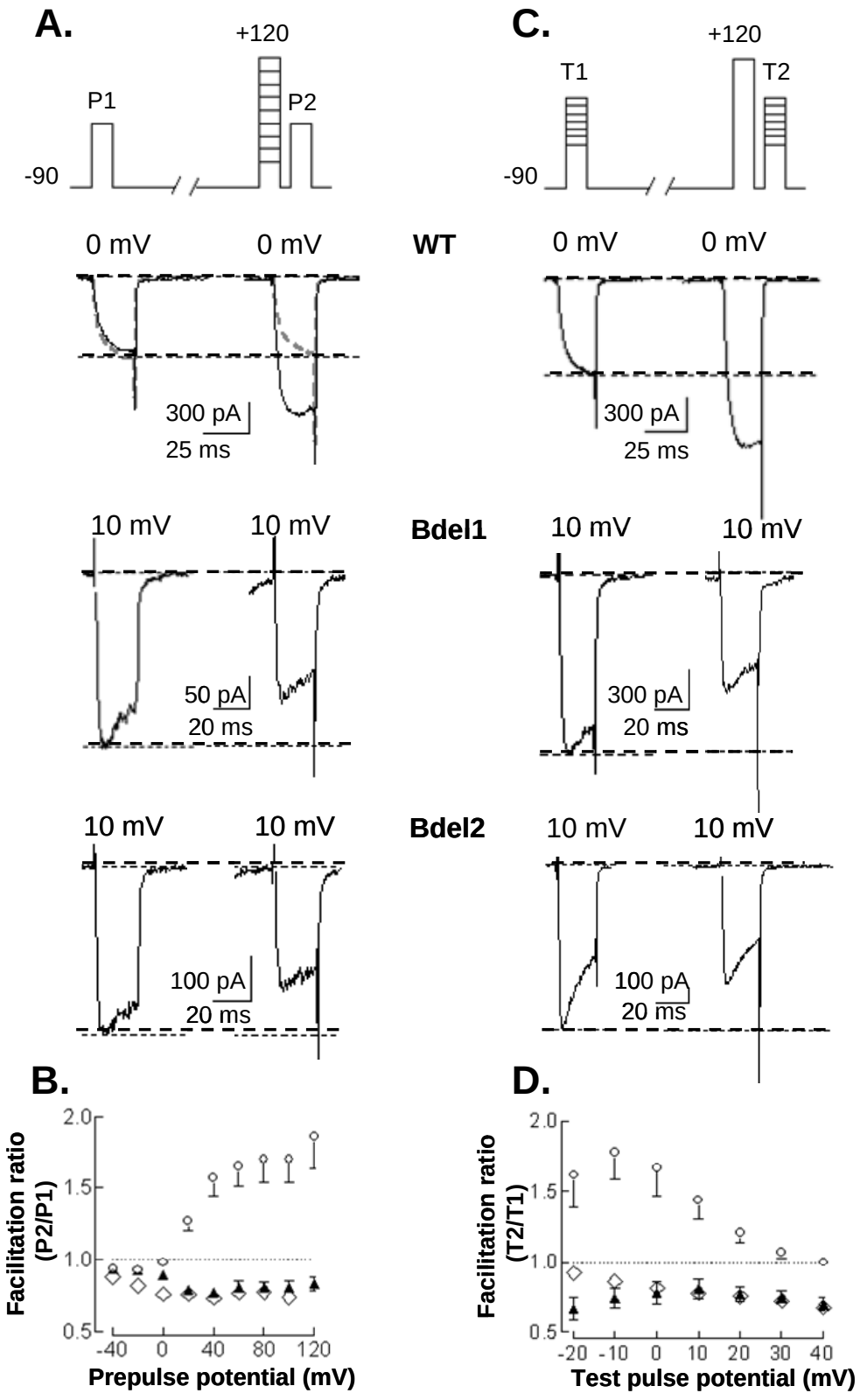
A.
+120
P1
P2
-90
0 mV
0 mV
300 pA
25 ms
10 mV
10 mV
50 pA
20 ms
10 mV
10 mV
100 pA
20 ms
B.
Facilitation ratio (P2/P1)
2.0
1.5
1.0
0.5
-40
0
40
80
120
Prepulse potential (mV)
C.
+120
T1
T2
-90
WT
0 mV
0 mV
300 pA
25 ms
Bdel1
10 mV
10 mV
300 pA
20 ms
Bdel2
10 mV
10 mV
100 pA
20 ms
D.
Facilitation ratio (T2/T1)
2.0
1.5
1.0
0.5
-20
-10
0
10
20
30
40
Test pulse potential (mV)

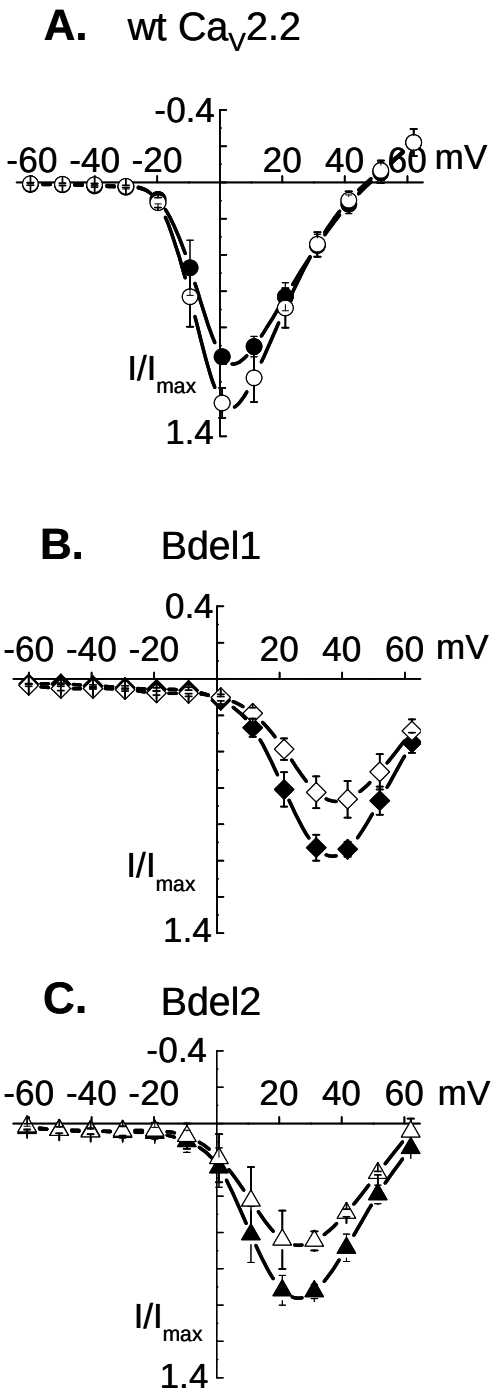

Figure 5.4 Tonic facilitation of currents is lost as observed in current voltage profiles **(A)** $Ca_V2.2$/β2a (○) **(B)** Bdel/ β2a (◊) **(C)** Bdel2/ β2a (▲). P1 indicated by closed symbols, P2 indicated by open symbols; n-3-4 per group.

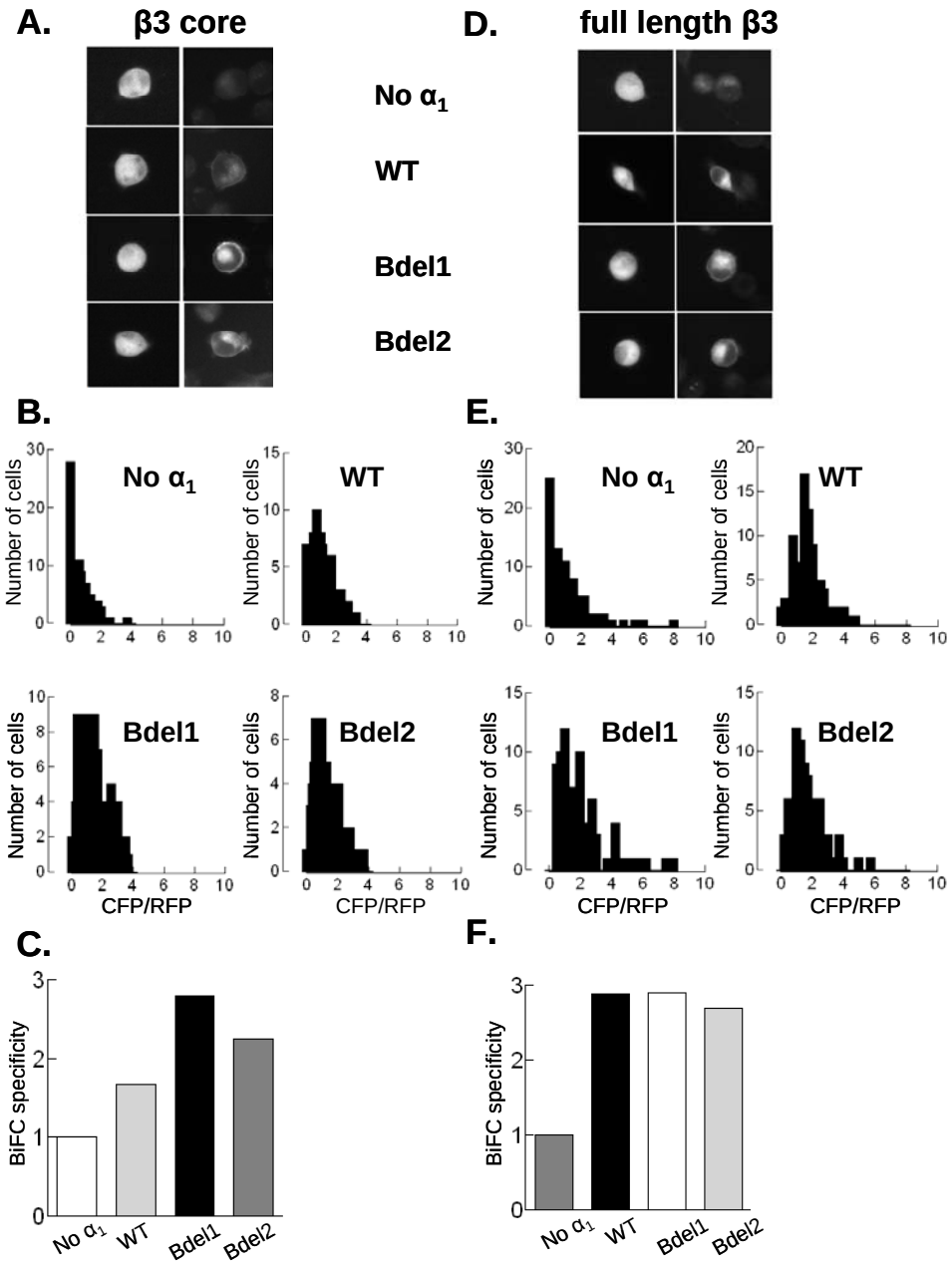

Figure 5.5 Interaction of Gβγ and Ca_Vβ is dependent on α1 subunit expression. **(A, D)** Images of representative cells obtained with bimolecular fluorescence complementation (BIFC) assay illustrate the close association of Gβγ with **(A)** β3 core or **(C)** full length β3 with no α1 or in the presence of wt Ca_V2.2, Bdel1 or Bdel2. **(B, E)** Histogram representing CFP/RFP ratio for wt Ca_V2.2, Bdel1 and Bdel2 in the presence of **(B)** β3 core or **(E)** full length β3. Summary of BIFC specificities obtained with **(C)** β3 core or **(F)** full length β3. n=94-138.

Figure 5.6 A single amino acid deletion in the IS6-AID segment disrupts inhibition and its relief by a prepulse. HEK-M1 cells were transiently transfected with D2R, Bdel1, $\alpha_2\delta$−1, β2a **(B, C)** or β3 **(E, F)**. **(A)** Working model where the single amino acid deletion in $Ca_V2.2$ (Bdel1) disrupts the orientation of β2a relative to Bdel1. **(B, E)** Individual sweeps taken before (con) and after application of 300 nM quin. **(C, F)** Summary of current inhibition by quin before and after a prepulse (n=5-6; NS denotes not significant). **(D)** Summary of facilitation ratio for wt with β2a (●), Bdel1 with either β2a (■) or β3 (**p<0.01; n=4-6 per group).

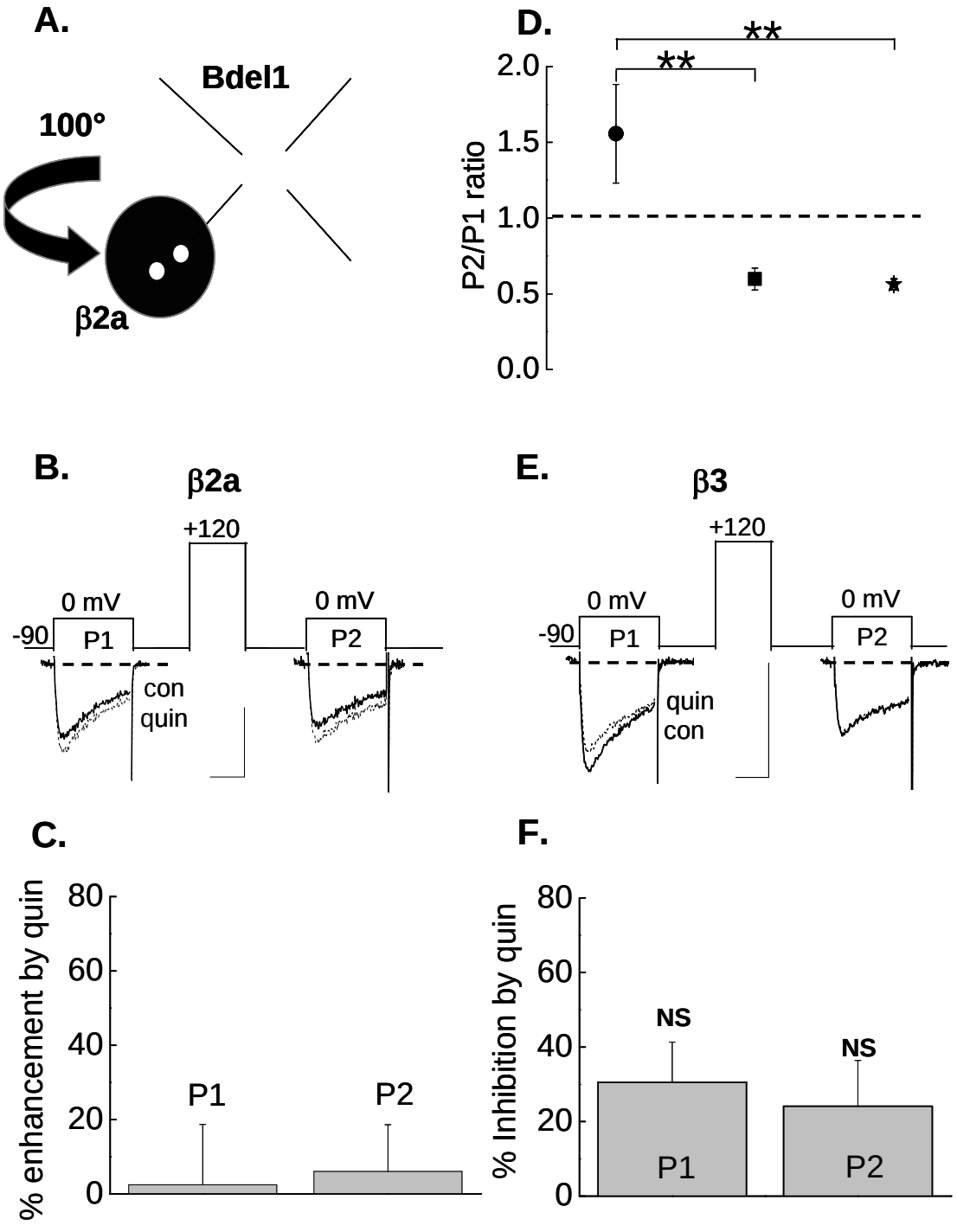
A.
Bdel1
100°
β2a
D.
**
**
2.0
1.5
1.0
0.5
0.0
P2/P1 ratio
B.
β2a
+120
0 mV
0 mV
-90
P1
P2
con
quin
E.
β3
+120
0 mV
0 mV
-90
P1
P2
quin
con
C.
% enhancement by quin
80
60
40
20
0
P1
P2
F.
% Inhibition by quin
80
60
40
20
0
NS
NS
P1
P2

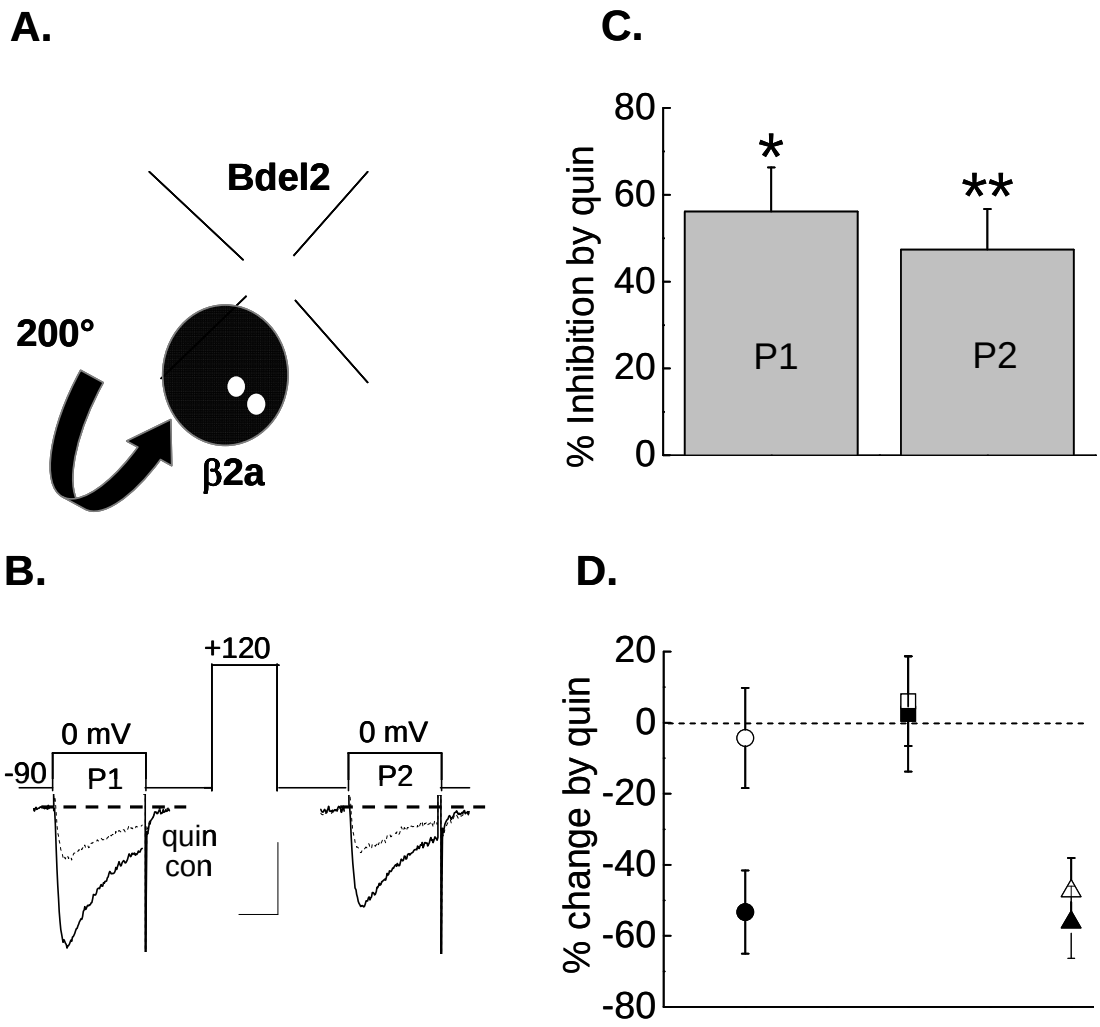

Figure 5.7 Current modulation by D2Rs is partially restored in Bdel2 channels. **(A)** Working model of Bdel2 where the orientation of β2a relative to Bdel2 is partially restored. β2a's palmitoyl groups are indicated by the two white dots. **(B)** Individual traces taken before (con) and after application of 300 nM quin. **(C)** Summary of N-current inhibition by quin before and after a prepulse. D) Summary of N-current inhibition before (filled) and after (open) a prepulse for wt (●), Bdel1 (■) and Bdel2 (▲); n=4-6 per group. *$p \leq 0.05$, **$p < 0.01$.

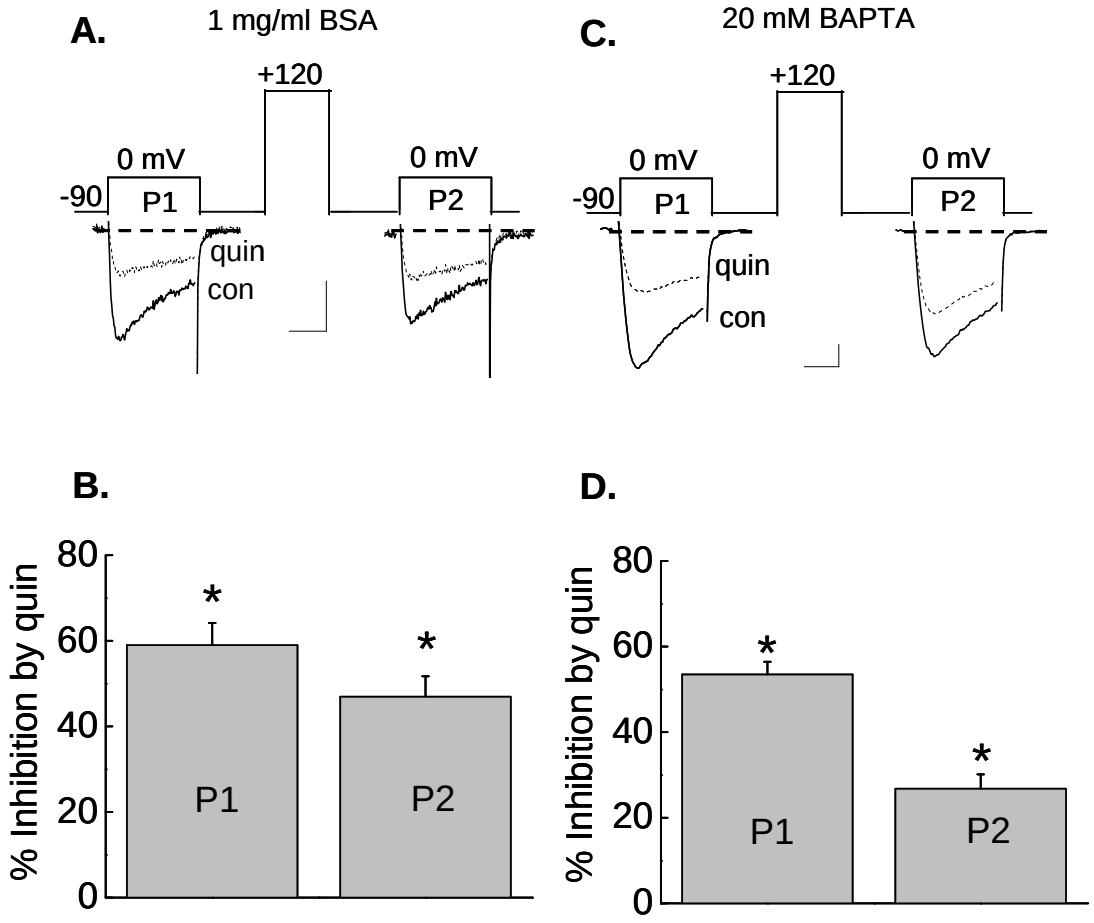

Figure 5.8 Inhibition of Bdel2 current by quin is voltage-independent but not mediated by a free fatty acid. **(A)** Individual traces taken after preincubation with BSA in the before (solid) and after (dashed) application of 300 nM quin. **(B)** Summary of current inhibition due to quin in the presence of BSA before (P1) and after (P2) a prepulse (n = 5 per group; *$p < 0.05$ compared to control current amplitude before and after a prepulse). **(C)** Example traces and **(D)** summary of mean current inhibition by quin with 20 mM BAPTA in the pipette solution (n = 5 pergroup, *$p<0.05$ compared to control peak currents before and after a prepulse).

CHAPTER VI:

Discussion

In this thesis, I have studied the modulation of N-channels by NK-1R and the role of $Ca_V\beta$ subunits in determining which form of modulation dominates. I have used a recombinant system to study N-channels in isolation without having to pharmacologically block other channels. I have summarized my key findings and discussed their functional implications at the cellular and molecular level and where appropriate, in terms of pain therapy. I have also discussed key outstanding questions that remain and what experiments I would do in the future to try to answer them. Lastly, I summarize my vision of how I could imagine $Ca_V\beta$s serving as a therapeutic target for treating neuropathic pain.

1) The slow pathway mediates N-current modulation by SP

Rapid turnover of phospholipids upon stimulation of pancreatic slices by acetylcholine was first observed in the 1950s (Hokin and Hokin, 1953). Although it is well known that prostaglandins and other metabolites of AA released during pain and inflammation are important inter- and intracellular signaling molecules (Hannun and Obeid, 2008), the role of AA as a signaling molecule mediating N-current modulation has not been readily accepted (Delmas et al., 2005; Michailidis et al., 2007). Consequently the actions of AA on neuronal calcium channel functioning are not understood

mechanistically. Therefore, as my first question, I used a pharmacological approach in Chapter II to examine whether inhibition of N-current by SP involves phospholipid breakdown by the slow pathway. I tested antagonists against components that appear to participate in slow pathway modulation of N-channel activity by other GPCRs such as the M_1R (Liu and Rittenhouse, 2003). My findings are consistent with ERK1/2, PLA_2 and a free fatty acid, most likely AA, participating in N-current inhibition by NK-1Rs (Fig 6.1). These findings link SP and the inflammatory signaling that normally occurs during pain to N-channel modulation. Recently, the enzyme diacylglycerol lipase was shown to be necessary for modulation of N-current by M_1R (Liu et al., 2008) in addition to PLC and PLA_2 (Liu and Rittenhouse, 2003a). Hence it is possible that this lipase and other enzymes are also involved in modulation of N-current by NK-1Rs. The data in Chapters II-IV indicate that as with M_1R signaling, NK-1Rs utilize the same signaling cascade to modulate N-current.

The requirement of several phospholipases for N-current inhibition (Liu and Rittenhouse, 2003a; Gamper et al., 2004) suggests that N-channel modulation arises from a coordinated breakdown of phospholipids occurring in close proximity to the channel. A proximal location of the enzymes and precursors could provide specificity and efficiency of signaling. An example of enzyme location optimizing function is diacylglycerol lipase, which synthesizes 2-arachidonoyl-glycerol from diacylglycerol (Bisogno et al., 2003). Diacylglycerol lipase is specifically targeted to the neck and not the body of postsynaptic spines in cerebellar Purkinje neurons. Its location ensures that diacylglycerol in spines can activate protein kinase C sufficiently before its rising concentration reaches the neck

of the spine and undergoes metabolism to yield 2-arachidonoyl-glycerol (2AG). Once synthesized, 2AG will diffuse into the synaptic cleft away from the postsynaptic membrane where it rapidly binds to presynaptic cannabinoid receptors ensuring efficient retrograde signaling (Yoshida et al., 2006).

The involvement of phospholipid metabolism in N-current modulation by SP comes as no surprise, given the role of the enzymes phospholipase A_2, C and D in pain and inflammation (Steed and Chow, 2001; Svensson and Yaksh, 2002; Drdla and Sandkuhler, 2008). However, identifying the specific components of this G_q signaling pathway that act on N-channels is an important step forward in understanding the possible molecular changes occurring during pain transmission because, given the diversity of signaling molecules, not all GPCRs modulate ion channels the same way. For example, bradykinin is a key mediator of inflammatory responses and its receptor activation leads to activation of PLC, PLA_2 and release of diacylglycerol (Farmer and Burch, 1992). Yet, bradykinin modulates Ca^{2+} currents by a pathway distinct from M_1Rs or NK-1Rs (Wilk-Blaszczak et al., 1994; Delmas et al., 2002; Gamper et al., 2004). Interestingly, despite overlapping downstream signaling molecules with muscarinic agonists and SP, bradykinin's receptor couples to a G_{13}-coupled receptor (Wilk-Blaszczak et al., 1994). These findings suggest that perhaps the G-protein is critical in creating signaling microdomains that then determine the enzymes contained within it. My studies predict that other receptors, which couple to G_q, also should utilize the same pathway to modulate N-current. This possibility is supported by findings that angiotensin II also inhibits N-current in SCG neurons via a diffusible messenger (Shapiro et al.,

1994b). Moreover, these GPCRs should not only modulate N-current in peripheral and spinal neurons but also in the brain wherever G_q-coupled receptors are found (Stewart et al., 1999).

Future Direction: What is the role of $cPLA_2$ in shaping an action potential in dorsal horn neurons?

My findings were collected using recombinant N-channels. Could one of the enzymes, for example $cPLA_2$, discussed in Chapter II participate in modulation of Ca^{2+} currents when SP is released onto the dorsal horn neurons? Moreover, how would the modulation of Ca^{2+} currents affect the shape of the action potentials in the dorsal horn? To answer these questions, I would generate action potentials by injecting current into dorsal horn neurons before and after applying SP. I would then compare the action potential profiles from wild-type neurons with similar recordings from dorsal horn neurons isolated from $cPLA_2^{-/-}$ mice. I would expect $cPLA_2$ to be important in modulation of Ca^{2+} currents in the dorsal horn neurons. I would predict that while SP application in the neurons from wt mice would affect the action potential duration and/or frequency of action potentials, these parameters would be unaffected in neurons from $cPLA_2^{-/-}$ mice. Unpublished data from Dr. Liwang Liu indicates that SCG neurons from the $cPLA_2^{-/-}$ mice display unanticipated hyperexcitability in control conditions. Whether adding back $cPLA_2$ would restore the membrane excitability remains untested.

2) $Ca_V\beta$ subunit expression determines whether enhancement or inhibition dominates N-current modulation

In Chapter III, I extended the observation made by Dr. John Heneghan in his thesis that modulation of N-channels by M_1R changes from inhibition to enhancement depending on which $Ca_V\beta$ subunit is co-expressed, by testing whether a similar profile of modulation is observed when stimulating NK-1Rs with SP. Whereas inhibition is observed with $Ca_V\beta3$, I found that N-current enhancement occurs when the palmitoylated $Ca_V\beta2a$ is present (Fig 6.1). Additionally, I advanced our understanding of how $Ca_V\beta2a$ appears to block inhibition to reveal enhancement. From studies with mutated and chimeric $Ca_V\beta$ subunits we showed that block of inhibition required palmitoylation of $Ca_V\beta2a$ and I discovered that free palmitic acid is sufficient to block N-current inhibition by SP. These findings suggest that the palmitic acids are necessary and sufficient for blocking inhibition.

While the role of $Ca_V\beta$ was earlier conceived as being confined to regulating the channel's expression and kinetic properties, separation of inhibition and enhancement based on the subtype of $Ca_V\beta$ that is co-expressed with $Ca_V2.2$ identified a new role for $Ca_V\beta$ in channel modulation by the slow pathway. Biophysical and biochemical studies, presented in Chapter V, indicate that N-current enhancement occurs via the same pathway that mediates inhibition, but it is not clear whether enhancement occurs via a site that is located on the channel or on the $Ca_V\beta$ subunit.

While direct interaction of AA with specific sites on N-channels has been proposed as a mechanism for channel modulation, this direct interaction could occur at an

extracellular site, an intracellular site or within transmembrane regions (Meves, 2008). N-current enhancement by exogenous AA occurs faster than inhibition, indicating two different sites of action (Barrett et al., 2001). In the presence of BSA in the bath, both N-current inhibition and enhancement by Oxo-M are lost (Liu and Rittenhouse, 2003a). Internal dialysis of SCG neurons with BSA eliminates inhibition when Oxo-M is applied and application of arachidonoyl coenzyme AA, an AA analog that cannot cross the cell membrane, mimics enhancement but not inhibition (Barrett et al., 2001). These four experiments suggest that enhancement occurs extracellularly or within the outer leaflet of the membrane while inhibition occurs intracellularly or within the inner leaflet. Alternatively the enhancement site could be within the inner leaflet, but exhibit higher affinity for AA such that residual AA that remains in the presence of BSA or that accompanies the arachidonyl CoA, but crosses the cell membrane, can act at the internal site.

Both internal and external sites of action have been observed for K^+ channel modulation by AA (Ordway et al., 1991). For example, in a study examining the effects of AA on the transient K-current I_A, an internal inhibitory site was proposed since intracellular application of a low concentration of AA (1pM) inhibited I_A while a 10^6-fold increase in AA concentration was required when applied extracellularly (Bittner and Muller, 1999). An explanation for this observation is that, when a higher concentration of AA was applied extracellularly, the AA must cross the cell membrane to interact with the inhibitory site for inhibition to occur. The existence of an inhibitory site for AA on N-channels is further revealed in the finding that exogenous palmitic acid can block this inhibition (Chapter III), most likely by occupying this same site. Determining the exact

location of the regions of N-channels that confer enhancement and inhibition should provide a detailed, molecular understanding of how the modulation occurs.

Future direction: Is the interaction of $Ca_V\beta$ subunits with $Ca_V2.2$ subunits dynamic?

I would be very interested in determining whether the distribution of $Ca_V\beta2a$ and $Ca_V\beta3$ subunits changes during conditions of neuropathic pain. The ratios of $Ca_V\beta$ subunits expressed in individual neurons have not been studied in any brain region. By performing immunocytochemistry on dorsal horn tissue samples from animals before and after nerve injury, a change in the subunit ratio could be measured acutely and over a period of days. The findings should be quite relevant to pain management because the $Ca_V\beta$ expression pattern should determine whether inhibition or enhancement of N-current occurs in the presence of SP. In turn the change in N-current is predicted to alter neuronal firing; in other words, $Ca_V\beta$ subunit expression should affect membrane excitability. The possible contributions of the two different $Ca_V\beta$ subunits to membrane excitability will be discussed below in a later section.

3) Role of palmitoylation in N-channel modulation

From the studies in Chapter III, I realized that by further understanding the role of palmitoylation in N-channel modulation, I could gain mechanistic insight on how NK-1Rs inhibit N-current. Therefore in Chapter IV, I tried to determine whether the palmitic acids might be interacting with $Ca_V2.2$ to somehow disrupt N-current inhibition by SP. I tested mutant N-channels where $Ca_V\beta2a$ associates with $Ca_V2.2$ in a different orientation

(Vitko et al., submitted). I found that while current enhancement occurs with $Ca_V\beta2a$ expression with wt channels, deletions in the IS6-AID segment that change $Ca_V\beta2a$'s orientation in relation to $Ca_V2.2$, result in current inhibition by the slow pathway. While changing $Ca_V\beta2a$'s orientation still allows it to bind to mutant N-channels, the data seem to indicate that with a sufficient change in orientation, the palmitoyl groups acquire a new position whereby they no longer block N-current inhibition when SP is applied. Thus, inhibition dominates N-current modulation. I cannot yet claim to completely understand what causes current enhancement. However, the data in Chapter IV give an image of a missing key, palmitic acid in this case, which when absent (as in $Ca_V\beta3$) or displaced (when $Ca_V\beta2a$ associates with Bdel2), allows current inhibition, and when added back in the form of free palmitic acid can block inhibition. The data also show for the first time that in addition to the subtype of $Ca_V\beta$ subunit that associates with N-channels, it is also the orientation of the $Ca_V\beta$ subunit that determines the form of modulation observed following exposure to SP. When SP is applied, Bdel2/$Ca_V\beta2a$ currents do not show current enhancement even when palmitic acid is added back, hence it is possible that the determinants of current enhancement (discussed below) are present in $Ca_V\beta2a$; however since its orientation is changed compared to when it is associated with wt $Ca_V2.2$, the enhancement site(s) also is not available.

The novel role of palmitoylation as an antagonist of lipid signaling raises questions about an unanticipated role for palmitoylation in the pain pathway. While palmitoylation of $Ca_V\beta2a$ is a dynamic process (Hurley et al., 2000), inhibiting palmitoyl acyltransferases by the nucleoside antibiotic, tunicamycin, causes neuronal growth cones

to collapse within 10 mins of application (Patterson and Skene, 1994). This effect can be reversed by application of exogenous palmitic acid indicating a role for palmitoylation in neurite extension and axon regeneration. This leads one to wonder whether the palmitoyl acyltransferase could be specifically up- or down-regulated during neuropathic pain. Regulation of palmitoyl acyltransferases may be a mechanism to regulate neuronal excitability by changing the levels of palmitoylated proteins including Cavβ2a. Preliminary experiments indicate that besides N-channels, dorsal horn neurons also express Ca_Vβ2a and Ca_Vβ3 subunits as early as postnatal day 3 (Fig 6.2). Could a toggling of N-channel modulation by dynamic palmitoylation of Ca_Vβ subunits be observed at this stage of development? Answers to these questions await future studies.

Future Direction: Where are the enhancement and inhibitory sites located?

While the sites for current modulation are still not known, two potential sites are along the S6 segments of Ca_V2.2, which line the channel's pore forming an inverted tepee, and the variable D2 region of Ca_Vβs- both of which have been implicated in regulating channel inactivation. I am interested in this question because finding an inhibitory site would not only help in better understanding the modulation of Ca_V2.2, but it would also establish Ca_V2.2 as a lipid-binding protein. Mutating residues in the S6 region possesses the risk of destabilizing the tepee but careful amino acid substitutions may help in overcoming the challenge. Of particular interest is a key asparagine residue in the S6 region that is conserved among Na_V and Ca_V channel families (Fig 6.3a). This N406S mutation is a mutation in Na_V1.5 that contributes to aberrant electrocardiograph

patterns in Brugada syndrome, also known as Sudden Unexpected Death Syndrome (Brugada et al., 2005). The asparagine residue is part of a sequence of amino acid residues that is highly conserved in both Na^+ and Ca^{2+} channel families (Fig 6.3b). Mutation of this residue to serine in the cardiac voltage-gated Na^+ channel, $Na_V1.5$, accelerates inactivation kinetics. Compared to wt channels, in the presence of a fatty acid, the mutant channels show faster recovery from inactivation, less current inhibition and enhancement of current (Xiao et al., 2001; Itoh et al., 2005; Itoh et al., 2007). Hence it seems that while the S6 region is important for inactivation (Hering et al., 2000), it could also be important for current inhibition by fatty acids.

I am particularly curious about the role of $Ca_V\beta2a$ in current enhancement. If the palmitoylated $Ca_V\beta2a$ blocks inhibition revealing latent enhancement, is there a structural component of the $Ca_V\beta$ subunit that promotes enhancement? As pointed out earlier, a determinant of N-current enhancement could be present in the $Ca_V\beta2a$ subunit. One region of interest that could be easily tested is a variable D3 region which is longest in $Ca_V\beta2a$ compared to $Ca_V\beta1b$, $Ca_V\beta3$ and $Ca_V\beta4$ (Birnbaumer et al., 1998). This D3 region, also referred to as the HOOK region (Fig 6.4) connects the two highly conserved SH3 and guanylate kinase (GK) domains of the $Ca_V\beta$ subunits and is usually involved in interaction of membrane-associated guanylate kinases with other proteins (Chien et al., 1998; Hanlon et al., 1999; Chen et al., 2004; Opatowsky et al., 2004; Van Petegem et al., 2004). Coincidentally, enhancement of current was observed with a peptide containing the SH3-HOOK-GK region (De Waard et al., 1994). But since an artificial peptide generated from a shift in the reading-frame of the SH3-HOOK-GK region when dialyzed

into Xenopus oocytes also caused current enhancement, the enhancement was considered to be a non-specific effect due to lack of a mechanistic explanation (Chen et al., 2004) . However, increase in current was also seen when a peptide containing $Ca_V\beta$'s GK domain but not when the SH3 and GK regions from PSD95 were co-expressed in the oocytes (Chen et al., 2004). With careful analysis, it is possible that the HOOK region by itself or together with the SH3 and GK domains indeed contributes to current enhancement.

One way to test the involvement of the SH3-HOOK-GK region is to use the recently published $Ca_V\beta2a$ mutants that lack the SH3, GK or the connecting HOOK region (Dresviannikov et al., 2008). If enhancement of $Ca_V2.2$ current is lost in the presence of one of these mutant $Ca_V\beta2a$ subunits, one could focus on the deleted sequence as a potential site for enhancement. It would be interesting to see whether all the $Ca_V\beta$ subunits share the same sequence or if the site is unique to $Ca_V\beta2a$. In any case, discovery of a site on $Ca_V\beta2a$ that contributes to current enhancement would be a key finding since most studies tend to focus on N-current inhibition. Yet, current enhancement at sub-zero membrane potentials is crucial when cells undergo short depolarizations during a postsynaptic potential or an action potential, such as during transmission of nociceptive information. On the other hand, if the inhibitory site for AA can be identified, it would potentially offer opportunities to develop novel strategies to manage pain, injury and stroke, where the impetus would be on developing drugs that target the inhibitory site to prevent uncontrolled modulation by AA.

4) Moving $Ca_V\beta$2a's orientation alters membrane-delimited inhibition

In chapter V, I have shown that $Ca_V\beta$'s normal orientation to Ca_V2.2 is necessary to observe both membrane-delimited inhibition and relief of this inhibition following a depolarizing pulse. The data in this chapter serve as a control for the data in Chapter IV because it shows that $Ca_V\beta$2a's orientation is not only important for modulation via the slow pathway but also for a different form of modulation of N-current, the membrane-delimited inhibition. These findings suggest that $Ca_V\beta$'s orientation with the wt Ca_V2.2 allows it to move with the electric field during a step depolarization. This movement serves to displace $G\beta\gamma$ and thereby relieve N-current inhibition. When $Ca_V\beta$'s orientation to Ca_V2.2 is changed as with Bdel1 or Bdel2, $Ca_V\beta$ can no longer harness the kinetic energy of Ca_V2.2's movements or the electrical field across the cell membrane to "budge" $G\beta\gamma$ and hence inhibition is maintained. What the data in this chapter does not clarify is how the altered orientation alters the voltage-dependence of inhibition; but it does provide the insight that altered orientation of $Ca_V\beta$ disrupts $Ca_V\beta$'s ability to dislodge $G\beta\gamma$ during positive test pulses. As with Chapter IV, the way to move this forward conceptually would be to determine whether the palmitic acids of $Ca_V\beta$2a directly interact with Ca_V2.2 as described above. Tethering $Ca_V\beta$2a to Ca_V2.2 may efficiently couple $Ca_V\beta$-subunit movement to positive shifts in voltage. Indeed, when comparing the effectiveness of $Ca_V\beta$ subunits, the greatest prepulse facilitation of inhibited current is observed with $Ca_V\beta$2a (De Waard, 2005).

Final comments on the role of SP and Ca^{2+} channel in neuropathic pain

Neuropathic pain arises from damage to nerve fibres which are located either peripherally or in the dorsal root (Zieglgansberger et al., 2005) and may occur following disease or surgery. In animal pain models, peripheral neurons show increased membrane excitability after nerve injury that results in hyperalgesia (intense pain) or allodynia (increased response to normally innocuous stimuli) (Hogan, 2007). DRG neurons show prolonged action potential duration, decreased amplitude and duration of afterhyperpolarization and decreases in high-voltage activated Ca^{2+} currents following nerve injury.

Influx of Ca^{2+} is tightly coupled to Ca^{2+}-sensitive K^+ channels, which generate $I_{K(Ca2+)}$ that underlies the afterhyperpolarization in many neurons (Fig 6.5a). Thus loss of Ca^{2+} currents, which could arise from inhibition of Ca^{2+} currents by SP, following nerve injury causes decreased outward $I_{K(Ca2+)}$ and reduces the amplitude and duration of afterhyperpolarization (Fig 6.5b). These changes would be predicted to increase neuronal firing rates. A prolonged action potential is likely to release more neurotransmitter (such as SP) at the synapse between DRG and dorsal horn neurons while reduced afterhyper-polarization increases membrane excitability and burst firing. Increased rate of firing of dorsal horn neurons in response to nociceptive inputs is one of the mechanisms that leads to central sensitization of neurons that causes hyperalgesia (Campbell and Meyer, 2006). Increased burst firing increases nociceptive transmission via secondary neurons in the dorsal horn. However, after peripheral nerve injury, a reduction in SP immunoreactivity and an increase in NK-1R immunoreactivity in dorsal horn neurons (Malmberg and

Basbaum, 1998) could be an indication of increased downstream signaling leading to increase in ion channel modulation. Thus if the expression of $Ca_V\beta 2a$ subunits can be increased in spinal cord neurons pharmacologically or by gene manipulation, the released SP might elicit larger Ca^{2+} currents that will restore $I_{K(Ca2+)}$ and reduce membrane excitability (Fig 6.5c).

While expression of ion channels changes with neuropathic pain, targeting individual $Ca_V\beta$ subunits may be unrealistic and pose a challenge for therapeutic management. Anti-convulsive drugs such as gabapentin and pregabalin, aimed at the $\alpha_2\delta$-1 subunit, are currently used to treat neuropathic pain (Galluzzi, 2007) despite uncertainty surrounding their exact mechanism of action. With the advent of RNAi technology, such selective targeting of $Ca_V\beta$ subunits could be used to restore membrane excitability and provide relief from neuropathic pain. Thus, future experiments using genetic knockout mice, such as $cPLA_2^{-/-}$ (Bonventre et al., 1997) combined with cellular, molecular and pharmacological techniques will provide crucial answers regarding the role of N-current modulation by phospholipids, such as AA, in health and disease.

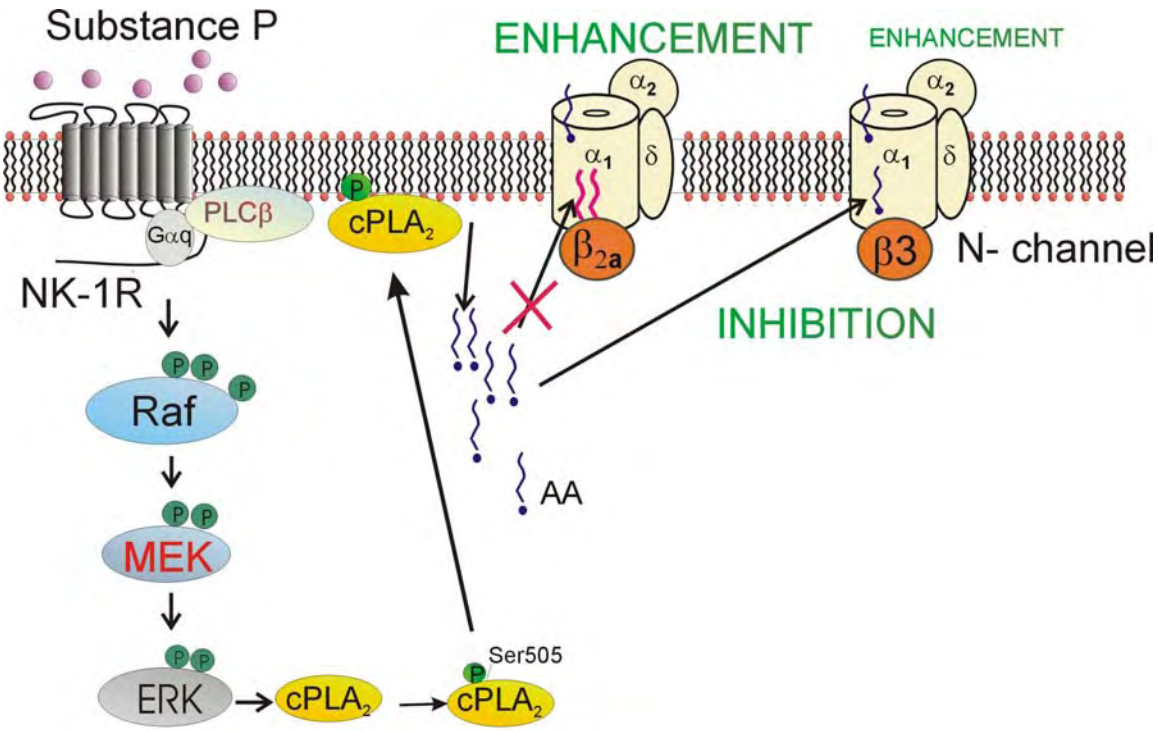

Figure 6.1 A working model of the signaling pathway involved in modulation of N-channels by SP. SP either enhances or inhibits N-current depending on the $Ca_V\beta$ subunit that is co-expressed. The studies in this thesis indicate involvement of ERK1/2, $cPLA_2$ and free AA in N-current modulation by SP. The presence of a $Ca_V\beta2a$ subunit blocks inhibition when SP is applied and the net effect is enhancement of current. On the contrary, when a $Ca_V\beta3$ subunit is present, inhibition predominates over enhancement.

Figure 6.2 Postnatal day 3 dorsal horn (DH) neurons express $Ca_V\beta2a$ as well as $Ca_V\beta3$ in addition to $Ca_V2.2$ and NK-1R. Homogenized tissue samples were lysed in 0.8 ml TRIzol reagent (Invitrogen). After separating RNA from DNA using phenol-chloroform phase separation, RNA was precipitated using isopropyl alcohol and washed with 75% ethanol. After drying, the RNA pellet was dissolved in RNase-free water. Subsequently, reverse transcription was carried out using 1.0 µl 10X buffer RT, 1.0 µl dNTP mix (5 mM each dNTP), 1.0 µl Oligo-dT primer (0.5 mg/ml), 0.125 µl RNase inhibitor (40 U/µl, Promega), 0.5 µl Omniscript Reverse Transcriptase and RNase-free water to make up a total volume of 10 µl (all reagents from QIAGEN, Valencia, CA unless otherwise noted). The mixture was incubated at 37ºC for 1 h. The mixture was then heated at 93ºC for 5 min followed by cooling on ice to rapidly inactivate the transcriptase. Aliquots of RT-PCR product were amplified by PCR using the following primers: α1B: 5'-CAC ATG CCA ACG CCA GCG AAT G-3' and 5'-GAC AGG CCT CCA GGA GCT TGG TG-3' (633 bp product) (Lin et al., 1996), NK-1R: 5'-AGG ACA GTG ACC AAT TAT TTC CTG G-3' and 5'-CTG CTG GAT GAA CTT CTT-3' (668 bp product) (Goto et al., 2007) and β2a: 5'- ATA ACC ACA GAG AGG AGA GCC ACA-3' and 5'-TAT ACA TCC CTG TTC CAC TCG CCA-3' (258 bp product) and β3 5'- TCC CTG GAC TTC AGA ACC AGC AG-3' and 5'- TTG TGG TCA TGC TCC GAG TCC TG-3' (368 bp) (Lin et al., 1996). Reaction mixtures for PCR contained 2 µl template cDNA, 2.5 µl 10X Buffer, 0.5 µl dNTP mix, 2 µl each of forward and reverse primer and made up in distilled water to a final volume of 25 µl. The protocol for amplification was 94°C for 4 mins, followed by 33 cycles of 94 °C for 45 secs, 60 °C for 45 secs, 72 °C for 1 min and held at 72 °C for 10 mins for last extension. PCR products were run on 1.8% agarose gel stained with ethidium bromide along with 1000 bp DNA ladder (Fermentas Life Sciences). Postnatal day 3 SCG neurons serve as a positive control for the presence of NK-1R, $Ca_V2.2$ and $Ca_V\beta2a$.

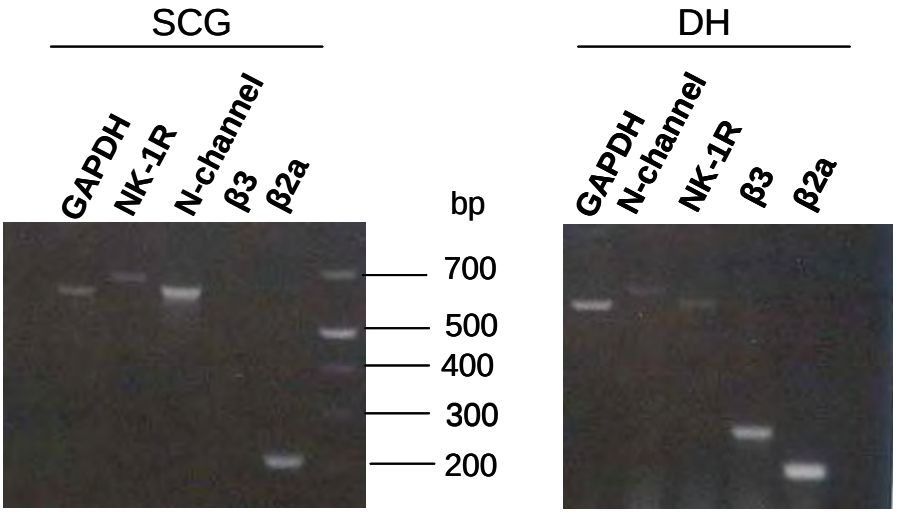
SCG
DH
GAPDH
NK-1R
N-channel
β3
β2a
bp
700
500
400
300
200
GAPDH
N-channel
NK-1R
β3
β2a

A.

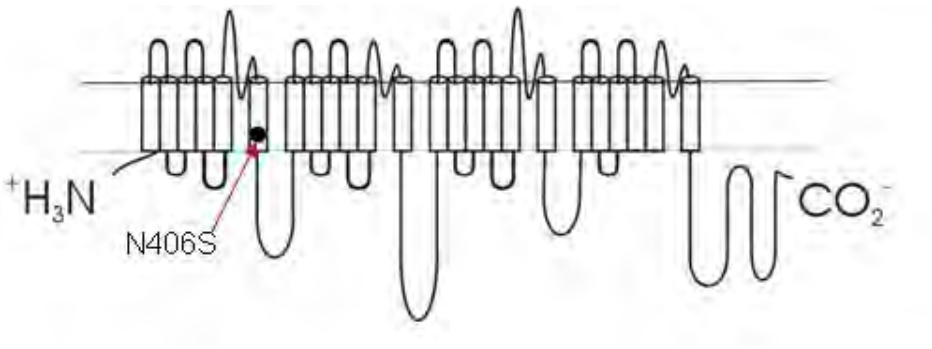

B.

hSCN5A	390	MIFFMLVIFLGSFYLVNLILAVVA	415 (N406)
rCav1.2	411	PWVYFVSLVIFGSFFVLNLVLGVLS	435 (N428)
rCav1.3	382	PWVYFVSLIILGSFFVLNLVLGVLS	406 (N399)
hCav1.4	348	PWVYFVSLVIFGSFFVLNLVLGVLS	372 (N365)
rCav2.1	338	NWLYFIPLIIIGSFFMLNLVLGVLS	362 (N355)
rCav2.2	332	NWLYFIPLIIIGSFFMLNLVLGVLS	356 (N349)
rCav2.3	278	NWLYFIPLIIIGSFFVLNLVLGVLS	302 (N295)
rCav3.1	371	NFIYFILLIIVGSFFMINLCLVVIA	395 (N388)
rCav3.2	395	NFIYFILLIIMGSFFMINLCLVVIA	419 (N412)
rCav3.3	372	NFIYFILLIIVGSFFMINLCLVVIA	396 (N389)

Adapted from Itoh et al., *J Cardiovasc Electrophysiol.* 2005 Apr;16(4):378-83.

Figure 6.3 The S6 region is an important site for channel modulation based on sequence comparison across Na^+ and Ca^{2+} channels. **(A)** Schematic representation of the location of the human point mutation in the gene *SCN*5A that encodes the pore-forming α subunit of $Na_V1.5$ channels. **(B)** A comparison of the homologous sequences from domain I S6 region of $Na_V1.5$ and Ca_V families. The conserved sequence of amino acids including asparagine could be a key site that mediates current inhibition by AA release during stimulation of the slow pathway since this residue confers fatty acid sensitivity to $Na_V1.5$.

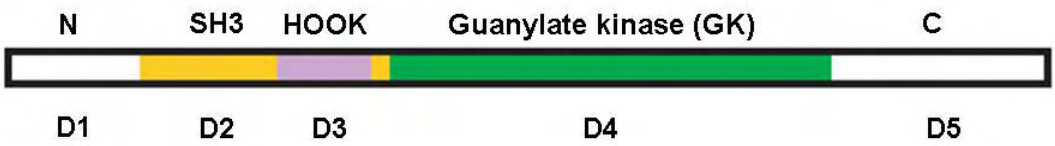

Adapted from Chen et al., *Nature* 2004 June; 429:675-680

Figure 6.4 Schematic representation of the structural organization of $Ca_V\beta$ subunits. $Ca_V\beta$ subunits all share the homologous D2 and D4 domains that are placed intermediately between the variable D1, D3 and D5 domains.

Figure 6.5 Schematic representation of altered membrane excitability that could occur in the presence of different $Ca_V\beta$ subunits. **(A)** Under normal conditions, influx of Ca^{2+} gives rise to an outward Ca^{2+}-activated K^+ current that contributes to the after-hyperpolarization following an action potential. **(B)** Upon nociceptive stimuli, released SP would modulate Ca^{2+} channel activity in the dorsal horn neurons by the slow pathway. If inhibition of Ca^{2+} currents occur due to the presence of $Ca_V\beta3$ subunit expression, a decrease in Ca^{2+}-activated K^+ currents would shorten the afterhyperpolarization, lead to an increased rate of firing, and contribute towards hyperalgesia. This could explain the hyperexcitability that occurs in neuropathic pain. **(C)** Following treatment, if expression of $Ca_V\beta2a$ became predominant, the resultant N-current enhancement following release of SP would increase the Ca^{2+}-activated K^+ current, restore the afterhyperpolarization, and bring membrane excitability to pre-injury levels.

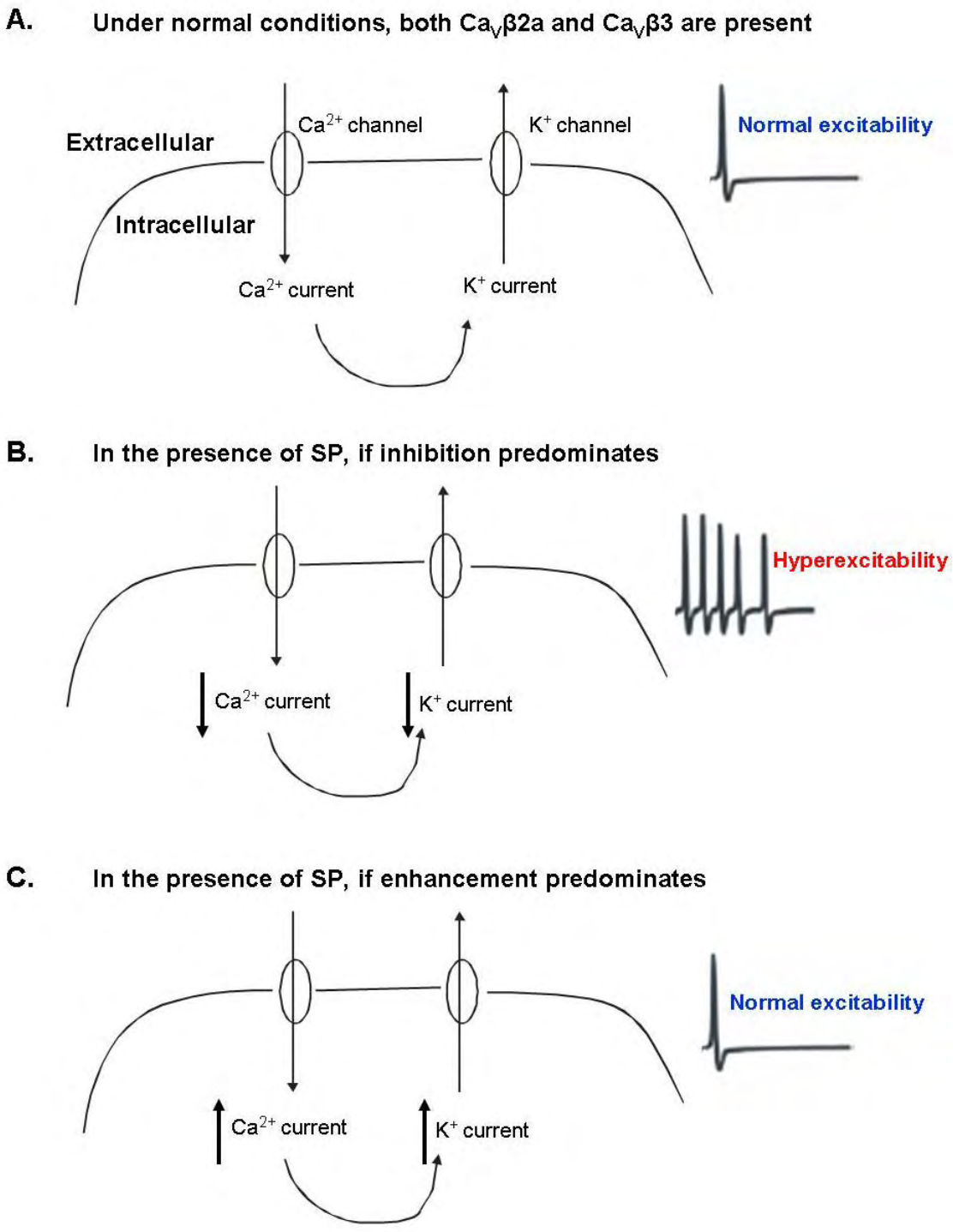

Adapted from Hogan *Croat Med J*. 2007;48:9-21

REFERENCES

Abdulla FA, Moran TD, Balasubramanyan S, Smith PA (2003) Effects and consequences of nerve injury on the electrical properties of sensory neurons. Can J Physiol Pharmacol 81:663-682.

Agler HL, Evans J, Tay LH, Anderson MJ, Colecraft HM, Yue DT (2005) G protein-gated inhibitory module of N-type (ca(v)2.2) ca2+ channels. Neuron 46:891-904.

Almeida TA, Rojo J, Nieto PM, Pinto FM, Hernandez M, Martin JD, Candenas ML (2004) Tachykinins and tachykinin receptors: structure and activity relationships. Curr Med Chem 11:2045-2081.

Altier C, Khosravani H, Evans RM, Hameed S, Peloquin JB, Vartian BA, Chen L, Beedle AM, Ferguson SS, Mezghrani A, Dubel SJ, Bourinet E, McRory JE, Zamponi GW (2006) ORL1 receptor-mediated internalization of N-type calcium channels. Nat Neurosci 9:31-40.

Arias JM, Murbartian J, Vitko I, Lee JH, Perez-Reyes E (2005) Transfer of beta subunit regulation from high to low voltage-gated Ca2+ channels. FEBS Lett 579:3907-3912.

Arikkath J, Campbell KP (2003) Auxiliary subunits: essential components of the voltage-gated calcium channel complex. Curr Opin Neurobiol 13:298-307.

Balsinde J, Winstead MV, Dennis EA (2002) Phospholipase A(2) regulation of arachidonic acid mobilization. FEBS Lett 531:2-6.

Bannister RA, Melliti K, Adams BA (2004) Differential modulation of CaV2.3 Ca2+ channels by Galphaq/11-coupled muscarinic receptors. Mol Pharmacol 65:381-388.

Barrett CF, Rittenhouse AR (2000) Modulation of N-type calcium channel activity by G-proteins and protein kinase C. J Gen Physiol 115:277-286.

Barrett CF, Liu L, Rittenhouse AR (2001) Arachidonic acid reversibly enhances N-type calcium current at an extracellular site. Am J Physiol Cell Physiol 280:C1306-1318.

Bean BP (1989) Neurotransmitter inhibition of neuronal calcium currents by changes in channel voltage dependence. Nature 340:153-156.

Beech DJ, Bernheim L, Hille B (1992) Pertussis toxin and voltage dependence distinguish multiple pathways modulating calcium channels of rat sympathetic neurons. Neuron 8:97-106.

Beech DJ, Bernheim L, Mathie A, Hille B (1991) Intracellular Ca2+ buffers disrupt muscarinic suppression of Ca2+ current and M current in rat sympathetic neurons. Proc Natl Acad Sci U S A 88:652-656.

Bell TJ, Thaler C, Castiglioni AJ, Helton TD, Lipscombe D (2004) Cell-specific alternative splicing increases calcium channel current density in the pain pathway. Neuron 41:127-138.

Bernheim L, Beech DJ, Hille B (1991) A diffusible second messenger mediates one of the pathways coupling receptors to calcium channels in rat sympathetic neurons. Neuron 6:859-867.

Bichet D, Cornet V, Geib S, Carlier E, Volsen S, Hoshi T, Mori Y, De Waard M (2000) The I-II loop of the Ca2+ channel alpha1 subunit contains an endoplasmic reticulum retention signal antagonized by the beta subunit. Neuron 25:177-190.

Birnbaumer L, Qin N, Olcese R, Tareilus E, Platano D, Costantin J, Stefani E (1998) Structures and functions of calcium channel beta subunits. J Bioenerg Biomembr 30:357-375.

Bisogno T, Howell F, Williams G, Minassi A, Cascio MG, Ligresti A, Matias I, Schiano-Moriello A, Paul P, Williams EJ, Gangadharan U, Hobbs C, Di Marzo V, Doherty P (2003) Cloning of the first sn1-DAG lipases points to the spatial and temporal regulation of endocannabinoid signaling in the brain. J Cell Biol 163:463-468.

Bittner K, Muller W (1999) Oxidative downmodulation of the transient K-current IA by intracellular arachidonic acid in rat hippocampal neurons. J Neurophysiol 82:508-511.

Bonventre JV, Huang Z, Taheri MR, O'Leary E, Li E, Moskowitz MA, Sapirstein A (1997) Reduced fertility and postischaemic brain injury in mice deficient in cytosolic phospholipase A2. Nature 390:622-625.

Bourinet E, Soong TW, Stea A, Snutch TP (1996) Determinants of the G protein-dependent opioid modulation of neuronal calcium channels. Proc Natl Acad Sci U S A 93:1486-1491.

Brice NL, Dolphin AC (1999) Differential plasma membrane targeting of voltage-dependent calcium channel subunits expressed in a polarized epithelial cell line. J Physiol 515 (Pt 3):685-694.

Brice NL, Berrow NS, Campbell V, Page KM, Brickley K, Tedder I, Dolphin AC (1997) Importance of the different beta subunits in the membrane expression of the alpha1A and alpha2 calcium channel subunits: studies using a depolarization-sensitive alpha1A antibody. Eur J Neurosci 9:749-759.

Brody DL, Patil PG, Mulle JG, Snutch TP, Yue DT (1997) Bursts of action potential waveforms relieve G-protein inhibition of recombinant P/Q-type Ca2+ channels in HEK 293 cells. J Physiol 499 (Pt 3):637-644.

Brosenitsch TA, Katz DM (2001) Physiological patterns of electrical stimulation can induce neuronal gene expression by activating N-type calcium channels. J Neurosci 21:2571-2579.

Brugada P, Brugada R, Antzelevitch C, Brugada J (2005) The Brugada Syndrome. Arch Mal Coeur Vaiss 98:115-122.

Caccavelli L, Cussac D, Pellegrini I, Audinot V, Jaquet P, Enjalbert A (1992) D2 dopaminergic receptors: normal and abnormal transduction mechanisms. Horm Res 38:78-83.

Campbell JN, Meyer RA (2006) Mechanisms of neuropathic pain. Neuron 52:77-92.

Campbell V, Berrow NS, Fitzgerald EM, Brickley K, Dolphin AC (1995) Inhibition of the interaction of G protein G(o) with calcium channels by the calcium channel beta-subunit in rat neurones. J Physiol 485 (Pt 2):365-372.

Canti C, Bogdanov Y, Dolphin AC (2000) Interaction between G proteins and accessory subunits in the regulation of 1B calcium channels in Xenopus oocytes. J Physiol 527 Pt 3:419-432.

Canti C, Page KM, Stephens GJ, Dolphin AC (1999) Identification of residues in the N terminus of alpha1B critical for inhibition of the voltage-dependent calcium channel by Gbeta gamma. J Neurosci 19:6855-6864.

Carbone E, Lux HD (1984) A low voltage-activated calcium conductance in embryonic chick sensory neurons. Biophys J 46:413-418.

Carbone E, Lux HD (1987) Single low-voltage-activated calcium channels in chick and rat sensory neurones. J Physiol 386:571-601.

Carraway R, Leeman SE (1979) The amino acid sequence of bovine hypothalamic substance P. Identity to substance P from colliculi and small intestine. J Biol Chem 254:2944-2945.

Castellano A, Wei X, Birnbaumer L, Perez-Reyes E (1993a) Cloning and expression of a neuronal calcium channel beta subunit. J Biol Chem 268:12359-12366.

Castellano A, Wei X, Birnbaumer L, Perez-Reyes E (1993b) Cloning and expression of a third calcium channel beta subunit. J Biol Chem 268:3450-3455.

Catalan RE, Martinez AM, Aragones MD, Miguel BG, Robles A, Hernandez F (1988) Dual mechanism of phosphatidylinositol hydrolysis by substance P in brain. Eur J Biochem 172:547-552.

Catterall WA (2000) Structure and regulation of voltage-gated Ca2+ channels. Annu Rev Cell Dev Biol 16:521-555.

Catterall WA, Perez-Reyes E, Snutch TP, Striessnig J (2005) International Union of Pharmacology. XLVIII. Nomenclature and structure-function relationships of voltage-gated calcium channels. Pharmacol Rev 57:411-425.

Chang MM, Leeman SE (1970) Isolation of a sialogogic peptide from bovine hypothalamic tissue and its characterization as substance P. J Biol Chem 245:4784-4790.

Chang MM, Leeman SE, Niall HD (1971) Amino-acid sequence of substance P. Nat New Biol 232:86-87.

Chemin J, Nargeot J, Lory P (2007) Chemical determinants involved in anandamide-induced inhibition of T-type calcium channels. J Biol Chem 282:2314-2323.

Chen YH, Li MH, Zhang Y, He LL, Yamada Y, Fitzmaurice A, Shen Y, Zhang H, Tong L, Yang J (2004) Structural basis of the alpha1-beta subunit interaction of voltage-gated Ca2+ channels. Nature 429:675-680.

Cheunsuang O, Maxwell D, Morris R (2002) Spinal lamina I neurones that express neurokinin 1 receptors: II. Electrophysiological characteristics, responses to primary afferent stimulation and effects of a selective mu-opioid receptor agonist. Neuroscience 111:423-434.

Chien AJ, Hosey MM (1998) Post-translational modifications of beta subunits of voltage-dependent calcium channels. J Bioenerg Biomembr 30:377-386.

Chien AJ, Gao T, Perez-Reyes E, Hosey MM (1998) Membrane targeting of L-type calcium channels. Role of palmitoylation in the subcellular localization of the beta2a subunit. J Biol Chem 273:23590-23597.

Chien AJ, Carr KM, Shirokov RE, Rios E, Hosey MM (1996) Identification of palmitoylation sites within the L-type calcium channel beta2a subunit and effects on channel function. J Biol Chem 271:26465-26468.

Cizkova D, Marsala J, Lukacova N, Marsala M, Jergova S, Orendacova J, Yaksh TL (2002) Localization of N-type Ca2+ channels in the rat spinal cord following chronic constrictive nerve injury. Exp Brain Res 147:456-463.

Clapham DE (2007) Calcium signaling. Cell 131:1047-1058.

Dai Y, Iwata K, Fukuoka T, Kondo E, Tokunaga A, Yamanaka H, Tachibana T, Liu Y, Noguchi K (2002) Phosphorylation of extracellular signal-regulated kinase in primary afferent neurons by noxious stimuli and its involvement in peripheral sensitization. J Neurosci 22:7737-7745.

Davies A, Hendrich J, Van Minh AT, Wratten J, Douglas L, Dolphin AC (2007) Functional biology of the alpha(2)delta subunits of voltage-gated calcium channels. Trends Pharmacol Sci 28:220-228.

De Waard M, Pragnell M, Campbell KP (1994) Ca2+ channel regulation by a conserved beta subunit domain. Neuron 13:495-503.

De Waard M, Hering J, Weiss N, Feltz A (2005) How do G proteins directly control neuronal Ca2+ channel function? Trends Pharmacol Sci 26:427-436.

De Waard M, Liu H, Walker D, Scott VE, Gurnett CA, Campbell KP (1997) Direct binding of G-protein betagamma complex to voltage-dependent calcium channels. Nature 385:446-450.

Delmas P, Brown DA (2005) Pathways modulating neural KCNQ/M (Kv7) potassium channels. Nat Rev Neurosci 6:850-862.

Delmas P, Coste B, Gamper N, Shapiro MS (2005) Phosphoinositide lipid second messengers: new paradigms for calcium channel modulation. Neuron 47:179-182.

Delmas P, Wanaverbecq N, Abogadie FC, Mistry M, Brown DA (2002) Signaling microdomains define the specificity of receptor-mediated InsP(3) pathways in neurons. Neuron 34:209-220.

Delmas P, Abogadie FC, Dayrell M, Haley JE, Milligan G, Caulfield MP, Brown DA, Buckley NJ (1998) G-proteins and G-protein subunits mediating cholinergic inhibition of N-type calcium currents in sympathetic neurons. Eur J Neurosci 10:1654-1666.

Dennis EA (1997) The growing phospholipase A2 superfamily of signal transduction enzymes. Trends Biochem Sci 22:1-2.

DeSilva DR, Jones EA, Favata MF, Jaffee BD, Magolda RL, Trzaskos JM, Scherle PA (1998) Inhibition of mitogen-activated protein kinase kinase blocks T cell proliferation but does not induce or prevent anergy. J Immunol 160:4175-4181.

Diaz A, Dickenson AH (1997) Blockade of spinal N- and P-type, but not L-type, calcium channels inhibits the excitability of rat dorsal horn neurones produced by subcutaneous formalin inflammation. Pain 69:93-100.

Dolphin AC (2003) Beta subunits of voltage-gated calcium channels. J Bioenerg Biomembr 35:599-620.

Doyle DA, Morais Cabral J, Pfuetzner RA, Kuo A, Gulbis JM, Cohen SL, Chait BT, MacKinnon R (1998) The structure of the potassium channel: molecular basis of K+ conduction and selectivity. Science 280:69-77.

Drdla R, Sandkuhler J (2008) Long-term potentiation at C-fibre synapses by low-level presynaptic activity in vivo. Mol Pain 4:18.

Dresviannikov AV, Page KM, Leroy J, Pratt WS, Dolphin AC (2008) Determinants of the voltage dependence of G protein modulation within calcium channel beta subunits. Pflugers Arch.

Dubel SJ, Starr TV, Hell J, Ahlijanian MK, Enyeart JJ, Catterall WA, Snutch TP (1992) Molecular cloning of the alpha-1 subunit of an omega-conotoxin-sensitive calcium channel. Proc Natl Acad Sci U S A 89:5058-5062.

Duffy RA (2004) Potential therapeutic targets for neurokinin-1 receptor antagonists. Expert Opin Emerg Drugs 9:9-21.

Dunlap K, Fischbach GD (1978) Neurotransmitters decrease the calcium ocmponent of sensory neurone action potentials. Nature 276:837-839.

Dunlap K, Fischbach GD (1981) Neurotransmitters decrease the calcium conductance activated by depolarization of embryonic chick sensory neurones. J Physiol 317:519-535.

El-Husseini Ael D, Schnell E, Dakoji S, Sweeney N, Zhou Q, Prange O, Gauthier-Campbell C, Aguilera-Moreno A, Nicoll RA, Bredt DS (2002) Synaptic strength regulated by palmitate cycling on PSD-95. Cell 108:849-863.

Elmslie KS, Zhou W, Jones SW (1990) LHRH and GTP-gamma-S modify calcium current activation in bullfrog sympathetic neurons. Neuron 5:75-80.

Evans JH, Fergus DJ, Leslie CC (2002) Inhibition of the MEK1/ERK pathway reduces arachidonic acid release independently of cPLA2 phosphorylation and translocation. BMC Biochem 3:30.

Farmer SG, Burch RM (1992) Biochemical and molecular pharmacology of kinin receptors. Annu Rev Pharmacol Toxicol 32:511-536.

Fatt P, Katz B (1953) The electrical properties of crustacean muscle fibres. J Physiol 120:171-204.

Favata MF, Horiuchi KY, Manos EJ, Daulerio AJ, Stradley DA, Feeser WS, Van Dyk DE, Pitts WJ, Earl RA, Hobbs F, Copeland RA, Magolda RL, Scherle PA, Trzaskos JM (1998) Identification of a novel inhibitor of mitogen-activated protein kinase kinase. J Biol Chem 273:18623-18632.

Feng ZP, Arnot MI, Doering CJ, Zamponi GW (2001) Calcium channel beta subunits differentially regulate the inhibition of N-type channels by individual Gbeta isoforms. J Biol Chem 276:45051-45058.

Fitzgerald EM (2000) Regulation of voltage-dependent calcium channels in rat sensory neurones involves a Ras-mitogen-activated protein kinase pathway. J Physiol 527 Pt 3:433-444.

Forscher P, Oxford GS, Schulz D (1986) Noradrenaline modulates calcium channels in avian dorsal root ganglion cells through tight receptor-channel coupling. J Physiol 379:131-144.

Fukata M, Fukata Y, Adesnik H, Nicoll RA, Bredt DS (2004) Identification of PSD-95 palmitoylating enzymes. Neuron 44:987-996.

Galluzzi KE (2007) Managing neuropathic pain. J Am Osteopath Assoc 107:ES39-48.

Gamper N, Reznikov V, Yamada Y, Yang J, Shapiro MS (2004) Phosphatidylinositol [correction] 4,5-bisphosphate signals underlie receptor-specific Gq/11-mediated modulation of N-type Ca2+ channels. J Neurosci 24:10980-10992.

Ghasemzadeh MB, Pierce RC, Kalivas PW (1999) The monoamine neurons of the rat brain preferentially express a splice variant of alpha1B subunit of the N-type calcium channel. J Neurochem 73:1718-1723.

Gray AC, Raingo J, Lipscombe D (2007) Neuronal calcium channels: splicing for optimal performance. Cell Calcium 42:409-417.

Guo J, Ikeda SR (2004) Endocannabinoids Modulate N-Type Calcium Channels and G-Protein-Coupled Inwardly Rectifying Potassium Channels via CB1 Cannabinoid Receptors Heterologously Expressed in Mammalian Neurons. Mol Pharmacol 65:665-674.

Hagiwara S, Ozawa S, Sand O (1975) Voltage clamp analysis of two inward current mechanisms in the egg cell membrane of a starfish. J Gen Physiol 65:617-644.

Haley JE, Delmas P, Offermanns S, Abogadie FC, Simon MI, Buckley NJ, Brown DA (2000) Muscarinic inhibition of calcium current and M current in Galpha q-deficient mice. J Neurosci 20:3973-3979.

Hamid J, Nelson D, Spaetgens R, Dubel SJ, Snutch TP, Zamponi GW (1999) Identification of an integration center for cross-talk between protein kinase C and G protein modulation of N-type calcium channels. J Biol Chem 274:6195-6202.

Hanlon MR, Berrow NS, Dolphin AC, Wallace BA (1999) Modelling of a voltage-dependent Ca2+ channel beta subunit as a basis for understanding its functional properties. FEBS Lett 445:366-370.

Hannun YA, Obeid LM (2008) Principles of bioactive lipid signalling: lessons from sphingolipids. Nat Rev Mol Cell Biol 9:139-150.

Hatakeyama S, Wakamori M, Ino M, Miyamoto N, Takahashi E, Yoshinaga T, Sawada K, Imoto K, Tanaka I, Yoshizawa T, Nishizawa Y, Mori Y, Niidome T, Shoji S (2001) Differential nociceptive responses in mice lacking the alpha(1B) subunit of N-type Ca(2+) channels. Neuroreport 12:2423-2427.

He LL, Zhang Y, Chen YH, Yamada Y, Yang J (2007) Functional modularity of the beta-subunit of voltage-gated Ca2+ channels. Biophys J 93:834-845.

Hering S (2002) beta-Subunits: fine tuning of Ca(2+) channel block. Trends Pharmacol Sci 23:509-513.

Hering S, Berjukow S, Sokolov S, Marksteiner R, Weiss RG, Kraus R, Timin EN (2000) Molecular determinants of inactivation in voltage-gated Ca2+ channels. J Physiol 528 Pt 2:237-249.

Herlitze S, Hockerman GH, Scheuer T, Catterall WA (1997) Molecular determinants of inactivation and G protein modulation in the intracellular loop connecting domains I and II of the calcium channel alpha1A subunit. Proc Natl Acad Sci U S A 94:1512-1516.

Herlitze S, Garcia DE, Mackie K, Hille B, Scheuer T, Catterall WA (1996) Modulation of Ca2+ channels by G-protein beta gamma subunits. Nature 380:258-262.

Hernandez-Lopez S, Tkatch T, Perez-Garci E, Galarraga E, Bargas J, Hamm H, Surmeier DJ (2000) D2 dopamine receptors in striatal medium spiny neurons reduce L-type Ca2+ currents and excitability via a novel PLC[beta]1-IP3-calcineurin-signaling cascade. J Neurosci 20:8987-8995.

Hildebrand ME, David LS, Hamid J, Mulatz K, Garcia E, Zamponi GW, Snutch TP (2007) Selective inhibition of Cav3.3 T-type calcium channels by Galphaq/11-coupled muscarinic acetylcholine receptors. J Biol Chem 282:21043-21055.

Hille B (1994) Modulation of ion-channel function by G-protein-coupled receptors. Trends Neurosci 17:531-536.

Hille B (2001) Ion Channels of Excitable Membranes, 3rd. Edition. Sunderland,MA: Sinauer Associates.

Hille B, Beech DJ, Bernheim L, Mathie A, Shapiro MS, Wollmuth LP (1995) Multiple G-protein-coupled pathways inhibit N-type Ca channels of neurons. Life Sci 56:989-992.

Hirning LD, Fox AP, McCleskey EW, Olivera BM, Thayer SA, Miller RJ, Tsien RW (1988) Dominant role of N-type Ca2+ channels in evoked release of norepinephrine from sympathetic neurons. Science 239:57-61.

Hogan QH (2007) Role of decreased sensory neuron membrane calcium currents in the genesis of neuropathic pain. Croat Med J 48:9-21.

Hokin MR, Hokin LE (1953) Enzyme secretion and the incorporation of P32 into phospholipides of pancreas slices. J Biol Chem 203:967-977.

Holz GGt, Rane SG, Dunlap K (1986) GTP-binding proteins mediate transmitter inhibition of voltage-dependent calcium channels. Nature 319:670-672.

Houliston RA, Pearson JD, Wheeler-Jones CP (2001) Agonist-specific cross talk between ERPKs and p38(mapk) regulates PGI(2) synthesis in endothelium. Am J Physiol Cell Physiol 281:C1266-1276.

Hummer A, Delzeith O, Gomez SR, Moreno RL, Mark MD, Herlitze S (2003) Competitive and synergistic interactions of G protein beta(2) and Ca(2+) channel beta(1b) subunits with Ca(v)2.1 channels, revealed by mammalian two-hybrid and fluorescence resonance energy transfer measurements. J Biol Chem 278:49386-49400.

Hurley JH, Cahill AL, Currie KP, Fox AP (2000) The role of dynamic palmitoylation in Ca2+ channel inactivation. Proc Natl Acad Sci U S A 97:9293-9298.

Ikeda SR (1991) Double-pulse calcium channel current facilitation in adult rat sympathetic neurones. J Physiol 439:181-214.

Ikeda SR (1996) Voltage-dependent modulation of N-type calcium channels by G-protein beta gamma subunits. Nature 380:255-258.

Itoh H, Shimizu M, Takata S, Mabuchi H, Imoto K (2005) A novel missense mutation in the SCN5A gene associated with Brugada syndrome bidirectionally affecting blocking actions of antiarrhythmic drugs. J Cardiovasc Electrophysiol 16:486-493.

Itoh H, Tsuji K, Sakaguchi T, Nagaoka I, Oka Y, Nakazawa Y, Yao T, Jo H, Ashihara T, Ito M, Horie M, Imoto K (2007) A paradoxical effect of lidocaine for the N406S mutation of SCN5A associated with Brugada syndrome. Int J Cardiol 121:239-248.

Ji RR, Baba H, Brenner GJ, Woolf CJ (1999) Nociceptive-specific activation of ERK in spinal neurons contributes to pain hypersensitivity. Nat Neurosci 2:1114-1119.

Jiang Y, Ruta V, Chen J, Lee A, MacKinnon R (2003) The principle of gating charge movement in a voltage-dependent K+ channel. Nature 423:42-48.

Kamatchi GL, Franke R, Lynch C, 3rd, Sando JJ (2004) Identification of sites responsible for potentiation of type 2.3 calcium currents by acetyl-beta-methylcholine. J Biol Chem 279:4102-4109.

Kammermeier PJ, Ruiz-Velasco V, Ikeda SR (2000) A voltage-independent calcium current inhibitory pathway activated by muscarinic agonists in rat sympathetic neurons requires both Galpha q/11 and Gbeta gamma. J Neurosci 20:5623-5629.

Kandel ER, Schwartz JH, Jessell TM (2000) Principles of neural science, 4th. Edition: McGraw-Hill.

Kangawa K, Minamino N, Fukuda A, Matsuo H (1983) Neuromedin K: a novel mammalian tachykinin identified in porcine spinal cord. Biochem Biophys Res Commun 114:533-540.

Kanterman RY, Mahan LC, Briley EM, Monsma FJ, Jr., Sibley DR, Axelrod J, Felder CC (1991) Transfected D2 dopamine receptors mediate the potentiation of arachidonic acid release in Chinese hamster ovary cells. Mol Pharmacol 39:364-369.

Kerppola TK (2006) Design and implementation of bimolecular fluorescence complementation (BiFC) assays for the visualization of protein interactions in living cells. Nat Protoc 1:1278-1286.

Keyser DO, Alger BE (1990) Arachidonic acid modulates hippocampal calcium current via protein kinase C and oxygen radicals. Neuron 5:545-553.

Kimura S, Goto K, Ogawa T, Sugita Y, Kanazawa I (1984) Pharmacological characterization of novel mammalian tachykinins, neurokinin alpha and neurokinin beta. Neurosci Res 2:97-104.

Klugbauer N, Marais E, Hofmann F (2003) Calcium channel alpha2delta subunits: differential expression, function, and drug binding. J Bioenerg Biomembr 35:639-647.

Lawson SN (2002) Phenotype and function of somatic primary afferent nociceptive neurones with C-, Adelta- or Aalpha/beta-fibres. Exp Physiol 87:239-244.

Lewis R (2005) A Sketch of the Subjective. Supplement to The Scientist:3-11.

Lie AA, Blumcke I, Volsen SG, Wiestler OD, Elger CE, Beck H (1999) Distribution of voltage-dependent calcium channel beta subunits in the hippocampus of patients with temporal lobe epilepsy. Neuroscience 93:449-456.

Liman ER, Hess P, Weaver F, Koren G (1991) Voltage-sensing residues in the S4 region of a mammalian K+ channel. Nature 353:752-756.

Lin LL, Wartmann M, Lin AY, Knopf JL, Seth A, Davis RJ (1993) cPLA2 is phosphorylated and activated by MAP kinase. Cell 72:269-278.

Lin Y, McDonough SI, Lipscombe D (2004) Alternative splicing in the voltage-sensing region of N-Type CaV2.2 channels modulates channel kinetics. J Neurophysiol 92:2820-2830.

Lin Z, Harris C, Lipscombe D (1996) The molecular identity of Ca channel alpha 1-subunits expressed in rat sympathetic neurons. J Mol Neurosci 7:257-267.

Lin Z, Haus S, Edgerton J, Lipscombe D (1997) Identification of functionally distinct isoforms of the N-type Ca2+ channel in rat sympathetic ganglia and brain. Neuron 18:153-166.

Lin Z, Lin Y, Schorge S, Pan JQ, Beierlein M, Lipscombe D (1999) Alternative splicing of a short cassette exon in alpha1B generates functionally distinct N-type calcium channels in central and peripheral neurons. J Neurosci 19:5322-5331.

Liu L, Rittenhouse AR (2000) Effects of arachidonic acid on unitary calcium currents in rat sympathetic neurons. J Physiol 525 Pt 2:391-404.

Liu L, Rittenhouse AR (2003a) Arachidonic acid mediates muscarinic inhibition and enhancement of N-type Ca2+ current in sympathetic neurons. Proc Natl Acad Sci U S A 100:295-300.

Liu L, Rittenhouse AR (2003b) Pharmacological discrimination between muscarinic receptor signal transduction cascades with bethanechol chloride. Br J Pharmacol 138:1259-1270.

Liu L, Barrett CF, Rittenhouse AR (2001) Arachidonic acid both inhibits and enhances whole cell calcium currents in rat sympathetic neurons. Am J Physiol Cell Physiol 280:C1293-1305.

Liu L, Roberts ML, Rittenhouse AR (2004) Phospholipid metabolism is required for M1 muscarinic inhibition of N-type calcium current in sympathetic neurons. Eur Biophys J 33:255-264.

Liu L, Gonzalez PK, Barrett CF, Rittenhouse AR (2003) The calcium channel ligand FPL 64176 enhances L-type but inhibits N-type neuronal calcium currents. Neuropharmacology 45:281-292.

Liu L, Heneghan JF, Michael GJ, Stanish LF, Egertova M, Rittenhouse AR (2008) L- and N-current but not M-current inhibition by M1 muscarinic receptors requires DAG lipase activity. J Cell Physiol 216:91-100.

Liu L, Zhao R, Bai Y, Stanish LF, Evans JE, Sanderson MJ, Bonventre JV, Rittenhouse AR (2006) M1 muscarinic receptors inhibit L-type Ca2+ current and M-current by divergent signal transduction cascades. J Neurosci 26:11588-11598.

Llinas R, Sugimori M, Lin JW, Cherksey B (1989) Blocking and isolation of a calcium channel from neurons in mammals and cephalopods utilizing a toxin fraction (FTX) from funnel-web spider poison. Proc Natl Acad Sci U S A 86:1689-1693.

Lopez HS, Brown AM (1991) Correlation between G protein activation and reblocking kinetics of Ca2+ channel currents in rat sensory neurons. Neuron 7:1061-1068.

Lu Q, Dunlap K (1999) Cloning and functional expression of novel N-type Ca(2+) channel variants. J Biol Chem 274:34566-34575.

Macdonald SG, Dumas JJ, Boyd ND (1996) Chemical cross-linking of the substance P (NK-1) receptor to the alpha subunits of the G proteins Gq and G11. Biochemistry 35:2909-2916.

MacKinnon R (1991) Using mutagenesis to study potassium channel mechanisms. J Bioenerg Biomembr 23:647-663.

Malmberg AB, Yaksh TL (1994) Voltage-sensitive calcium channels in spinal nociceptive processing: blockade of N- and P-type channels inhibits formalin-induced nociception. J Neurosci 14:4882-4890.

Malmberg AB, Basbaum AI (1998) Partial sciatic nerve injury in the mouse as a model of neuropathic pain: behavioral and neuroanatomical correlates. Pain 76:215-222.
Martin SW, Butcher AJ, Berrow NS, Richards MW, Paddon RE, Turner DJ, Dolphin AC, Sihra TS, Fitzgerald EM (2006) Phosphorylation sites on calcium channel alpha1 and beta subunits regulate ERK-dependent modulation of neuronal N-type calcium channels. Cell Calcium 39:275-292.
Mathie A, Bernheim L, Hille B (1992) Inhibition of N- and L-type calcium channels by muscarinic receptor activation in rat sympathetic neurons. Neuron 8:907-914.
McCleskey EW, Fox AP, Feldman DH, Cruz LJ, Olivera BM, Tsien RW, Yoshikami D (1987) Omega-conotoxin: direct and persistent blockade of specific types of calcium channels in neurons but not muscle. Proc Natl Acad Sci U S A 84:4327-4331.
McGivern JG, McDonough SI (2004) Voltage-gated calcium channels as targets for the treatment of chronic pain. Curr Drug Targets CNS Neurol Disord 3:457-478.
Meir A, Bell DC, Stephens GJ, Page KM, Dolphin AC (2000) Calcium channel beta subunit promotes voltage-dependent modulation of alpha 1 B by G beta gamma. Biophys J 79:731-746.
Melliti K, Meza U, Adams BA (2001) RGS2 blocks slow muscarinic inhibition of N-type Ca(2+) channels reconstituted in a human cell line. J Physiol 532:337-347.
Meves H (2008) Arachidonic acid and ion channels: an update. Br J Pharmacol.
Meza U, Thapliyal A, Bannister RA, Adams BA (2007) Neurokinin 1 receptors trigger overlapping stimulation and inhibition of CaV2.3 (R-type) calcium channels. Mol Pharmacol 71:284-293.
Michailidis IE, Zhang Y, Yang J (2007) The lipid connection-regulation of voltage-gated Ca(2+) channels by phosphoinositides. Pflugers Arch.
Millan MJ (1999) The induction of pain: an integrative review. Prog Neurobiol 57:1-164.
Mumby SM (1997) Reversible palmitoylation of signaling proteins. Curr Opin Cell Biol 9:148-154.
Mussap CJ, Geraghty DP, Burcher E (1993) Tachykinin receptors: a radioligand binding perspective. J Neurochem 60:1987-2009.
Nawa H, Doteuchi M, Igano K, Inouye K, Nakanishi S (1984) Substance K: a novel mammalian tachykinin that differs from substance P in its pharmacological profile. Life Sci 34:1153-1160.
Noda M, Shimizu S, Tanabe T, Takai T, Kayano T, Ikeda T, Takahashi H, Nakayama H, Kanaoka Y, Minamino N, et al. (1984) Primary structure of Electrophorus electricus sodium channel deduced from cDNA sequence. Nature 312:121-127.
Nowycky MC, Fox AP, Tsien RW (1985) Three types of neuronal calcium channel with different calcium agonist sensitivity. Nature 316:440-443.
Olcese R, Qin N, Schneider T, Neely A, Wei X, Stefani E, Birnbaumer L (1994) The amino terminus of a calcium channel beta subunit sets rates of channel inactivation independently of the subunit's effect on activation. Neuron 13:1433-1438.

Oliver D, Lien CC, Soom M, Baukrowitz T, Jonas P, Fakler B (2004) Functional conversion between A-type and delayed rectifier K+ channels by membrane lipids. Science 304:265-270.

Opatowsky Y, Chomsky-Hecht O, Hirsch JA (2004) Expression, purification and crystallization of a functional core of the voltage-dependent calcium channel beta subunit. Acta Crystallogr D Biol Crystallogr 60:1301-1303.

Ordway RW, Singer JJ, Walsh JV, Jr. (1991) Direct regulation of ion channels by fatty acids. Trends Neurosci 14:96-100.

Page KM, Canti C, Stephens GJ, Berrow NS, Dolphin AC (1998) Identification of the amino terminus of neuronal Ca2+ channel alpha1 subunits alpha1B and alpha1E as an essential determinant of G-protein modulation. J Neurosci 18:4815-4824.

Pan JQ, Lipscombe D (2000) Alternative splicing in the cytoplasmic II-III loop of the N-type Ca channel alpha 1B subunit: functional differences are beta subunit-specific. J Neurosci 20:4769-4775.

Patterson SI, Skene JH (1994) Novel inhibitory action of tunicamycin homologues suggests a role for dynamic protein fatty acylation in growth cone-mediated neurite extension. J Cell Biol 124:521-536.

Peralta EG, Ashkenazi A, Winslow JW, Ramachandran J, Capon DJ (1988) Differential regulation of PI hydrolysis and adenylyl cyclase by muscarinic receptor subtypes. Nature 334:434-437.

Perez-Reyes E, Castellano A, Kim HS, Bertrand P, Baggstrom E, Lacerda AE, Wei XY, Birnbaumer L (1992) Cloning and expression of a cardiac/brain beta subunit of the L-type calcium channel. J Biol Chem 267:1792-1797.

Perez JF, Sanderson MJ (2005) The frequency of calcium oscillations induced by 5-HT, ACH, and KCl determine the contraction of smooth muscle cells of intrapulmonary bronchioles. J Gen Physiol 125:535-553.

Plummer MR, Logothetis DE, Hess P (1989) Elementary properties and pharmacological sensitivities of calcium channels in mammalian peripheral neurons. Neuron 2:1453-1463.

Pragnell M, Sakamoto J, Jay SD, Campbell KP (1991) Cloning and tissue-specific expression of the brain calcium channel beta-subunit. FEBS Lett 291:253-258.

Pragnell M, De Waard M, Mori Y, Tanabe T, Snutch TP, Campbell KP (1994) Calcium channel beta-subunit binds to a conserved motif in the I-II cytoplasmic linker of the alpha 1-subunit. Nature 368:67-70.

Qin N, Platano D, Olcese R, Stefani E, Birnbaumer L (1997) Direct interaction of gbetagamma with a C-terminal gbetagamma-binding domain of the Ca2+ channel alpha1 subunit is responsible for channel inhibition by G protein-coupled receptors. Proc Natl Acad Sci U S A 94:8866-8871.

Qin N, Platano D, Olcese R, Costantin JL, Stefani E, Birnbaumer L (1998) Unique regulatory properties of the type 2a Ca2+ channel beta subunit caused by palmitoylation. Proc Natl Acad Sci U S A 95:4690-4695.

Randall A, Tsien RW (1995) Pharmacological dissection of multiple types of Ca2+ channel currents in rat cerebellar granule neurons. J Neurosci 15:2995-3012.

Resh MD (2006) Palmitoylation of ligands, receptors, and intracellular signaling molecules. Sci STKE 2006:re14.

Restituito S, Cens T, Barrere C, Geib S, Galas S, De Waard M, Charnet P (2000) The [beta]2a subunit is a molecular groom for the Ca2+ channel inactivation gate. J Neurosci 20:9046-9052.

Reuter H (1974) Localization of beta adrenergic receptors, and effects of noradrenaline and cyclic nucleotides on action potentials, ionic currents and tension in mammalian cardiac muscle. J Physiol 242:429-451.

Rittenhouse AR, Zigmond RE (1999) Role of N- and L-type calcium channels in depolarization-induced activation of tyrosine hydroxylase and release of norepinephrine by sympathetic cell bodies and nerve terminals. J Neurobiol 40:137-148.

Roche JP, Treistman SN (1998) Ca2+ channel beta3 subunit enhances voltage-dependent relief of G-protein inhibition induced by muscarinic receptor activation and Gbetagamma. J Neurosci 18:4883-4890.

Roche JP, Anantharam V, Treistman SN (1995) Abolition of G protein inhibition of alpha 1A and alpha 1B calcium channels by co-expression of the beta 3 subunit. FEBS Lett 371:43-46.

Saegusa H, Kurihara T, Zong S, Kazuno A, Matsuda Y, Nonaka T, Han W, Toriyama H, Tanabe T (2001) Suppression of inflammatory and neuropathic pain symptoms in mice lacking the N-type Ca2+ channel. Embo J 20:2349-2356.

Sah P, Faber ES (2002) Channels underlying neuronal calcium-activated potassium currents. Prog Neurobiol 66:345-353.

Sanderson MJ, Parker I (2003) Video-rate confocal microscopy. Methods Enzymol 360:447-481.

Sandoz G, Lopez-Gonzalez I, Grunwald D, Bichet D, Altafaj X, Weiss N, Ronjat M, Dupuis A, De Waard M (2004) Cavbeta-subunit displacement is a key step to induce the reluctant state of P/Q calcium channels by direct G protein regulation. Proc Natl Acad Sci U S A 101:6267-6272.

Santarelli L, Gobbi G, Blier P, Hen R (2002) Behavioral and physiologic effects of genetic or pharmacologic inactivation of the substance P receptor (NK1). J Clin Psychiatry 63 Suppl 11:11-17.

Schinelli S, Paolillo M, Corona GL (1994) Opposing actions of D1- and D2-dopamine receptors on arachidonic acid release and cyclic AMP production in striatal neurons. J Neurochem 62:944-949.

Schroeder CI, Doering CJ, Zamponi GW, Lewis RJ (2006) N-type calcium channel blockers: novel therapeutics for the treatment of pain. Med Chem 2:535-543.

Scott VE, De Waard M, Liu H, Gurnett CA, Venzke DP, Lennon VA, Campbell KP (1996) Beta subunit heterogeneity in N-type Ca2+ channels. J Biol Chem 271:3207-3212.

Sculptoreanu A, de Groat WC (2003) Protein kinase C is involved in neurokinin receptor modulation of N- and L-type Ca2+ channels in DRG neurons of the adult rat. J Neurophysiol 90:21-31.

Senogles SE, Benovic JL, Amlaiky N, Unson C, Milligan G, Vinitsky R, Spiegel AM, Caron MG (1987) The D2-dopamine receptor of anterior pituitary is functionally associated with a pertussis toxin-sensitive guanine nucleotide binding protein. J Biol Chem 262:4860-4867.

Shapiro MS, Hille B (1993) Substance P and somatostatin inhibit calcium channels in rat sympathetic neurons via different G protein pathways. Neuron 10:11-20.

Shapiro MS, Wollmuth LP, Hille B (1994a) Modulation of Ca2+ channels by PTX-sensitive G-proteins is blocked by N-ethylmaleimide in rat sympathetic neurons. J Neurosci 14:7109-7116.

Shapiro MS, Wollmuth LP, Hille B (1994b) Angiotensin II inhibits calcium and M current channels in rat sympathetic neurons via G proteins. Neuron 12:1319-1329.

Sharp AH, Black JL, 3rd, Dubel SJ, Sundarraj S, Shen JP, Yunker AM, Copeland TD, McEnery MW (2001) Biochemical and anatomical evidence for specialized voltage-dependent calcium channel gamma isoform expression in the epileptic and ataxic mouse, stargazer. Neuroscience 105:599-617.

Shyu YJ, Liu H, Deng X, Hu CD (2006) Identification of new fluorescent protein fragments for bimolecular fluorescence complementation analysis under physiological conditions. Biotechniques 40:61-66.

Singer D, Biel M, Lotan I, Flockerzi V, Hofmann F, Dascal N (1991) The roles of the subunits in the function of the calcium channel. Science 253:1553-1557.

Smith MT, Cabot PJ, Ross FB, Robertson AD, Lewis RJ (2002) The novel N-type calcium channel blocker, AM336, produces potent dose-dependent antinociception after intrathecal dosing in rats and inhibits substance P release in rat spinal cord slices. Pain 96:119-127.

Snutch TP (2005) Targeting chronic and neuropathic pain: the N-type calcium channel comes of age. NeuroRx 2:662-670.

Steed PM, Chow AH (2001) Intracellular signaling by phospholipase D as a therapeutic target. Curr Pharm Biotechnol 2:241-256.

Stephens GJ, Canti C, Page KM, Dolphin AC (1998) Role of domain I of neuronal Ca2+ channel alpha1 subunits in G protein modulation. J Physiol 509 (Pt 1):163-169.

Stewart AE, Yan Z, Surmeier DJ, Foehring RC (1999) Muscarine modulates Ca2+ channel currents in rat sensorimotor pyramidal cells via two distinct pathways. J Neurophysiol 81:72-84.

Stocker M (2004) Ca(2+)-activated K+ channels: molecular determinants and function of the SK family. Nat Rev Neurosci 5:758-770.

Stotz SC, Zamponi GW (2001) Structural determinants of fast inactivation of high voltage-activated Ca(2+) channels. Trends Neurosci 24:176-181.

Sugiura T, Kobayashi Y, Oka S, Waku K (2002) Biosynthesis and degradation of anandamide and 2-arachidonoylglycerol and their possible physiological significance. Prostaglandins Leukot Essent Fatty Acids 66:173-192.

Suh BC, Hille B (2002) Recovery from muscarinic modulation of M current channels requires phosphatidylinositol 4,5-bisphosphate synthesis. Neuron 35:507-520.

Surmeier DJ, Bargas J, Hemmings HC, Jr., Nairn AC, Greengard P (1995) Modulation of calcium currents by a D1 dopaminergic protein kinase/phosphatase cascade in rat neostriatal neurons. Neuron 14:385-397.

Svensson CI, Yaksh TL (2002) The spinal phospholipase-cyclooxygenase-prostanoid cascade in nociceptive processing. Annu Rev Pharmacol Toxicol 42:553-583.

Swartz KJ (1993) Modulation of Ca2+ channels by protein kinase C in rat central and peripheral neurons: disruption of G protein-mediated inhibition. Neuron 11:305-320.

Swartz KJ, Merritt A, Bean BP, Lovinger DM (1993) Protein kinase C modulates glutamate receptor inhibition of Ca2+ channels and synaptic transmission. Nature 361:165-168.

Tai C, Kuzmiski JB, MacVicar BA (2006) Muscarinic enhancement of R-type calcium currents in hippocampal CA1 pyramidal neurons. J Neurosci 26:6249-6258.

Takahashi SX, Mittman S, Colecraft HM (2003) Distinctive modulatory effects of five human auxiliary beta2 subunit splice variants on L-type calcium channel gating. Biophys J 84:3007-3021.

Talavera K, Staes M, Janssens A, Droogmans G, Nilius B (2004) Mechanism of arachidonic acid modulation of the T-type Ca2+ channel alpha1G. J Gen Physiol 124:225-238.

Tanabe T, Takeshima H, Mikami A, Flockerzi V, Takahashi H, Kangawa K, Kojima M, Matsuo H, Hirose T, Numa S (1987) Primary structure of the receptor for calcium channel blockers from skeletal muscle. Nature 328:313-318.

Tanaka O, Sakagami H, Kondo H (1995) Localization of mRNAs of voltage-dependent Ca(2+)-channels: four subtypes of alpha 1- and beta-subunits in developing and mature rat brain. Brain Res Mol Brain Res 30:1-16.

Tedford HW, Zamponi GW (2006) Direct G protein modulation of Cav2 calcium channels. Pharmacol Rev 58:837-862.

Tence M, Cordier J, Premont J, Glowinski J (1994) Muscarinic cholinergic agonists stimulate arachidonic acid release from mouse striatal neurons in primary culture. J Pharmacol Exp Ther 269:646-653.

Todd AJ (2002) Anatomy of primary afferents and projection neurones in the rat spinal dorsal horn with particular emphasis on substance P and the neurokinin 1 receptor. Exp Physiol 87:245-249.

Ulfers AL, Piserchio A, Mierke DF (2002) Extracellular domains of the neurokinin-1 receptor: structural characterization and interactions with substance P. Biopolymers 66:339-349.

Van Petegem F, Clark KA, Chatelain FC, Minor DL, Jr. (2004) Structure of a complex between a voltage-gated calcium channel beta-subunit and an alpha-subunit domain. Nature 429:671-675.

Wanke E, Ferroni A, Malgaroli A, Ambrosini A, Pozzan T, Meldolesi J (1987) Activation of a muscarinic receptor selectively inhibits a rapidly inactivated Ca2+ current in rat sympathetic neurons. Proc Natl Acad Sci U S A 84:4313-4317.

West AE, Chen WG, Dalva MB, Dolmetsch RE, Kornhauser JM, Shaywitz AJ, Takasu MA, Tao X, Greenberg ME (2001) Calcium regulation of neuronal gene expression. Proc Natl Acad Sci U S A 98:11024-11031.

Westenbroek RE, Hoskins L, Catterall WA (1998) Localization of Ca2+ channel subtypes on rat spinal motor neurons, interneurons, and nerve terminals. J Neurosci 18:6319-6330.

Wilk-Blaszczak MA, Singer WD, Gutowski S, Sternweis PC, Belardetti F (1994) The G protein G13 mediates inhibition of voltage-dependent calcium current by bradykinin. Neuron 13:1215-1224.

Wisgirda ME, Dryer SE (1994) Functional dependence of Ca(2+)-activated K+ current on L- and N-type Ca2+ channels: differences between chicken sympathetic and parasympathetic neurons suggest different regulatory mechanisms. Proc Natl Acad Sci U S A 91:2858-2862.

Witcher DR, De Waard M, Sakamoto J, Franzini-Armstrong C, Pragnell M, Kahl SD, Campbell KP (1993) Subunit identification and reconstitution of the N-type Ca2+ channel complex purified from brain. Science 261:486-489.

Woolf CJ, Salter MW (2000) Neuronal plasticity: increasing the gain in pain. Science 288:1765-1769.

Wu L, Bauer CS, Zhen XG, Xie C, Yang J (2002) Dual regulation of voltage-gated calcium channels by PtdIns(4,5)P2. Nature 419:947-952.

Xiao YF, Gomez AM, Morgan JP, Lederer WJ, Leaf A (1997) Suppression of voltage-gated L-type Ca2+ currents by polyunsaturated fatty acids in adult and neonatal rat ventricular myocytes. Proc Natl Acad Sci U S A 94:4182-4187.

Xiao YF, Ke Q, Wang SY, Auktor K, Yang Y, Wang GK, Morgan JP, Leaf A (2001) Single point mutations affect fatty acid block of human myocardial sodium channel alpha subunit Na+ channels. Proc Natl Acad Sci U S A 98:3606-3611.

Xue L, Gollapalli DR, Maiti P, Jahng WJ, Rando RR (2004) A palmitoylation switch mechanism in the regulation of the visual cycle. Cell 117:761-771.

Yaksh TL (2006) Calcium channels as therapeutic targets in neuropathic pain. J Pain 7:S13-30.

Yan Z, Song WJ, Surmeier J (1997) D2 dopamine receptors reduce N-type Ca2+ currents in rat neostriatal cholinergic interneurons through a membrane-delimited, protein-kinase-C-insensitive pathway. J Neurophysiol 77:1003-1015.

Yang J, Ellinor PT, Sather WA, Zhang JF, Tsien RW (1993) Molecular determinants of Ca2+ selectivity and ion permeation in L-type Ca2+ channels. Nature 366:158-161.

Yasuda T, Chen L, Barr W, McRory JE, Lewis RJ, Adams DJ, Zamponi GW (2004) Auxiliary subunit regulation of high-voltage activated calcium channels expressed in mammalian cells. Eur J Neurosci 20:1-13.

Yoshida T, Fukaya M, Uchigashima M, Miura E, Kamiya H, Kano M, Watanabe M (2006) Localization of diacylglycerol lipase-alpha around postsynaptic spine suggests close proximity between production site of an endocannabinoid, 2-arachidonoyl-glycerol, and presynaptic cannabinoid CB1 receptor. J Neurosci 26:4740-4751.

Zamponi GW, Snutch TP (1998) Decay of prepulse facilitation of N type calcium channels during G protein inhibition is consistent with binding of a single Gbeta subunit. Proc Natl Acad Sci U S A 95:4035-4039.

Zamponi GW, Bourinet E, Nelson D, Nargeot J, Snutch TP (1997) Crosstalk between G proteins and protein kinase C mediated by the calcium channel alpha1 subunit. Nature 385:442-446.

Zhang JF, Ellinor PT, Aldrich RW, Tsien RW (1996) Multiple structural elements in voltage-dependent Ca2+ channels support their inhibition by G proteins. Neuron 17:991-1003.

Zhang Y, Cribbs LL, Satin J (2000) Arachidonic acid modulation of alpha1H, a cloned human T-type calcium channel. Am J Physiol Heart Circ Physiol 278:H184-193.

Zhao R, Liu L, Rittenhouse AR (2007) Ca2+ influx through both L- and N-type Ca2+ channels increases c-fos expression by electrical stimulation of sympathetic neurons. Eur J Neurosci 25:1127-1135.

Zhu Y, Ikeda SR (1994) VIP inhibits N-type Ca2+ channels of sympathetic neurons via a pertussis toxin-insensitive but cholera toxin-sensitive pathway. Neuron 13:657-669.

Zieglgansberger W, Berthele A, Tolle TR (2005) Understanding neuropathic pain. CNS Spectr 10:298-308.